

**POLITECNICO DI TORINO**

**Collegio di Ingegneria Civile**

**Master of Science Course  
in Civil Engineering**

**Master of Science Thesis**

**Fire Resistance of Rubber  
Concrete Structures**



**Politecnico  
di Torino**

**Supervisor**

Prof. Alessandro Pasquale Fantilli

**Candidate**

Julian Ricardo Poveda Briceno

March 2025



## ***Acknowledgments***

*Este logro alcanzado se lo quiero dedicar y agradecer especialmente a mi mamá y a mi abuelo, quienes me han acompañado y apoyado durante toda mi vida para alcanzar todas mis metas y sueños. Gracias a su esfuerzo y sus enseñanzas soy la persona que soy hoy en día y he logrado llegar donde me encuentro. Sin ellos, nada de esto habría sido posible. Esta meta alcanzada también es de ellos.*

*Agradezco también a mis tías, tíos, primos, primas y a Leo, quienes me han brindado su apoyo, sus palabras de aliento y ánimo para sacar todos mis proyectos adelante y que, a pesar de la lejanía, siempre los he sentido muy cerca. A mis amigos más cercanos, tanto en Colombia como en Italia, que han hecho parte de este camino y me han acompañado en todo este proceso.*



## **Abstract**

One of the most used construction materials around the world is the concrete thanks to its versatility and durability. However, its environmental impact has been a topic of several investigations in order to find more sustainable alternatives. One alternative that has emerged during the last years is rubber concrete, which incorporates recycled tyre rubber as a partial replacement of natural aggregate. This innovative solution not only provides a great repurposing of waste tyres, but also offers potential benefits in terms of insulation, flexibility, and reduced density.

As it is a relatively new alternative, researchers have focused on understanding its behaviour and determine its different properties. One special field of interest is the behaviour when subjected to a fire scenario. Fire resistance is a critical aspect of building design and therefore, evaluating the fire resistance of rubber concrete structures is essential for ensuring compliance with current regulations.

This thesis aims to investigate the fire resistance of rubber concrete structures by analyzing their mechanical and thermal behaviour at elevated temperatures, considering the present normative and codes, as well as different add mixtures with different percentage of rubber replacement. Variation of thermal and mechanical properties with variation of temperature are proposed and its influence on its strength and distribution of temperature within concrete elements is analyzed.



## Index

1. Introduction .....	1
1.1. Concrete Behaviour Under Fire.....	1
1.1.1. Fire.....	2
1.1.2. Influence of temperature.....	3
1.1.3. Explosive spalling .....	4
1.1.3.1. Pore pressure increment.....	5
1.1.3.2. Restrained thermal dilatation.....	5
1.1.4. Critical temperatures.....	5
1.1.5. Temperature distribution.....	5
1.1.5.1. Thermal conductivity.....	6
1.1.5.2. Specific heat .....	7
1.1.5.3. Density.....	9
1.1.6. Fire resistance .....	10
1.1.6.1. Load-bearing/Resistance (R) .....	10
1.1.6.2. Integrity (E) .....	11
1.1.6.3. Insulation (I) .....	11
1.1.7. Residual strength of concrete .....	11
1.1.7.1. Residual compressive strength .....	11
1.1.7.2. Residual tensile strength.....	11
1.1.8. Failures of structural elements in fire .....	11
1.1.8.1. Loss of bending or tensile strength.....	12
1.1.8.2. Loss of bond strength .....	12
1.1.8.3. Loss of shear or torsional strength.....	12
1.1.8.4. Loss of compressive strength .....	12
2. Rubber Concrete .....	13

2.1.	Rubber .....	13
2.2.	Rubber concrete as an alternative .....	14
2.3.	Mechanical properties of rubber concrete .....	15
2.3.1.	Density.....	15
2.3.2.	Compressive strength .....	16
2.3.3.	Elastic Modulus .....	16
2.3.4.	Overview .....	16
2.4.	Rubber Concrete at High Temperature .....	16
2.4.1.	Mechanical properties.....	17
2.4.1.1.	Compressive strength .....	17
2.4.2.	Thermal properties.....	17
2.4.2.1.	Density.....	18
2.4.2.2.	Thermal conductivity.....	18
2.4.2.3.	Specific heat .....	18
2.4.2.4.	Remarks .....	18
3.	Structural Analysis of Rubber Concrete at High Temperatures.....	19
3.1.	Thermal analysis.....	19
3.2.	Mechanical analysis.....	21
3.3.	Input data .....	22
3.3.1.	Proposed density data .....	23
3.3.2.	Proposed thermal conductivity data .....	29
3.3.3.	Proposed specific heat data.....	36
3.3.4.	Compressive strength data.....	43
3.3.5.	Choose data summary and comparison .....	43
3.4.	Model definition .....	45
3.4.1.	Materials .....	45



3.4.2.	Geometry .....	48
3.4.3.	Exposure .....	49
3.4.4.	Space-time discretization.....	50
3.4.5.	Models resume.....	51
4.	Results and Analysis.....	53
4.1.	Case of study .....	53
4.2.	Base analysis from CDM Dolmen Srl. comparison .....	54
4.3.	Proposed models.....	59
4.3.1.	Temperature of reinforcement .....	59
4.3.2.	Bending moment resistance.....	62
4.3.3.	Axial resistance.....	70
4.3.4.	Bending moment – axial diagram (M-N interaction domain).....	76
5.	Conclusions .....	83
6.	References .....	85
Appendix A.	Density Values for Different Rubber Concrete Mixtures .....	88
Appendix B.	Input Data for Model with 0.45 Water-Cement Ratio .....	89
Appendix C.	Input Data for Model with 0.50 Water-Cement Ratio .....	91
Appendix D.	Input Data for Model with 0.55 Water-Cement Ratio .....	93
Appendix E.	Results of Temperature of Bottom Reinforcement.....	95
Appendix F.	Results of Bending Moment Resistance.....	97
Appendix G.	Results of Axial Resistance .....	99

## Figure Index

Figure 1-1. Components of the fire triangle .	2
Figure 1-2. Nominal temperature-time curves according to Eurocode 1.	3
Figure 1-3. Thermal conductivity of concrete as function of the temperature according to Eurocode 2 and 4.	7
Figure 1-4. Specific heat of concrete as function of the temperature according to Eurocode 2.	8
Figure 1-5. Specific heat of concrete as function of the temperature when moisture content is not considered in the analysis, according to Eurocode 2.	9
Figure 1-6. Density of concrete as function of the temperature according to Eurocode 2.	10
Figure 2-1. Tyres in landfills. <a href="https://www.metrorecycling.net/post/tires-in-landfills">https://www.metrorecycling.net/post/tires-in-landfills</a> ...	13
Figure 2-2. Process of shredding of waste tyres. Image from Mhaya et al., 2021.	14
Figure 3-1. Reduction coefficient of characteristic strength of concrete according to EUROCODE 2 (European Commission, 2002b).	21
Figure 3-2. Reduction coefficient of characteristic strength of reinforcement steel according to EUROCODE 2 (European Commission, 2002b).	22
Figure 3-3. Density values for different rubber concrete mixtures (Ling, 2011a).	24
Figure 3-4. Density as function of temperature for 0% of rubber content.	25
Figure 3-5. Density as function of temperature for 5% of rubber content.	25
Figure 3-6. Density as function of temperature for 10% of rubber content.	26
Figure 3-7. Density as function of temperature for 15% of rubber content.	26
Figure 3-8. Density as function of temperature for 20% of rubber content.	27
Figure 3-9. Density as function of temperature for 25% of rubber content.	27
Figure 3-10. Density as function of temperature for 30% of rubber content.	28
Figure 3-11. Density as function of temperature for 40% of rubber content.	28
Figure 3-12. Density as function of temperature for 50% of rubber content.	29
Figure 3-13. Variation of thermal conductivity as a function of hardened density of concrete (Bilal Nasar et al., 2020a).	30
Figure 3-14. Thermal conductivity as function of temperature for 0% of rubber content.	31

Figure 3-15. Thermal conductivity as function of temperature for 5% of rubber content.	32
Figure 3-16. Thermal conductivity as function of temperature for 10% of rubber content.	32
Figure 3-17. Thermal conductivity as function of temperature for 15% of rubber content.	33
Figure 3-18. Thermal conductivity as function of temperature for 20% of rubber content.	33
Figure 3-19. Thermal conductivity as function of temperature for 25% of rubber content.	34
Figure 3-20. Thermal conductivity as function of temperature for 30% of rubber content.	34
Figure 3-21. Thermal conductivity as function of temperature for 40% of rubber content.	35
Figure 3-22. Thermal conductivity as function of temperature for 50% of rubber content.	35
Figure 3-23. Variation of specific heat as a function of density of rubber concrete.....	37
Figure 3-24. Specific heat as function of temperature for 0% of rubber content. ....	39
Figure 3-25. Specific heat as function of temperature for 5% of rubber content. ....	39
Figure 3-26. Specific heat as function of temperature for 10% of rubber content. ....	40
Figure 3-27. Specific heat as function of temperature for 15% of rubber content. ....	40
Figure 3-28. Specific heat as function of temperature for 20% of rubber content. ....	41
Figure 3-29. Specific heat as function of temperature for 25% of rubber content. ....	41
Figure 3-30. Specific heat as function of temperature for 30% of rubber content. ....	42
Figure 3-31. Specific heat as function of temperature for 40% of rubber content. ....	42
Figure 3-32. Specific heat as function of temperature for 50% of rubber content. ....	43
Figure 3-33. Example of mechanic properties for mixture with 5% rubber content with $w/c=0.45$ , CDM DOLMEN Srl. ....	46
Figure 3-34. Example for thermal analysis parameters for mixture with 5% rubber content with $w/c=0.45$ , CDM DOLMEN Srl. ....	46
Figure 3-35. Example of thermal properties settings for mixture with 5% rubber content with $w/c=0.45$ , CDM DOLMEN Srl. ....	47

Figure 3-36. Example thermal conductivity graphic for mixture with 5% rubber content with w/c=0.45, CDM DOLMEN Srl. ....	47
Figure 3-37. Example of definition of the cross-section, CDM DOLMEN Srl. ....	48
Figure 3-38. Example of definition of longitudinal reinforcement, CDM DOLMEN Srl. ....	48
Figure 3-39. Example of cross-section with dimensions 50x25cm with reinforcement, CDM DOLMEN Srl. ....	49
Figure 3-40. Types of exposure present in the software "IS Fuoco", CDM DOLMEN Srl. ....	49
Figure 3-41. Assigned exposure to each surface of the cross-section, CDM DOLMEN Srl. ....	50
Figure 3-42. Mesh definition, CDM DOLMEN Srl. ....	50
Figure 3-43. Complete cross-section defined, CDM DOLMEN Srl. ....	51
Figure 3-44. Time discretization for thermal maps of the cross-section, CDM DOLMEN Srl. ....	51
Figure 4-1. Cross section under analysis (dimensions in mm).....	53
Figure 4-2. Thermal properties of CDM Dolmen analysis.....	54
Figure 4-3. Thermal map from CDM Dolmen model without rubber content.....	56
Figure 4-4. Thermal map from proposed model with w/c=0.5 without rubber content. ....	57
Figure 4-5. Thermal map from CDM Dolmen model with 30% of rubber content. ....	58
Figure 4-6. Thermal map from proposed model with w/c=0.5 with 30% rubber content. ....	58
Figure 4-7. Temperature of reinforcement in rubber concrete with different rubber content, Dolmen Models. ....	59
Figure 4-8. Temperature of reinforcement in rubber concrete with different rubber content, proposed models with w/c=0.45. ....	61
Figure 4-9. Temperature of reinforcement in rubber concrete with different rubber content, proposed models with w/c=0.50. ....	61
Figure 4-10. Temperature of reinforcement in rubber concrete with different rubber content, proposed models with w/c=0.55. ....	62
Figure 4-11. Bending moment resistance of rubber concrete with different rubber content, Dolmen Models. ....	63

Figure 4-12. Bending moment resistance of rubber concrete with different rubber content, proposed models with $w/c=0.45$ .....	64
Figure 4-13. Percentage of reduction of bending moment resistance from proposed models with $w/c=0.45$ .....	65
Figure 4-14. Bending moment resistance of rubber concrete with different rubber content, proposed models with $w/c=0.50$ .....	66
Figure 4-15. Percentage of reduction of bending moment resistance from proposed models with $w/c=0.50$ .....	66
Figure 4-16. Bending moment resistance of rubber concrete with different rubber content, proposed models with $w/c=0.55$ .....	67
Figure 4-17. Percentage of reduction of bending moment resistance from proposed models with $w/c=0.55$ .....	67
Figure 4-18. Variation of bending moment resistance with respect control concrete for models with $w/c: 0.45$ .....	69
Figure 4-19. Variation of bending moment resistance with respect control concrete for models with $w/c: 0.50$ .....	69
Figure 4-20. Variation of bending moment resistance with respect control concrete for models with $w/c: 0.55$ .....	70
Figure 4-21. Axial resistance of rubber concrete with different rubber content, Dolmen Models. ....	71
Figure 4-22. Axial resistance of rubber concrete with different rubber content, proposed models with $w/c=0.45$ . ....	71
Figure 4-23. Percentage of reduction of axial resistance from proposed models with $w/c=0.45$ . ....	72
Figure 4-24. Axial resistance of rubber concrete with different rubber content, proposed models with $w/c=0.50$ . ....	72
Figure 4-25. Percentage of reduction of axial resistance from proposed models with $w/c=0.50$ . ....	73
Figure 4-26. Axial resistance of rubber concrete with different rubber content, proposed models with $w/c=0.55$ . ....	73
Figure 4-27. Percentage of reduction of axial resistance from proposed models with $w/c=0.55$ . ....	74

Figure 4-28. Variation of axial resistance with respect control concrete for models with w/c: 0.45. ....	75
Figure 4-29. Variation of axial resistance with respect control concrete for models with w/c: 0.50. ....	75
Figure 4-30. Variation of axial resistance with respect control concrete for models with w/c: 0.55. ....	76
Figure 4-31. M-N interaction domain for control concrete with w/c: 0.45. ....	77
Figure 4-32. M-N interaction domain for concrete rubber content of 5% and w/c: 0.45. ....	77
Figure 4-33. M-N interaction domain for concrete rubber content of 10% and w/c: 0.45. ....	78
Figure 4-34. M-N interaction domain for concrete rubber content of 15% and w/c: 0.45. ....	78
Figure 4-35. M-N interaction domain for concrete rubber content of 20% and w/c: 0.45. ....	79
Figure 4-36. M-N interaction domain for concrete rubber content of 25% and w/c: 0.45. ....	79
Figure 4-37. M-N interaction domain for concrete rubber content of 30% and w/c: 0.45. ....	80
Figure 4-38. M-N interaction domain for concrete rubber content of 40% and w/c: 0.45. ....	80
Figure 4-39. M-N interaction domain for concrete rubber content of 50% and w/c: 0.45. ....	81

# 1. Introduction

Concrete is one of the most consumed materials around the world due to its large and significant usage in the construction sector and most likely will continue to be so in the future. However, its production has as consequence elevated levels of pollution, which is a big concern nowadays. Consequently, many efforts are focused on developing more sustainable alternatives when using concrete to reduce the impact of its application and fulfill new environmental regulations that aim to mitigate the consequences of the activities in the construction sector.

One alternative that has emerged in recent years is the incorporation of recycled rubber into concrete, coming from disposed tyres. By doing so, it is being given a second usage to tyres that are no longer useful for its initial purpose. It is important to remark the fact that the disposal of tyres is also a big concern since it is difficult to process them once their service life has ended and generates a significant amount of pollution. Since it is a new alternative, several studies have been conducted to define and characterize the main properties of rubber concrete.

Among the main concerns regarding rubberized concrete, one is its behaviour when is exposed to fire. The effects of fire on concrete structures have been studied over the years to comprehend its behaviour and fulfill safety requirements when exposed to it. The research has been focused mainly on the variation of its mechanical properties (such as the compressive strength, the elastic modulus, and the density) when the temperature increases, and the definition of its thermal properties such as the specific heat capacity, and thermal conductivity, among others.

On the other hand, to comprehend the concrete behaviour when it is exposed to a fire, it is necessary to understand the nature of the fire itself, for which different fire models describing how the temperature varies during the time have been developed.

## *1.1. Concrete Behaviour Under Fire*

Concrete as a material, presents some advantages when exposed to fire. It is incombustible in comparison with other construction materials such as wood and it is a good insulation material thanks to its low thermal diffusivity, which helps to the

protection of the reinforcement. However, when it is exposed to elevated temperatures, its mechanical properties start deteriorating. At a certain point, it could occur explosive spalling, a phenomenon that results in the reduction of the section, loss of mass, and the exposure of the reinforcement . Two main factors influence concrete's behaviour when it is exposed to high temperatures: Material properties and environmental properties.

The material properties are referred specifically to those of the cement paste, the aggregate, and the bond between these two; while environmental properties refer to the heating rate during a fire, the temperature level, the duration of the fire, the applied loads, and the moisture content.

If the concrete is sealed or unsealed also influence on its behaviour. When unsealed, it relies mostly on the water loss in its different forms, while when it is sealed, chemical reactions due to heating are the responsible (Khoury, 2000).

In general, since the behaviour of concrete when subjected to a fire scenario depends on different parameters, the measurements of concrete's residual strength vary within a wide range and therefore is difficult to specify a typical strength behaviour when it is under fire conditions, unless the properties and the conditions are fully specified.

#### 1.1.1. Fire

For a fire to take place, three elements are needed: oxygen, heat, and fuel. Together, they are commonly known as 'the triangle of fire' . Therefore, the behaviour of each fire would be different when varying any of the previously mentioned factors.

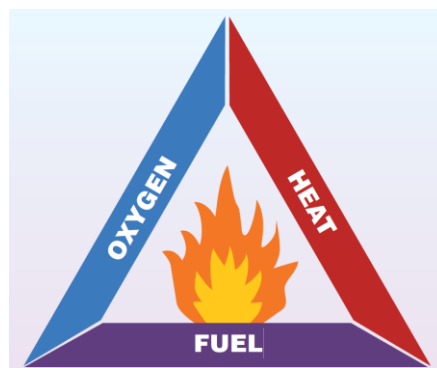


*Figure 1-1. Components of the fire triangle .*

Since the concrete structures must fulfill safety parameters and therefore, comply with codes and regulations, the temperature-fire curves presented in this document are the ones stipulated by Eurocode 1 specifically, Part 1-2 Section 3.2, where three different nominal



curves are presented. The different curves correspond to three different scenarios of fire which are standard, external, and hydrocarbon fire, as shown in Figure 1-2, and they are described by equations ( 1.1), ( 1.2), and ( 1.3), respectively .

$$\Theta_g = 20 + 345 \log_{10} (8t+1) \quad (1.1)$$

$$\Theta_g = 660 ( 1 - 0.687 e^{-0.32 t} - 0.313 e^{-3.8 t} ) + 20 \quad (1.2)$$

$$\Theta_g = 1080 ( 1 - 0.325 e^{-0.167 t} - 0.675 e^{-2.5 t} ) + 20 \quad (1.3)$$

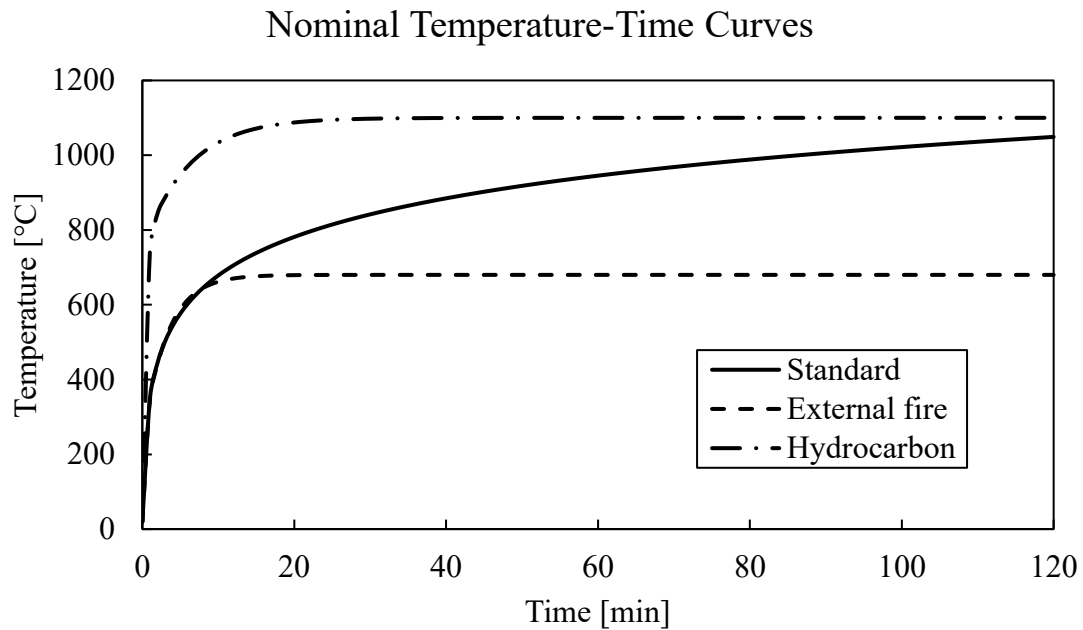


*Figure 1-2. Nominal temperature-time curves according to Eurocode 1.*

As can be seen in Figure 1-2, all three curves have an initial phase where the temperature rapidly increases. After this initial phase, the standard curve keeps increasing but at a lower rate, while the external fire and hydrocarbon curves practically maintain a constant temperature of 680 °C and 1100 °C, respectively. Additionally, none of the curves present a cooling phase.

It is important to highlight that depending on the structure being analyzed or designed, the use of one curve or another could change, depending on its characteristics and safety requirements.

### 1.1.2. Influence of temperature

Concrete has a particular behaviour when heated. At first, from ambient temperature up to reaching 80 °C, the compressive strength has an ‘apparent’ decrease, which could be

reversible by letting it cool. If temperature keeps increasing up to 200°C – 300°C, the compressive strength increases and could even be higher than the initial strength before heating (Khoury, 2000).

Above 300°C, most of the concretes could start losing its strength. The rate and the moment in which the resistance decrease depends on the type of aggregates and the water-cement ratio used. Some concretes could experience improvement in its strength up to 600 °C. However, it has be found that between 550°C and 600°C, the basic creep of cement paste increases considerably, which makes it structurally useless .

### 1.1.3. Explosive spalling

An important phenomenon that should be considered when addressing concrete's behaviour under a fire scenario is the spalling, which refers to the violent or not violent rupture of layers or pieces of concrete at temperatures that rises rapidly. This phenomenon can be group in four categories (Khoury, 2000):

- Aggregate spalling
- Explosive spalling
- Surface spalling
- Corner/sloughing-off spalling

In a fire scenario, during the first 20-30 minutes, the first three types of spalling mention above occur and are influenced by the heating rate, while after 30-60 minutes, the fourth one could occur and is influenced by the maximum temperature. The most critical form is the explosive spalling.

The occurrence of explosive spalling is influenced by several factors, which makes its prediction difficult. Based on different studies, these factors can be grouped in three main categories (material, geometric and environmental) and some of them are listed below (Benýšek, 2021):

- Heating rate
- Concrete's permeability
- Pore pressure
- Presence of reinforcement
- Applied loads

- Thermal properties (thermal conductivity, specific heat)

Although there are distinct factors which influences explosive spalling, there are two main theories explaining this phenomenon :

#### 1.1.3.1. *Pore pressure increment*

During heating, the water inside the concrete evaporates and causes the vapor pressure to increase. Depending on concrete's permeability, the rising on pore pressure will differ. If it has high permeability, vapor can be released easier, while for lower permeability the vaporized water remains trap and therefore, pressure increases. When pressure surpasses the tensile strength of concrete, parts of concrete fall off, causing spalling, which could be explosive, depending on other factors mentioned before (Khoury, 2000).

#### 1.1.3.2. *Restrained thermal dilatation*

Due to high temperatures, concrete tends to dilatate. However, according to this theory, concrete's thermal dilatation is restrained, causing increase on compressive stresses, which are later released in the form of brittle fracture, correspondent to spalling.

#### 1.1.4. Critical temperatures

According with Khoury and to different tests performed in concrete, there were identified three critical temperatures for concrete when subjected to high temperatures :

- I. Spalling critical surface temperature: surface spalling of concrete occurs between 250-420 °C.
- II. Strength loss critical temperature: concrete could start losing strength when temperature reaches around 300 °C but could vary depending on the type of aggregate.
- III. Generic loss of load-bearing capacity critical temperature: around 550-600°C concrete has considerable creep and would not be structurally useful.

#### 1.1.5. Temperature distribution

One key factor to understand concrete behaviour under fire is the development of temperature distribution within the material. Since concrete has good insulating properties, temperature gradient is large, leaving the core at relatively low temperatures in comparison with the external layer exposed to fire. The main properties influencing the

response of concrete when subjected to fire are the thermal conductivity, the specific heat, and the density.

#### 1.1.5.1. *Thermal conductivity*

Thermal conductivity is influenced by amount of moisture in concrete and as the name says, is the property of the material to conduct heat. It dictates the velocity in which the temperature raises within the concrete. Normal strength concrete has thermal conductivity ranging from 1.4 to 3.6 W/m·°C (Khoury, 2000). Although this property influences on the temperature distribution, the elevated temperature itself affects this property. In general, thermal conductivity decreases when temperature raises due to the variation on moisture content.

According to Eurocode 2, part 1-2, it proposes two limits for the variation of thermal conductivity of normal weight concrete as function of temperature, given by the following equations.

$$\lambda_c = 2 - 0.2451 (\theta/100) + 0.0107 (\theta/100)^2 \quad (1.1)$$

$$\lambda_c = 1.36 - 0.136 (\theta/100) + 0.0057 (\theta/100)^2 \quad (1.2)$$

In contrast, Eurocode 4, part 1-2 (European Commission, 2005), proposes a simpler approach for lightweight concretes.

$$\lambda_c = \lambda_{c0} \cdot [ 1 - (\theta/1600) ] \quad 20^\circ C \leq \theta \leq 800^\circ C \quad (1.3)$$

$$\lambda_c = \lambda_{c0} \cdot 0.5 \quad \theta > 800^\circ C \quad (1.4)$$

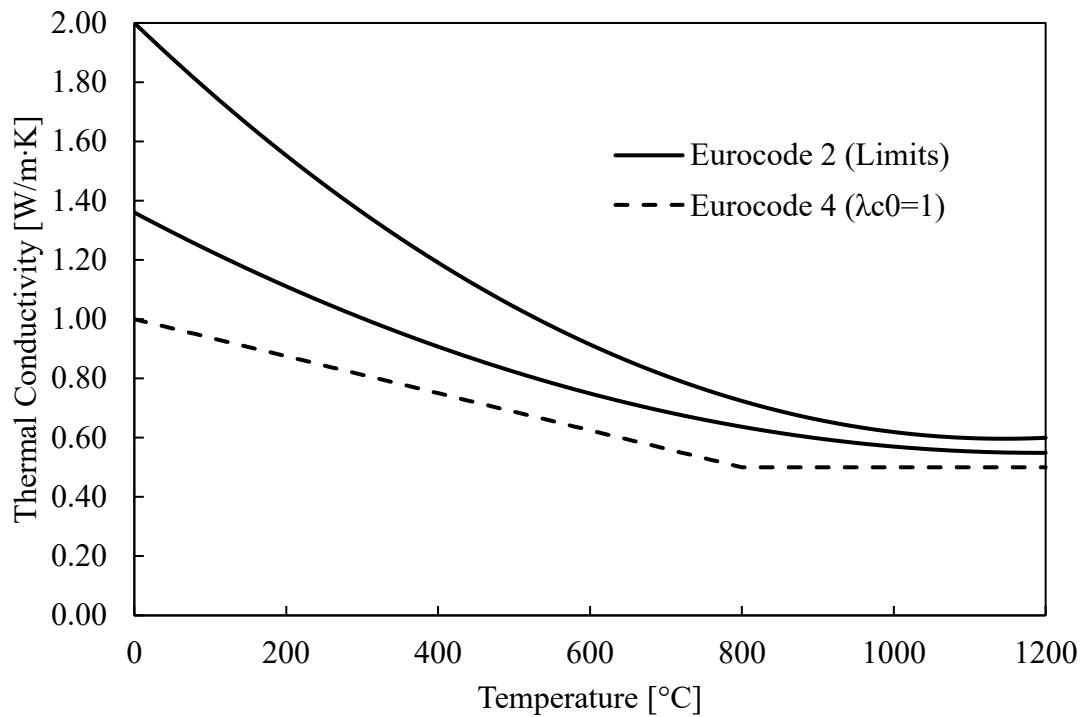


Figure 1-3. Thermal conductivity of concrete as function of the temperature according to Eurocode 2 and 4.

#### 1.1.5.2. Specific heat

Specific heat refers to the amount of heat required to change in one degree the temperature of the material. This property is influenced by type of aggregate, concrete's density, and the moisture content. As well as the thermal conductivity, specific heat also varies when concrete reaches high temperatures. Eurocode proposes the following equations for the specific heat as function of the temperature.

$$C_p = 900 \quad 20^\circ\text{C} \leq \theta \leq 100^\circ\text{C} \quad (1.5)$$

$$C_p = 900 + (\theta - 100) \quad 100^\circ\text{C} \leq \theta \leq 200^\circ\text{C} \quad (1.6)$$

$$C_p = 1000 + (\theta - 200)/2 \quad 200^\circ\text{C} \leq \theta \leq 400^\circ\text{C} \quad (1.7)$$

$$C_p = 1100 \quad 400^\circ\text{C} \leq \theta \leq 1200^\circ\text{C} \quad (1.8)$$

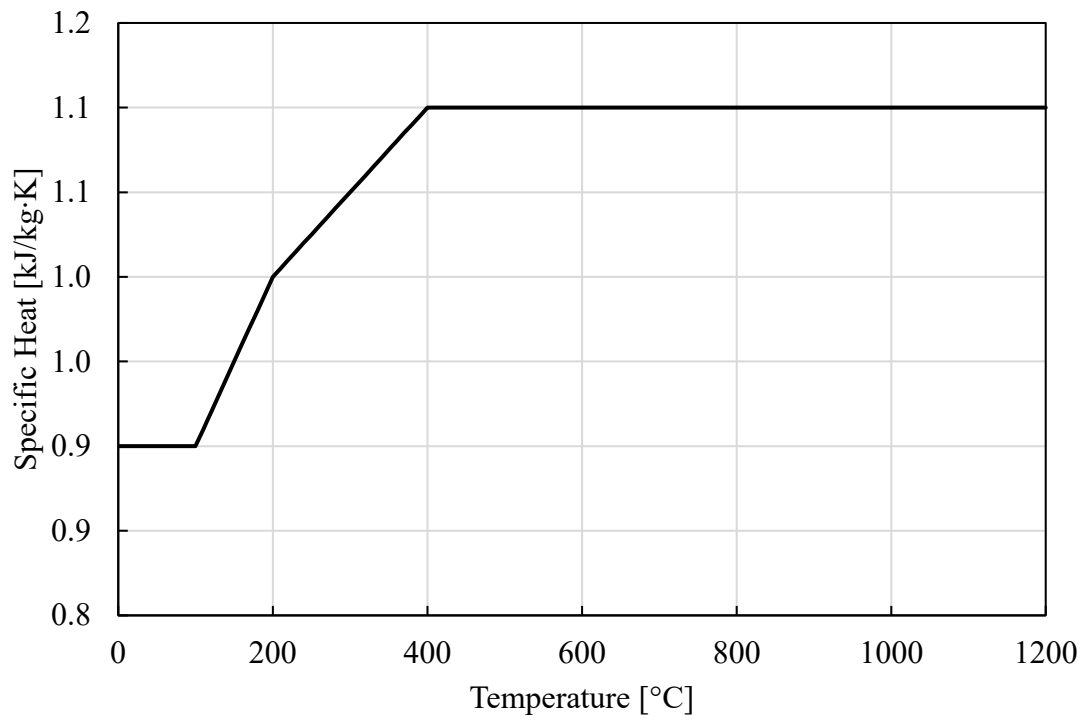


Figure 1-4. Specific heat of concrete as function of the temperature according to Eurocode 2.

Another set of equations is proposed when moisture content is not considered in the analysis.

$$C_p = C_0 \quad 20^\circ\text{C} \leq \theta \leq 100^\circ\text{C} \quad (1.9)$$

$$C_p = C_0 + C_{pu} \quad 100^\circ\text{C} < \theta \leq 115^\circ\text{C}$$

$$C_p = (C_0 + C_{pu}) - (C_{pu} - 100) (\theta - 115) / 85 \quad 115^\circ\text{C} < \theta \leq 200^\circ\text{C} \quad (1.10)$$

$$C_p = (C_0 + 100) + (\theta - 200) / 2 \quad 200^\circ\text{C} < \theta \leq 400^\circ\text{C} \quad (1.11)$$

$$C_p = C_0 + 200 \quad 400^\circ\text{C} < \theta \leq 1200^\circ\text{C} \quad (1.12)$$

Where  $C_0$  and  $C_{pu}$  correspond to the specific heat capacity at ambient temperature and the peak specific heat for a given moisture content.

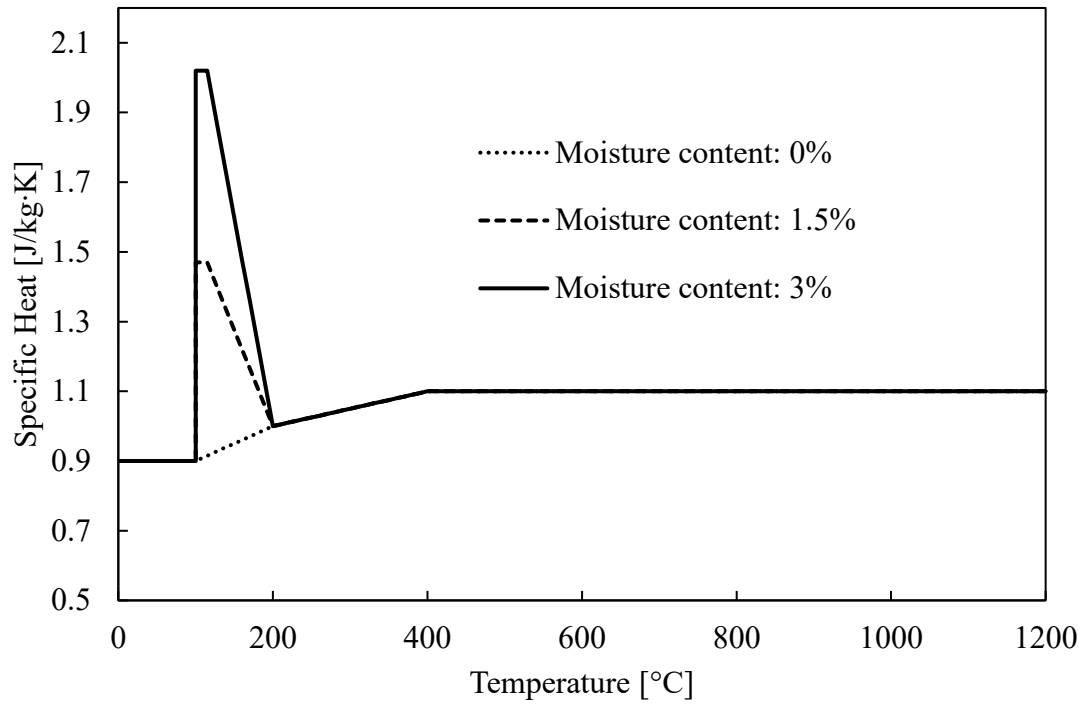


Figure 1-5. Specific heat of concrete as function of the temperature when moisture content is not considered in the analysis, according to Eurocode 2.

On contrast, the Eurocode 4 establish that the specific heat capacity of lightweight concrete may be considered independent of the concrete temperature, which means that remains constant when temperature rises.

#### 1.1.5.3. Density

Concretes are usually divided in two groups based on the density: normal-weight concrete and lightweight concrete. Due to the lost of moisture, concrete's density decreases when subjected to high temperatures. As well as with the previous properties, Eurocode proposes a set of equations to determine the density as function of temperature.

$$\rho = \rho_{(20^{\circ}\text{C})} \quad 20^{\circ}\text{C} \leq \theta \leq 115^{\circ}\text{C} \quad (1.13)$$

$$\rho = \rho_{(20^{\circ}\text{C})} \cdot (1 - 0.02 \cdot (\theta - 115) / 85) \quad 115^{\circ}\text{C} \leq \theta \leq 200^{\circ}\text{C} \quad (1.14)$$

$$\rho = \rho_{(20^{\circ}\text{C})} \cdot (0.98 - 0.03 \cdot (\theta - 200) / 200) \quad 200^{\circ}\text{C} \leq \theta \leq 400^{\circ}\text{C} \quad (1.15)$$

$$\rho = \rho_{(20^{\circ}\text{C})} \cdot (0.95 - 0.07 \cdot (\theta - 400) / 800) \quad 400^{\circ}\text{C} \leq \theta \leq 1200^{\circ}\text{C} \quad (1.16)$$

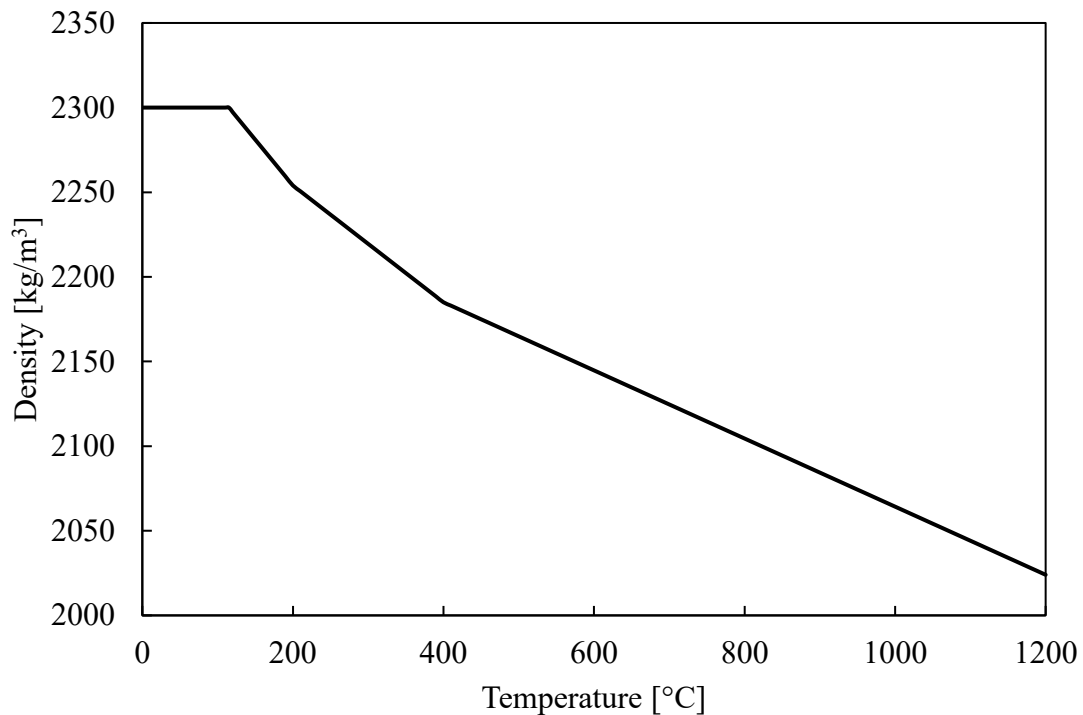


Figure 1-6. Density of concrete as function of the temperature according to Eurocode 2.

#### 1.1.6. Fire resistance

Fire resistance of concrete mainly refers to the element's capacity to maintain its design function at a certain moment during a fire event. It is evaluated by the time in which the structural element exhibits resistance with respect structural integrity, stability, and temperature transmission .

Fire resistance must fulfill three parameters or criteria: Resistance or load bearing (R), integrity (E) and insulation (I). Additionally, the fire resistance design of an element involves that the dimension of the element must be sufficient to withstand heat transfer, including the concrete cover, helping the protection of the internal reinforcement of the concrete element.

##### 1.1.6.1. Load-bearing/Resistance (R)

Load-bearing/resistance criteria refers to the capacity of the structural element to withstand the loads that are being applied during a fire scenario.

According to the code NTC18, the resistance to fire of an element or a structure is classified in different classes, which are 15, 20, 30, 45, 60, 90, 120, 180, 240 and 360,



referring to time, in minutes, in which the resistance to fire must be ensured (Ministero delle Infrastrutture e dei Trasporti, 2018).

#### 1.1.6.2. *Integrity (E)*

The element fulfills the integrity criteria if it does not allow the passage of flames or smoke, as a result of cracks formation. This criterion has great importance since prevents the propagation of fire to other areas in the structure .

#### 1.1.6.3. *Insulation (I)*

It is the capacity of a structural element to reduce the heat transfer from one side exposed to fire to other not exposed. Its main purpose is to avoid other objects on the other side from burning .

### 1.1.7. Residual strength of concrete

According to Khoury, the mechanical properties of concrete are of significant importance in terms of serviceability and failure criteria, when subjected to a fire scenario. In general, mechanical properties decrease at elevated temperatures. The compressive and the tensile strength are the ones of more interest since they influence the most to fire resistance.

#### 1.1.7.1. *Residual compressive strength*

Residual compressive strength is the great interest for researchers in terms of fire safety design. In general, what has been found in different studies is that concrete losses around 25% of its initial strength at room temperature when heated up to 300 °C. When temperature rises above 600°C, concrete could have a loss around 75% .

#### 1.1.7.2. *Residual tensile strength*

As it is well known, concrete is weak when subjected to tensile actions. From various research, as for compressive strength, tensile strength reduces when temperature rises and therefore, it is more susceptible to the appearance of cracks, up to the point where spalling could take place .

### 1.1.8. Failures of structural elements in fire

According to Khoury, when concrete elements are subjected to fire, they can present diverse types of failure.

#### 1.1.8.1. *Loss of bending or tensile strength*

Bending failure generally occurs when the reinforcement of an element subjected to bending (ex. beams), fails. The failure normally is evaluated with the mid span deflection being higher than  $L/30$ , being  $L$  the span's length. The main cause is the reduction of the steel strength due to heating during a fire scenario.

#### 1.1.8.2. *Loss of bond strength*

This failure occurs when the bond strength between reinforcement and concrete reduces due to heating. Usually appears together with loss of tensile strength failure.

#### 1.1.8.3. *Loss of shear or torsional strength*

Shear-torsion failure is more complex to determine than bending/tensile failure due to the lack of experimental experience on this regard. It is influenced by shear strength of concrete. It is not common to defined fire resistance for elements subjected to torsion, unless for specific cases when required. On the other hand, for shear elements, when fire resistance is required, special shear reinforcement is considered.

#### 1.1.8.4. *Loss of compressive strength*

Concrete elements subjected to compression usually fail during a fire due to reduction of strength caused by heating, causing compressive failure of concrete. For elements with low amount of reinforcement, the reduction of steel strength due to heating has no enormous impact, in comparison with elements with high amount of reinforcement, since both concrete and steel contributes in a significant matter to the compressive strength.

## 2. Rubber Concrete

Rubber or rubberized concrete is a type of concrete which implements crumb rubber from used tyres as a replacement of a portion of natural aggregate. This alternative arises as a more environmentally friendly solution in order to minimize the impact of concrete usage. It is a viable alternative since it gives a second usage to rubber from tyres, which is hard to recover and recycle (Azunna et al., 2024).

### 2.1. *Rubber*

According to Azunna et al., tyres disposal is of big concern in terms of pollution. In previous years, at the end of their life cycle, tyres were disposed in landfills, causing not only environmental impact, but also being a potential risk for human health. Another way used in the past to dispose waste tyres, which was cheaper, was burning them since they do not degrade. However, this alternative produced a huge amount of smoke with high content of dangerous components, being a considerable contaminant and a risk for health. Therefore, this alternative is not longer an option when considering the environmental and health impact of this practice.



Figure 2-1. Tyres in landfills. <https://www.metrorecycling.net/post/tires-in-landfills>

Due to the high ecological impact of burning tyres and its disposal in landfills, over the last years, these practices have decreased and new alternatives to recover rubber have emerged. One of these alternatives is the granulate recovery, which implies the chipping

and shredding of waste tyres, converting the tyres in granular small pieces that can be used in various applications, such as rubberized asphalt pavement or rubberized concrete, the focus of analysis of this document.



Figure 2-2. Process of shredding of waste tyres. Image from Mhaya et al., 2021.

Depending on the size of the final product, the material can be classified in fibres, coarse size, and fine size (Mhaya et al., 2021a). According to the study performed by Mhaya et al., focusing on the granular material, the coarse size rubber and the fine size rubber have sizes ranging between 5-8 mm and 1-4 mm, respectively.

## 2.2. *Rubber concrete as an alternative*

The use of such a product for civil applications have emerged as a sustainable development of construction materials. Fine size rubber or more commonly known as crumb rubber, according to Azunna et al., is used as partial replacement of natural fine aggregate in concrete. In comparison, physical properties of crumb rubber, such as specific gravity, water absorption and stiffness, are lower than those of natural fine aggregate. These differences have a considerable influence on the final product when crumb rubber is used as replacement for fine material.

From an economic perspective, there is not sufficient information in the literature regarding the use of crumb rubber in concrete for construction, which is also an important aspect that should be taken into account when considering the implementation of rubber

concrete as a construction material. However, according to Correia et al., regarding rubber concrete blocks, the cost of introducing crumb rubber increment between 4 and 17% the cost of its production.

In order to accurately assess the viability of crumb rubber as a replacement of natural aggregate in concrete, another aspect that should be consider are the mechanical properties of rubber concrete, since they are the ones that govern the structural behaviour and performance of concrete.

### 2.3. *Mechanical properties of rubber concrete*

The primary mechanical properties in which researchers focused on are the density, the compressive strength, and the elastic modulus. Azunna et al., made an investigation on this manner among various sources that have studied rubber concrete and summarized the different findings, which are present on this document.

#### 2.3.1. Density

According to the diverse sources considered by Azunna et al., replacing natural aggregate by crumb rubber influences the density of concrete by reducing it. The main reason for this effect is that the specific density of crumb rubber is considerably lower in comparison with natural aggregates. Generally speaking, natural aggregates have a specific gravity around 2.65 while crumb rubber has a specific gravity ranging between 0.6 to 1.15, which is less than half. By replacing a certain percentage of aggregate with rubber, there could be place for a considerable reduction in density, considering rubberized concrete as a lightweight concrete. According to the sources consulted by Azunna et al., for a 20% of replacement of aggregate with crumb rubber, the reduction of the density is around 9% of the density.

It is important to highlight that depending on the different mixtures of concrete, the value of the density is going to vary. However, the tendency of percentage of density reduction is similar among the different studies found in the literature.

On the whole, density is closely related to the strength of concrete, and it is no different for rubber concrete.

### 2.3.2. Compressive strength

As it was mentioned before, compressive strength of concrete is associated with its density. As a trend, concretes with high densities tend to have higher strengths, while lighter concretes have lower resistance. Therefore, in the case of rubber concrete, by increasing the percentage of replacement of aggregate by crumb rubber, the compressive strength reduces as well as its density. According to the research conducted by Fadiel et al., with a 20% replacement with crumb rubber, the reduction on the compressive strength was around 26%.

One key factor involved on the compressive strength of rubber concrete is the bond between the crumb particles and cement paste, due to the fact that crumb rubber has a hydrophobic nature (Mhaya et al., 2021). However, compressive strength can be improved by applying certain treatment to crumb rubber. Based on the findings of the study performed by Azunna et al., some of the treatments that could be used on crumb rubber are washing the rubber with water, treat it with cement, or coating the particles with cement mortar which proves to be the one with better results, reaching an increase of 40.6% of the compressive strength in comparison with other rubber concretes without any treatment of the rubber particles.

### 2.3.3. Elastic Modulus

As well as the compressive strength, elastic modulus tends to decrease when the percentage of rubber increase in the concrete mix. However, one of the studies present on the paper “Review on the characteristic properties of crumb rubber concrete” by Azunna et al., by treating the material there is an improvement, as well as in the case of the compressive strength.

### 2.3.4. Overview

In general, due to the fact that mechanical properties of rubber concrete have a trend to decrease when the percentage of rubber increases, in the literature is found that the usage of this alternative material is recommend for infrastructure or low strength applications.

## 2.4. *Rubber Concrete at High Temperature*

So far it has been shown that rubber concrete has a different behaviour in contrast with normal concrete; their mechanical properties change and therefore, its structural

performance also changes. However, as it has been mentioned on the present document, another aspect to consider is the resistance to fire. Therefore, not only the mechanical properties of rubber concrete, but also its thermal properties are of high importance, as well as how its behaviour is affected by elevated temperatures during a fire scenario.

It has been found that, up to temperatures of 300°C, rubber concrete does not present any noticeable change. However, once it reaches temperatures of 400°C, significant changes start to appear (El Marzak et al., 2022).

Evidence suggests that the usage of rubber within the concrete mixtures provides an insulation degree. Therefore, when it is subjected to high temperatures, heat transfer takes longer, which could lead advantageous for safety during a fire scenario (El Marzak et al., 2022).

#### 2.4.1. Mechanical properties

As has been mentioned before, as well as for standard concrete, rubber concrete also presents a degradation of its mechanical properties when it is subjected to elevated temperatures.

##### 2.4.1.1. *Compressive strength*

A reduction on the compressive strength of rubber concrete is present when it is exposed to high temperatures and this reduction is more noticeable as the temperature increases. However, this reduction is less severe in rubber concretes, according with different studies. As an example, in the article written by Fadiel et al., the samples with higher rubber content presented a lower reduction on its compressive strength. Some possible reasons for the reduction of the compressive strength have been mentioned on the present document: the increase in the internal pressure due to the evaporation of the internal water, leading to the appearance of small fractures, and chemical changes in the cement paste.

#### 2.4.2. Thermal properties

The main thermal properties to consider are the thermal conductivity, the specific heat and density, which is actually a mechanical property, but as it influences in the performance of the concrete against a fire scenario, it should be considered when analyzing the thermal behaviour of this material.

#### 2.4.2.1. *Density*

Based on the investigation conducted by Fadiel et al., when temperature raises, density of rubber concrete decreases, just as it does in the case of normal concrete, which is closely related to the mass loss.

In the study carried out by Fadiel et al., the control concrete (without any rubber content) had a mass loss around 7%, while rubber concretes between 3.25% and 6.7%, at a temperature of 200°C. However, at 400°C, rubberized concretes presented higher mass losses in comparison with the control concrete, reaching losses around 10% for exposures of 600°C (Fadiel et al., 2023b).

#### 2.4.2.2. *Thermal conductivity*

Thermal conductivity decreases when the rubber content increases, providing a degree of insulation to the concrete elements. This reduction of the thermal conductivity can be explained by two main factors: air entrapment effect of crumb rubber and the thermal conductivity itself of the crumb rubber, which is significantly lower in comparison with the other components of the concrete mixture (Najim et al., 2011). A lower value of thermal conductivity implies that heat flows slower or with more difficulty across the material, leading to a lower rate of heating.

#### 2.4.2.3. *Specific heat*

In contrast with the other properties, specific heat of rubber concrete tends to increase. From the results obtained by Najim et al. it is noticeable that the specific heat of rubber concrete increases when rubber content increases. Higher values of specific heat capacity means that more energy is required to increase the temperature of the material.

#### 2.4.2.4. *Remarks*

The different thermal properties also vary when the temperature raises. Unfortunately, there has not been found any literature references on how the thermal properties of rubber concrete vary as function of the temperature. Therefore, there is a wide field of research regarding the properties of this material related to the fire resistance. It is of significant importance the determination of this variation so a proper structural analysis under a fire scenario can be carry out. However, from the current codes and laws, estimated variations of this properties is proposed, based on studies performed on normal concretes.



# 3. Structural Analysis of Rubber Concrete at High Temperatures

## 3.1. Thermal analysis

For a two-dimensional problem, the thermal analysis of a cross section requires the integration of the Fourier's law of heat conduction (CDM DOLMEN Srl, n.d.-a).

$$\begin{aligned}\nabla \cdot (\lambda(T) \nabla T) &= \rho(T) C(T) \frac{\partial T}{\partial t} \\ \frac{\partial}{\partial x} \left( \lambda(T) \frac{\partial T}{\partial x} \right) + \frac{\partial}{\partial y} \left( \lambda(T) \frac{\partial T}{\partial y} \right) &= \rho(T) C(T) \frac{\partial T}{\partial t} \\ \frac{\partial \lambda(T)}{\partial x} \frac{\partial T}{\partial x} + \frac{\partial^2 T}{\partial x^2} + \frac{\partial \lambda(T)}{\partial y} \frac{\partial T}{\partial y} + \frac{\partial^2 T}{\partial y^2} &= \rho(T) C(T) \frac{\partial T}{\partial t}\end{aligned}$$

Where  $T$  is the temperature,  $\lambda$  is the thermal conductivity,  $\rho$  is the density and  $C$  is the specific heat capacity, and the last three are function of the temperature.

Applying a time-space discretization by using the Taylor series expansion, the first and second order derivatives for the temperature and the thermal conductivity are given by the following equations, considering a central scheme for the finite difference method (Karim Serroukh et al., 2023a).

$$\begin{aligned}\frac{\partial T}{\partial t} &= \frac{T_{i,j}^{n+1} - T_{i,j}^n}{\Delta t} \\ \frac{\partial T}{\partial x} &= \frac{T_{i+1,j}^{n+1} - T_{i-1,j}^{n+1}}{2\Delta x} \\ \frac{\partial T}{\partial y} &= \frac{T_{i,j+1}^{n+1} - T_{i,j-1}^{n+1}}{2\Delta y} \\ \frac{\partial^2 T}{\partial x^2} &= \frac{T_{i+1,j}^{n+1} - 2T_{i,j}^{n+1} + T_{i-1,j}^{n+1}}{2\Delta x^2}\end{aligned}$$

$$\frac{\partial^2 T}{\partial y^2} = \frac{T_{i,j+1}^{n+1} - 2T_{i,j}^{n+1} + T_{i,j-1}^{n+1}}{2\Delta y}$$

$$\frac{\partial \lambda(T)}{\partial x} = \frac{\lambda_{i+1,j}^{n+1} - \lambda_{i,j}^{n+1}}{\Delta x}$$

$$\frac{\partial \lambda(T)}{\partial y} = \frac{\lambda_{i,j+1}^{n+1} - \lambda_{i,j}^{n+1}}{\Delta y}$$

In order to solve the problem, boundary conditions must be set. Considering an element that is subjected to a fire scenario, just before it starts, the initial temperature ( $T_0$ ) across the complete section is the ambient temperature, considered equal to 20°C. Then, during the fire, it can be calculated the net heat flux of the surface exposed to it and set it as a boundary condition. This net heat flux is computed according to equations 3.1, 3.2 and 3.3 of Eurocode 1, Part 1-2 (EN 1991-1-2) (European Commission, 2002a).

$$\nabla \cdot (\lambda(T) \nabla T) = \dot{h}_{net} \text{ (Boundary condition)}$$

$$\dot{h}_{net} = \dot{h}_{net,c} + \dot{h}_{net,r}$$

Where  $\dot{h}_{net,c}$  is the heat flux by convection and  $\dot{h}_{net,r}$  is the heat flux by radiation. Each of these components are determined as follow.

$$\dot{h}_{net,c} = \alpha_c (\theta_g - \theta_m)$$

Where  $\alpha_c$  is the coefficient of heat transfer by convection,  $\theta_g$  is the temperature of the gas in proximity of the exposed surface and  $\theta_m$  is the temperature of the exposed surface of the element. The value of the gas temperature is taken from the temperature-time curve adopted for the analysis.

$$\dot{h}_{net,r} = \Phi \varepsilon_m \varepsilon_f \sigma [(\theta_r + 273)^4 - (\theta_m + 273)^4]$$

Where  $\Phi$  is the configurations factor,  $\varepsilon_m$  is the surface emissivity of the element,  $\varepsilon_f$  is the emissivity of the fire,  $\sigma$  is the Stephan Boltzmann constant set equal to  $5.67 \times 10^{-8} \text{ W/m}^2\text{K}^4$  and  $\theta_r$  is the effective radiation temperature of the fire environment.

Recommend values according to the normative for  $\varepsilon_m$  and  $\varepsilon_f$  are 0.8 and 1.0, respectively, while for the configuration factor is set equal to 1. It also establishes that for each temperature-time curve a specific coefficient of heat transfer by convection ( $\alpha_c$ ). For the

standard, external and hydrocarbon curves, the values of the coefficient of heat transfer by convection are 25, 25 and 50 W/m<sup>2</sup>K, respectively (European Commission, 2002a).

Applying the finite difference method and the discretization for the Finite Element Method, the final result of the thermal analysis is the value of the temperature at the different vertex of each finite element composing the cross section, at various times of the fire scenario.

### 3.2. *Mechanical analysis*

For the mechanical analysis, the main objective is to obtain the resistance to axial force and bending moment. Table 3.1 of Eurocode 2, part 1-2 (EN 1992-1-2) (European Commission, 2002b), provides a reduction coefficient ( $K_c(\theta)$ ) for the characteristic strength of concrete at different temperatures, depending on the type of aggregate used in the concrete mix. For intermediate values, it is allowed the interpolation between the given values. Figure 3-1 plots coefficient  $K_c$  for both types of aggregates.

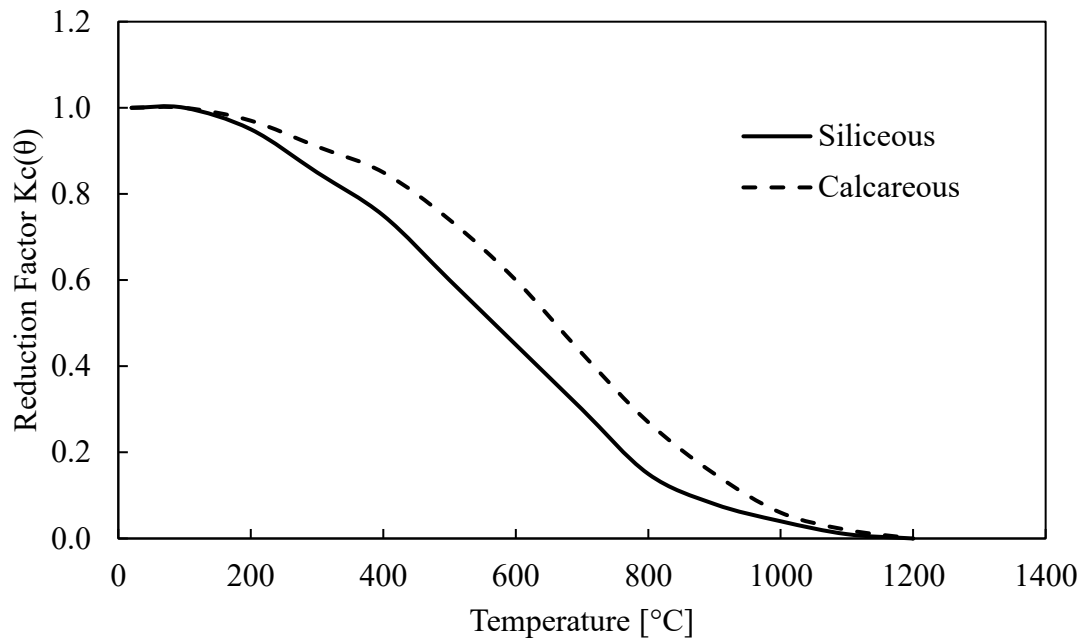


Figure 3-1. Reduction coefficient of characteristic strength of concrete according to EUROCODE 2 (European Commission, 2002b).

For reinforcement steel, code also provides a reduction coefficient ( $K_s(\theta)$ ) for its characteristic strength as function of its temperature, which varies if the reinforcement is hot rolled or cold worked.

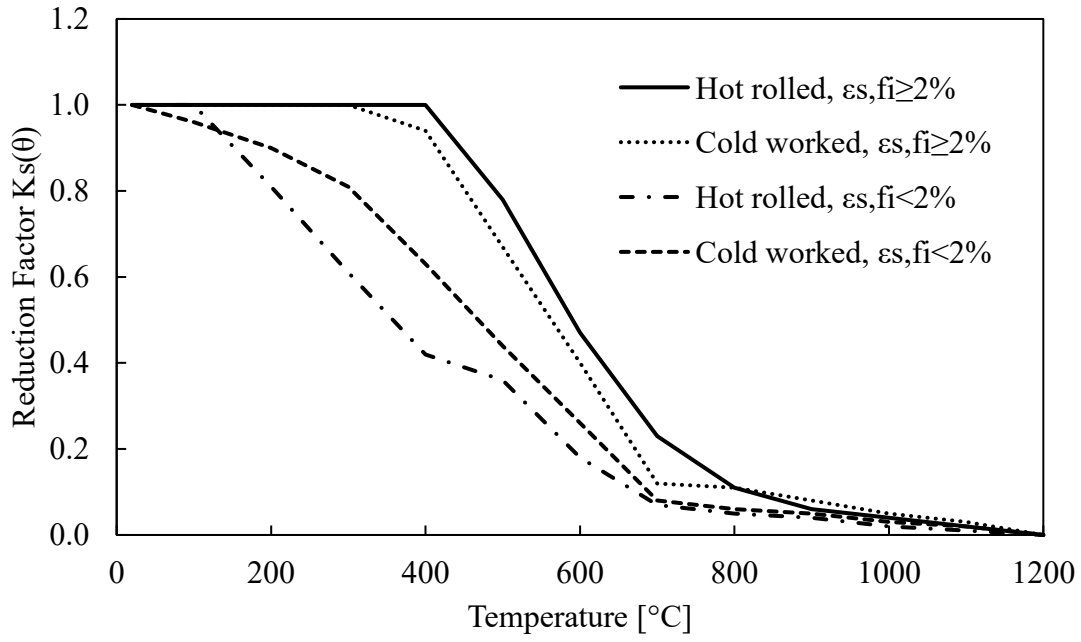


Figure 3-2. Reduction coefficient of characteristic strength of reinforcement steel according to EUROCODE 2 (European Commission, 2002b).

Since the temperatures across the transverse cross sections are obtained from the thermal analysis, and considering the reduction coefficient provided by Eurocode, it is possible to assign the correspondent strength to each one of the finite elements as function of its temperature.

Axial force and bending moment resistance are computed following constitutive laws of materials and integrating the internal stresses of each one of the finite elements (CDM DOLMEN Srl, n.d.-b).

$$N = \int_A \sigma_x dA = \int_{A_d} \sigma_d dA_d + \sum_i \sigma_{c,i} A_{c,i}$$

$$M_z = \int_A \sigma_x y dA = \int_{A_d} \sigma_d y dA_d + \sum_i \sigma_{c,i} y_{c,i} A_{c,i}$$

$$M_y = \int_A \sigma_x z dA = \int_{A_d} \sigma_d z dA_d + \sum_i \sigma_{c,i} z_{c,i} A_{c,i}$$

### 3.3. Input data

Since there is not still sufficient information on the literature available regarding the variation of the thermal properties of rubber concrete when temperature increases, it was

decided to use the equations provided by Eurocode to determine how these properties vary with the temperature (*see equations from (1.1 to (1.16)*). However, different experimental tests have been conducted with the objective of determining these properties at ambient temperature when natural aggregate is replaced by crumb rubber.

On the other hand, as has been mentioned several times, properties of rubber concrete vary depending on several factors such as percentage of replacement, type of aggregate, water-cement ratio, among others. Therefore, for the matter of the present thesis, studies of rubber concrete with similar characteristics were searched on the literature, with the purpose that the outcomes of the proposed analysis have certain correlation with the input data considered from the different studies performed.

Additionally, a base model with a different mixture is considered so a comparison can be made. The data for this model is taken from the investigation made by Karim Serroukh et al..

#### 3.3.1. Proposed density data

First of all, in the study performed by Ling, the values of density are provided. The research studied mixes with water/cement ratios of 0.45, 0.5 and 0.55, and for each one of them different percentages of replacement of fine aggregate by crumb rubber were considered with 5%, 10%, 15%, 20%, 25%, 30%, 40% and 50%. Figure 3-3 illustrates the results obtained regarding the density of the samples as function of the rubber content as replacement of fine aggregate. In the Appendix A can be found the actual values from the reference paper.

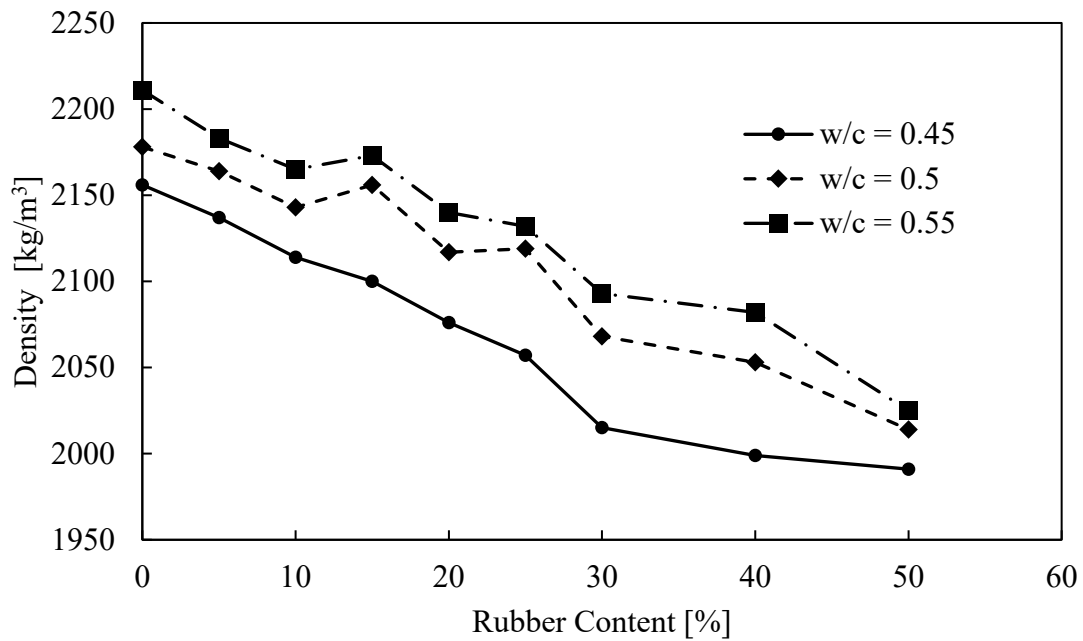


Figure 3-3. Density values for different rubber concrete mixtures (Ling, 2011a).

It is also important to highlight that the ratios aggregate/cement as well as fine aggregate/coarse aggregate were fixed with values of 5.6 and 0.5, respectively. These parameters are the based for the research of data for the other properties of rubber concrete.

With equations (1.13 to (1.16 is determine the variation of the density as function of the temperature, considering the initial one (at room temperature) as the ones obtained from Ling study. From Figure 3-4 to Figure 3-12 is shown the variation of density as function of the temperature for the different percentages of rubber concrete and water-cement ratios.

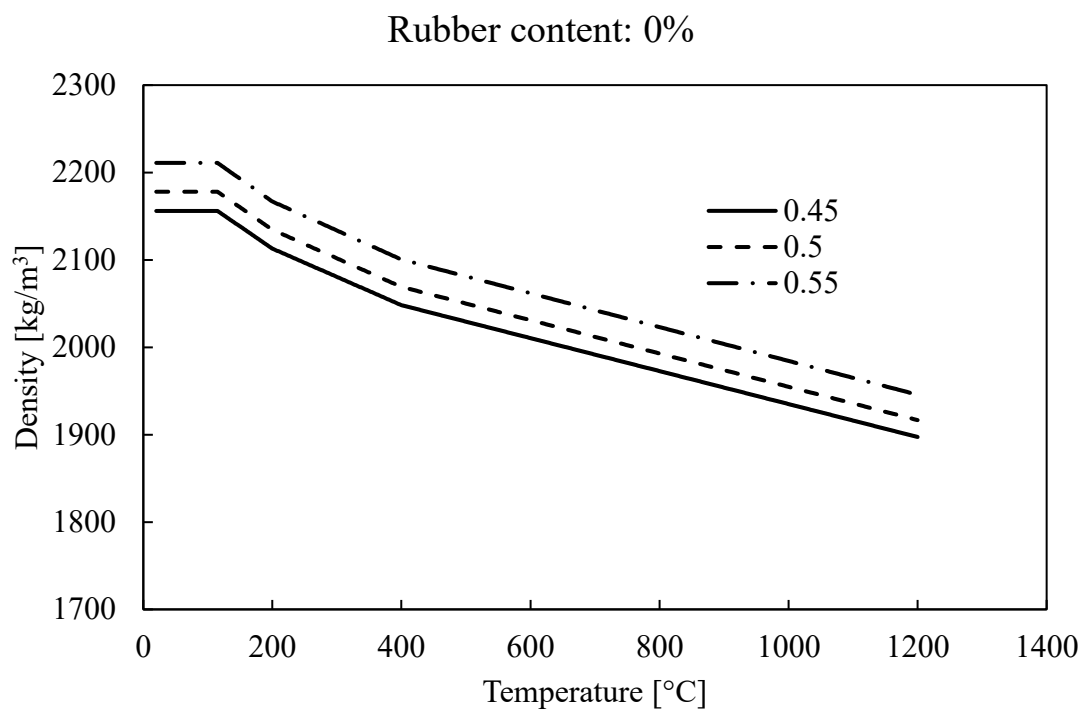


Figure 3-4. Density as function of temperature for 0% of rubber content.

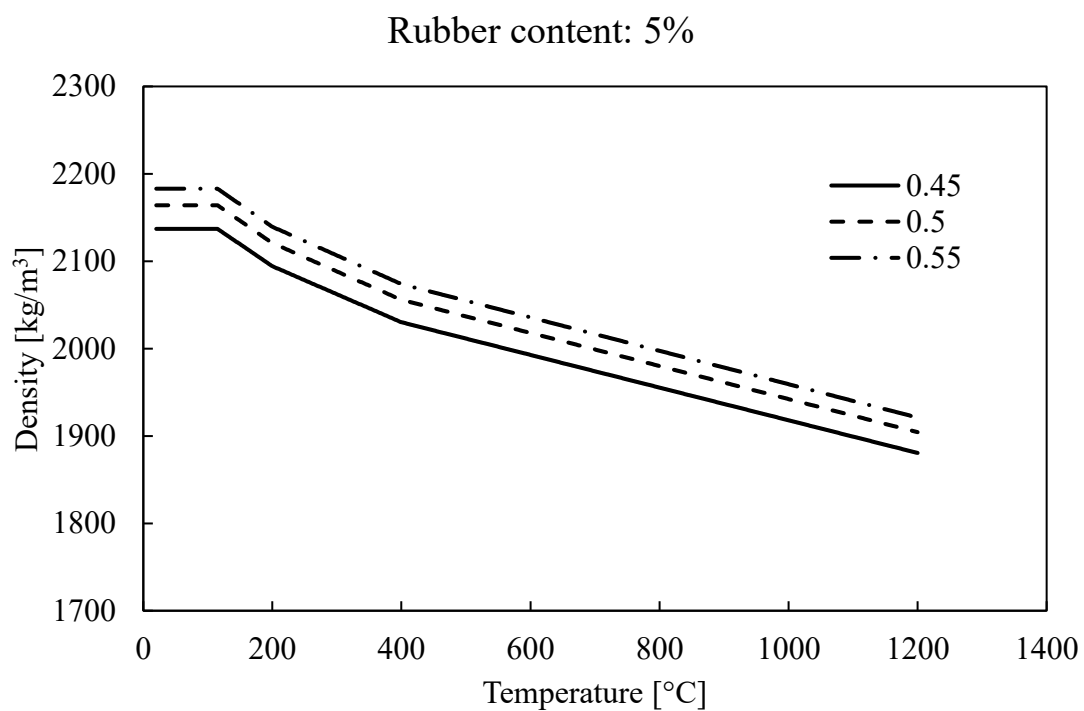


Figure 3-5. Density as function of temperature for 5% of rubber content.

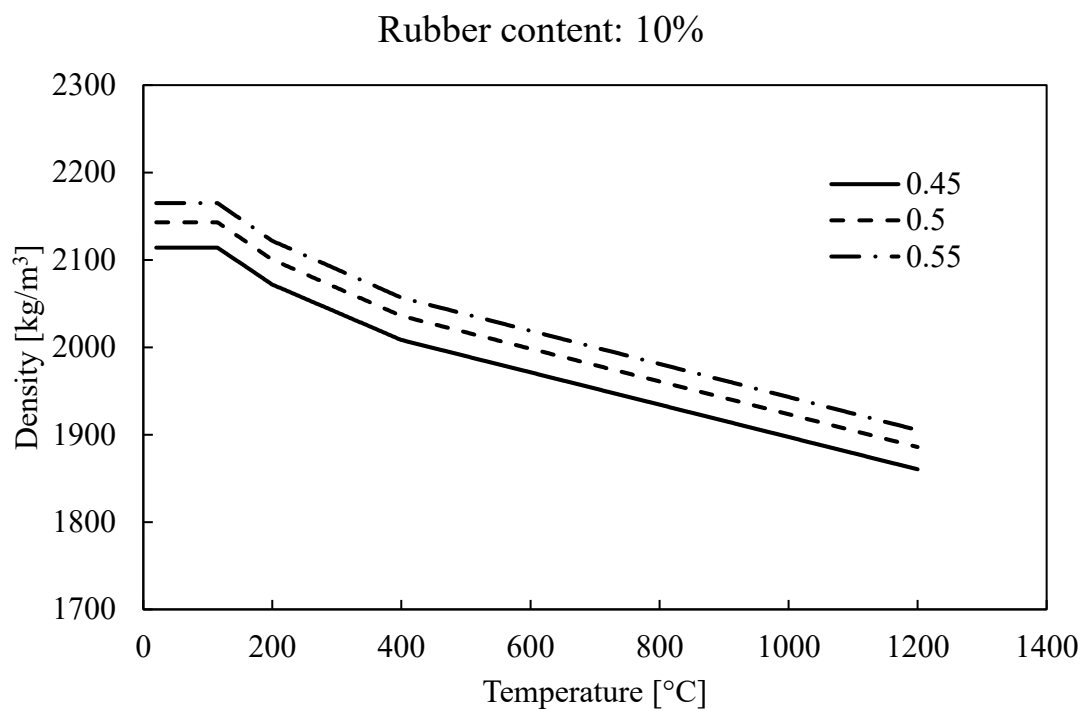


Figure 3-6. Density as function of temperature for 10% of rubber content.

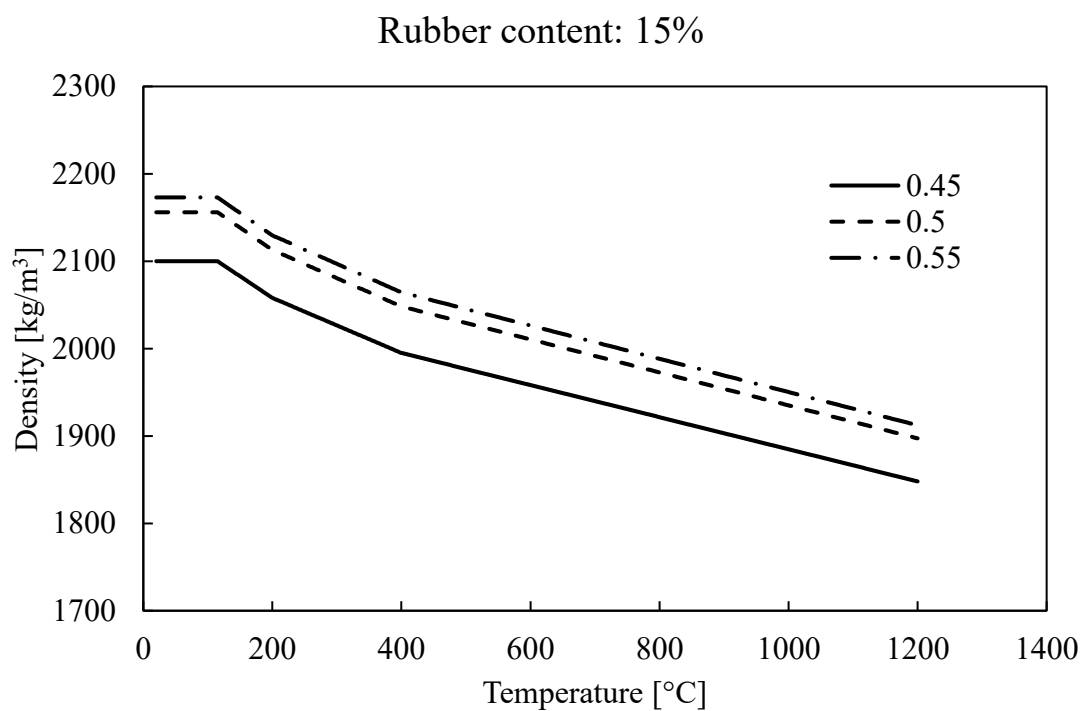


Figure 3-7. Density as function of temperature for 15% of rubber content.



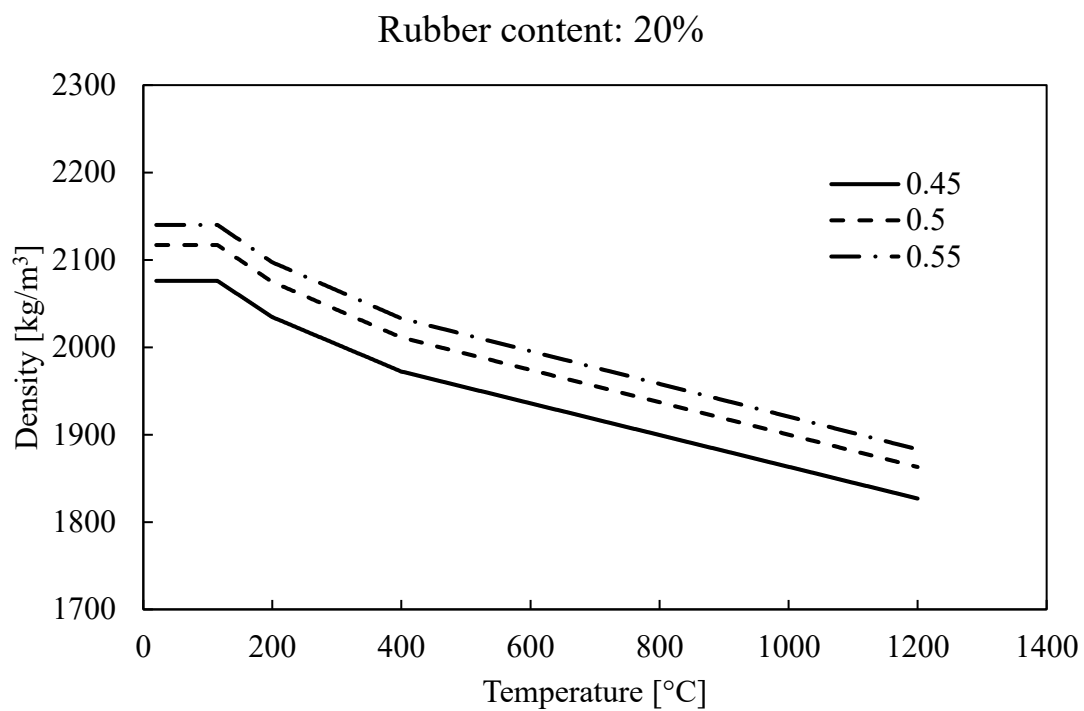


Figure 3-8. Density as function of temperature for 20% of rubber content.

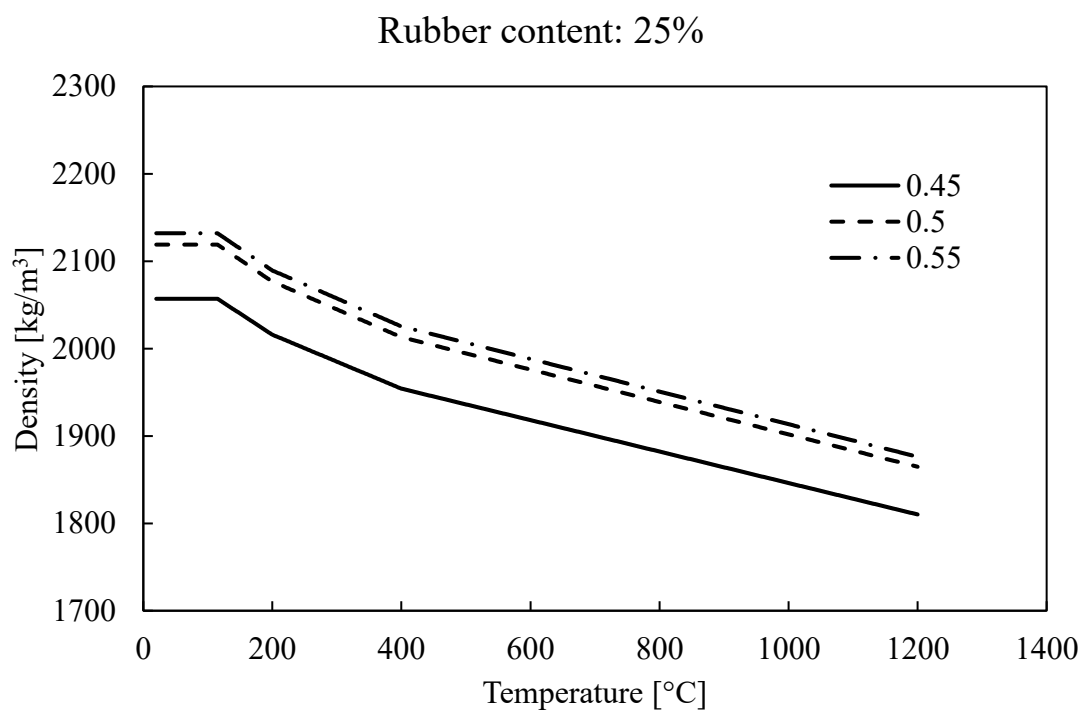


Figure 3-9. Density as function of temperature for 25% of rubber content.

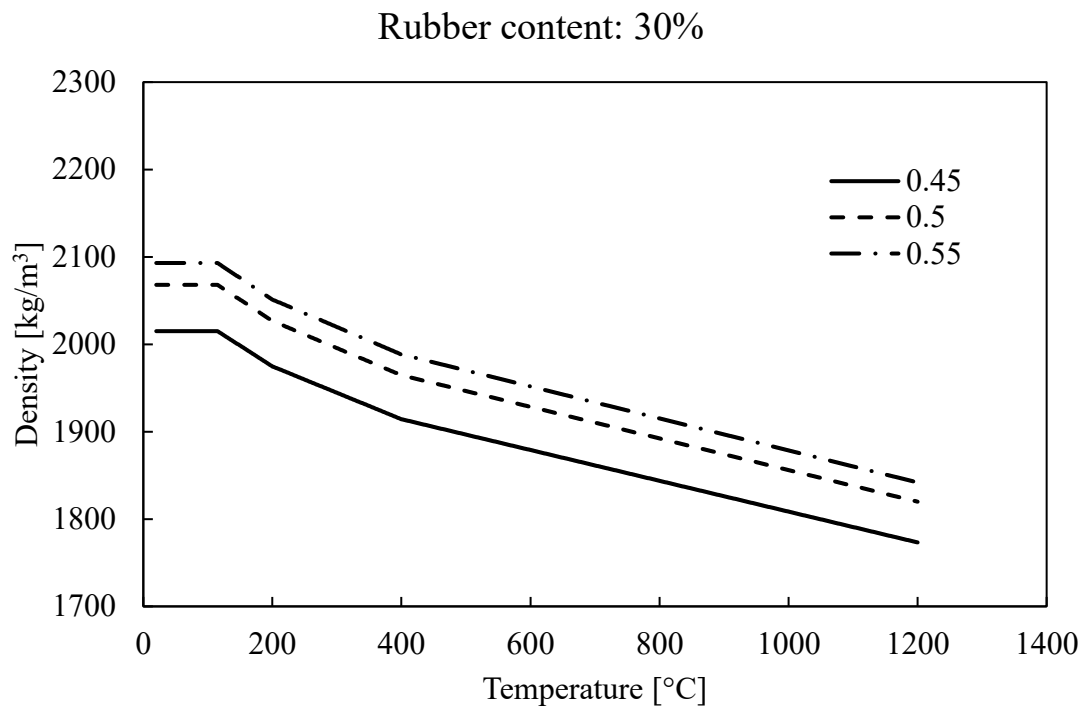


Figure 3-10. Density as function of temperature for 30% of rubber content.

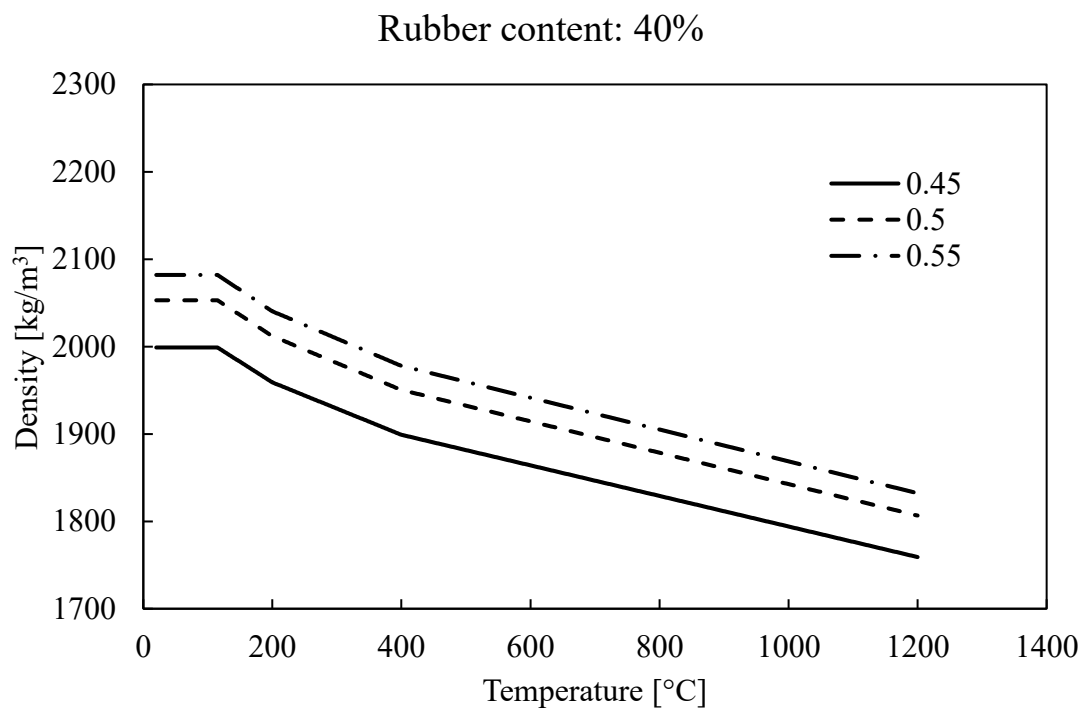


Figure 3-11. Density as function of temperature for 40% of rubber content.

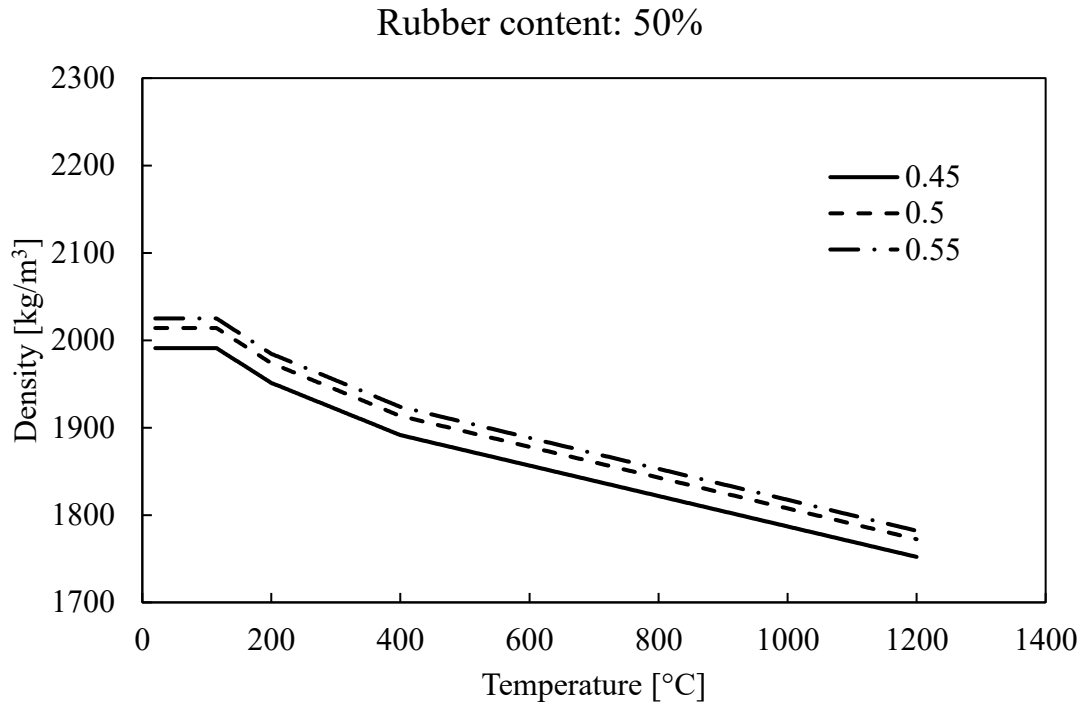


Figure 3-12. Density as function of temperature for 50% of rubber content.

### 3.3.2. Proposed thermal conductivity data

On the study conducted by Bilal Nasar et al., it is proposed an equation that relates the thermal conductivity of rubber concrete with the hardened density of the mix; all these properties measured at ambient temperature (20°C).

The different mixes had a water/cement ratio of 0.45, and the percentages of fine aggregate replacement with crumb rubber were 5%, 10% and 15%. The aggregate/cement ratio for all mixtures was fixed with a value of 4.7, while the coarse aggregate/fine aggregate ratio was fixed with a value of 0.5.

Figure 3-13 shows the results obtained by Bilal Nasar et al., as well as the linear relationship between thermal conductivity and hardened density with its corresponding value of the coefficient of determination, which has a value close to 1, meaning that the experimental results adjust to the proposed equation.

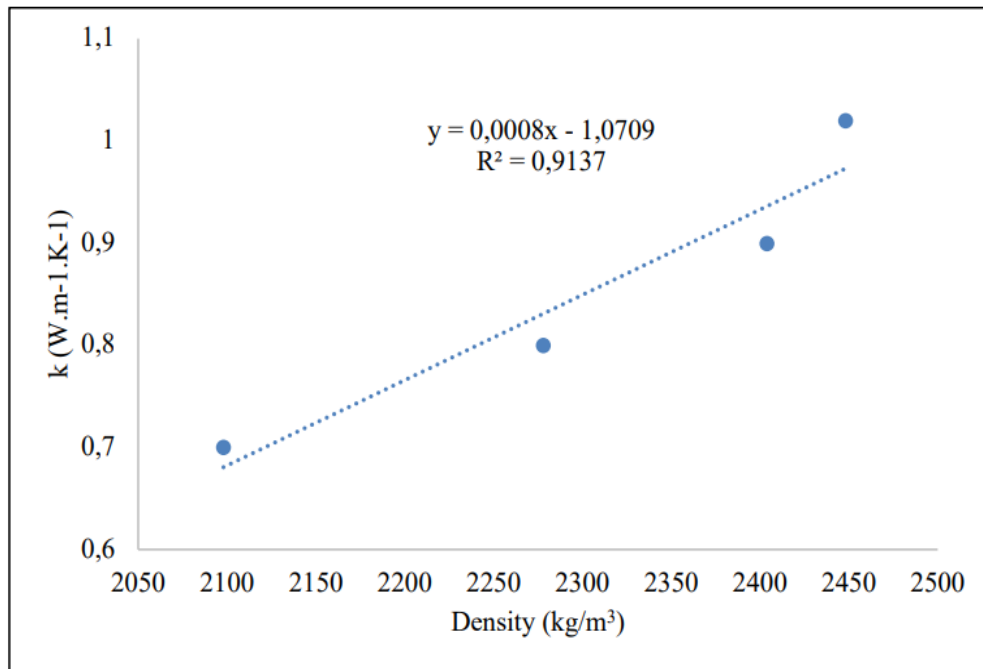


Figure 3-13. Variation of thermal conductivity as a function of hardened density of concrete  
(Bilal Nasar et al., 2020a).

Since the proposed relationship is at room temperature, it is possible to predict the value of the thermal conductivity at room temperature ( $\lambda_{c0}$ ) for each one of the samples from the study made by Ling.. Table 3-1 summarises the values of thermal conductivity for each rubber concrete mix from Ling.

Table 3-1. Thermal conductivity as function of density of various rubber concrete mixes, based on results obtained by Ling.

Rubber Content	w/c	Density [kg/m³]	Thermal Conductivity [W/m·K]
0%	0.45	2156	0.654
	0.5	2178	0.672
	0.55	2211	0.698
5%	0.45	2137	0.639
	0.5	2164	0.660
	0.55	2183	0.676
10%	0.45	2114	0.620
	0.5	2143	0.644
	0.55	2165	0.661
15%	0.45	2100	0.609
	0.5	2156	0.654
	0.55	2173	0.668

20%	0.45	2076	0.590
	0.5	2117	0.623
	0.55	2140	0.641
25%	0.45	2057	0.575
	0.5	2119	0.624
	0.55	2132	0.635
30%	0.45	2015	0.541
	0.5	2068	0.584
	0.55	2093	0.604
40%	0.45	1999	0.528
	0.5	2053	0.572
	0.55	2082	0.595
50%	0.45	1991	0.522
	0.5	2014	0.540
	0.55	2025	0.549

As well as for the density, the prediction of the thermal conductivity, at different temperatures, was done with the equations proposed by Eurocode for lightweight concrete (equations (1.3 and (1.4).

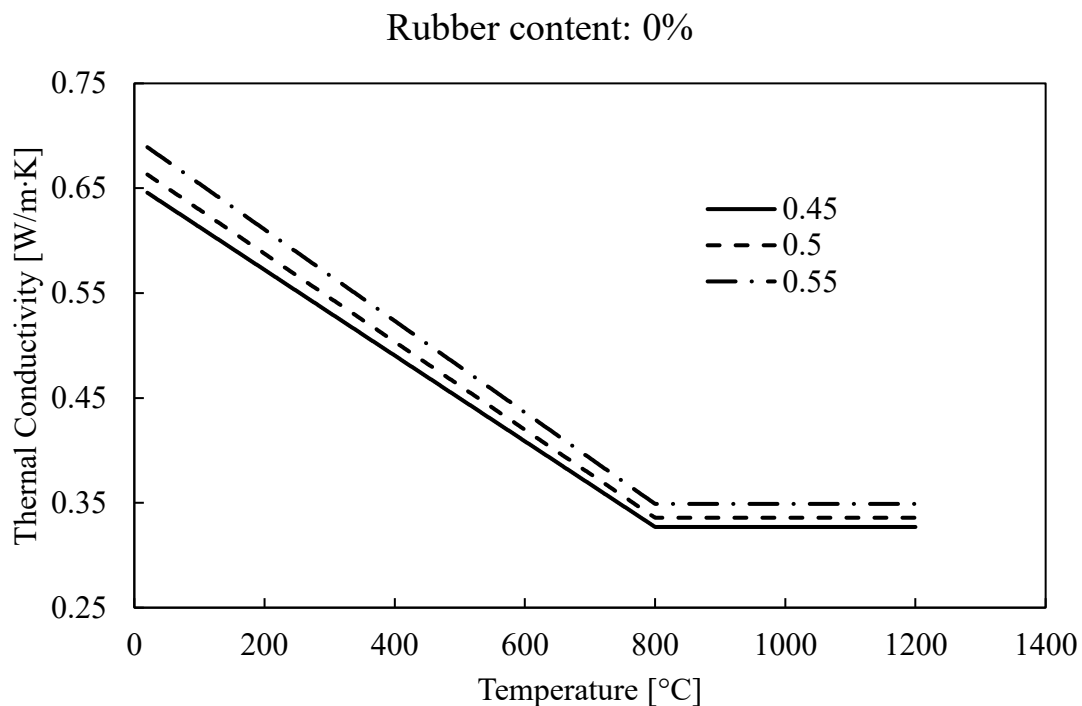


Figure 3-14. Thermal conductivity as function of temperature for 0% of rubber content.

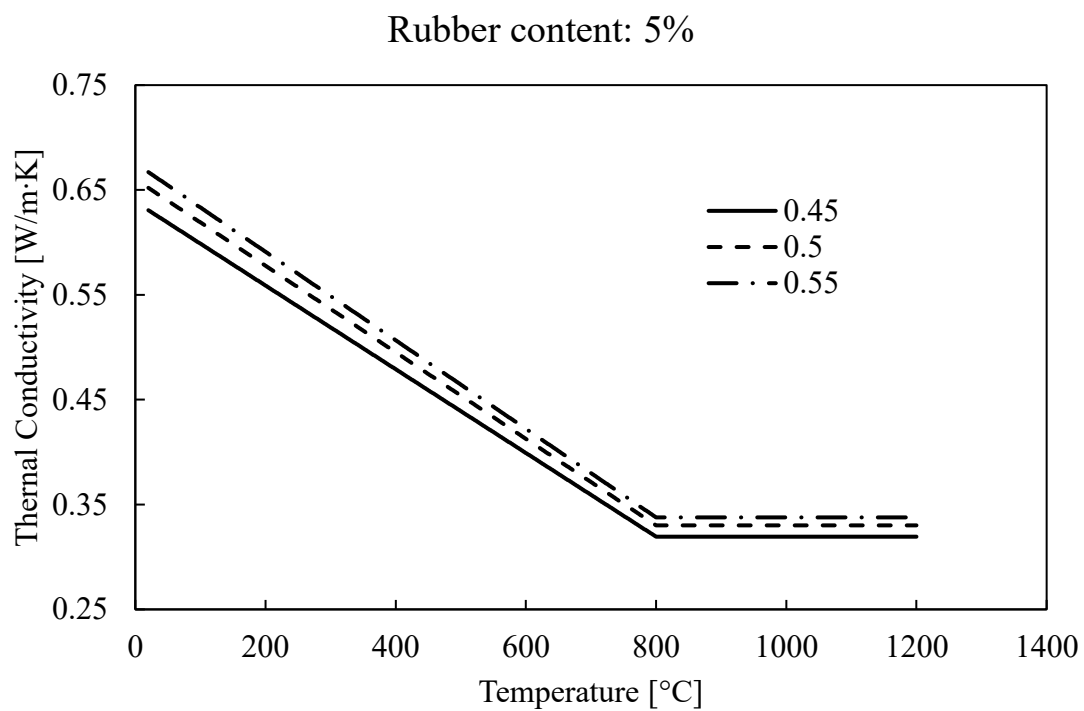


Figure 3-15. Thermal conductivity as function of temperature for 5% of rubber content.

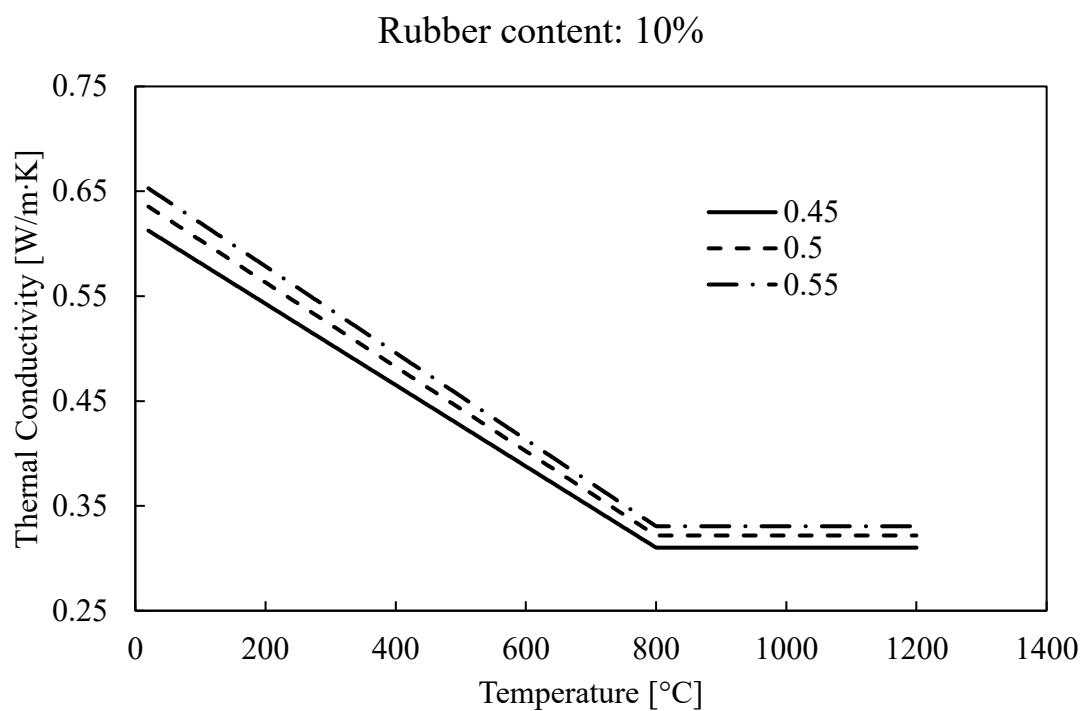


Figure 3-16. Thermal conductivity as function of temperature for 10% of rubber content.

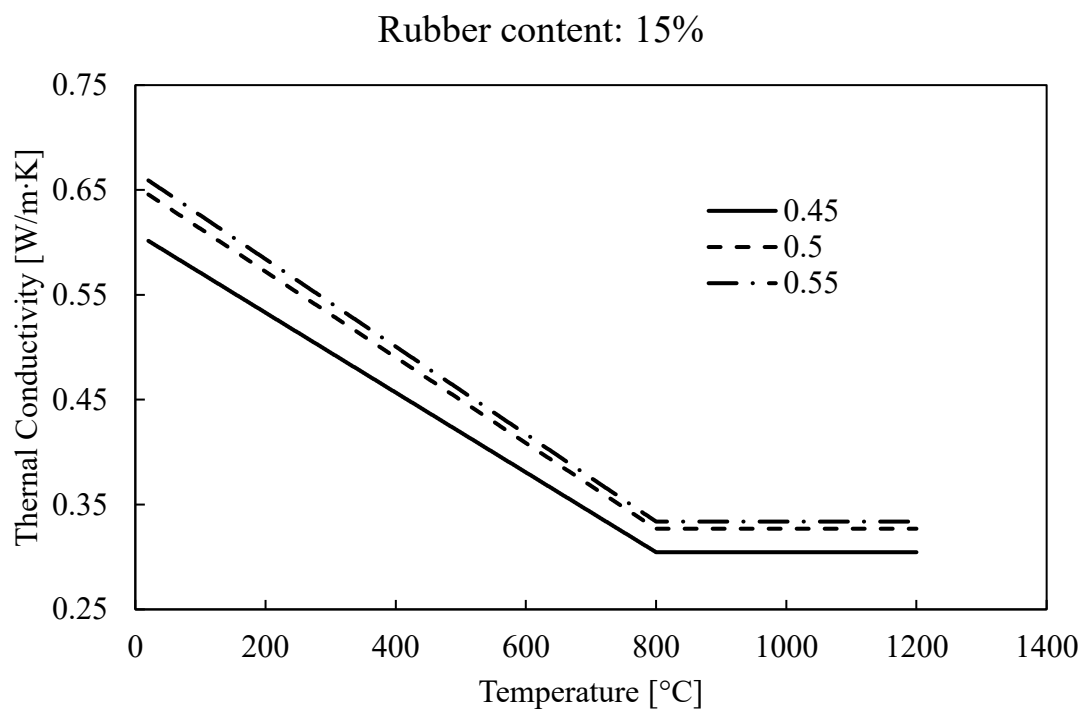


Figure 3-17. Thermal conductivity as function of temperature for 15% of rubber content.

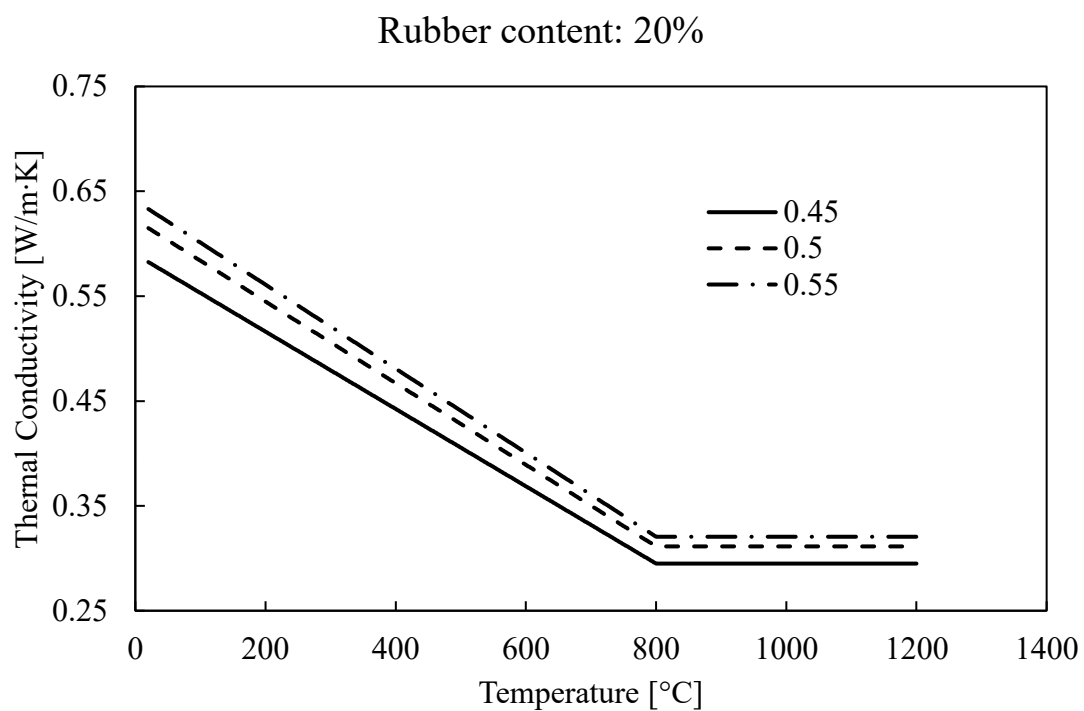


Figure 3-18. Thermal conductivity as function of temperature for 20% of rubber content.

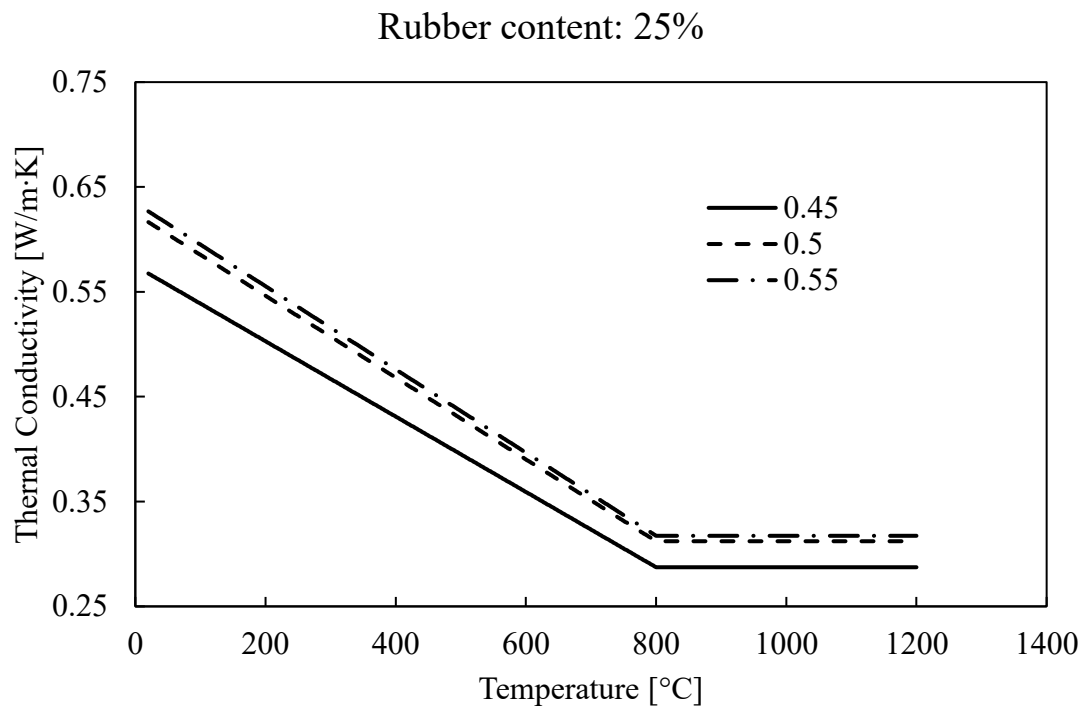


Figure 3-19. Thermal conductivity as function of temperature for 25% of rubber content.

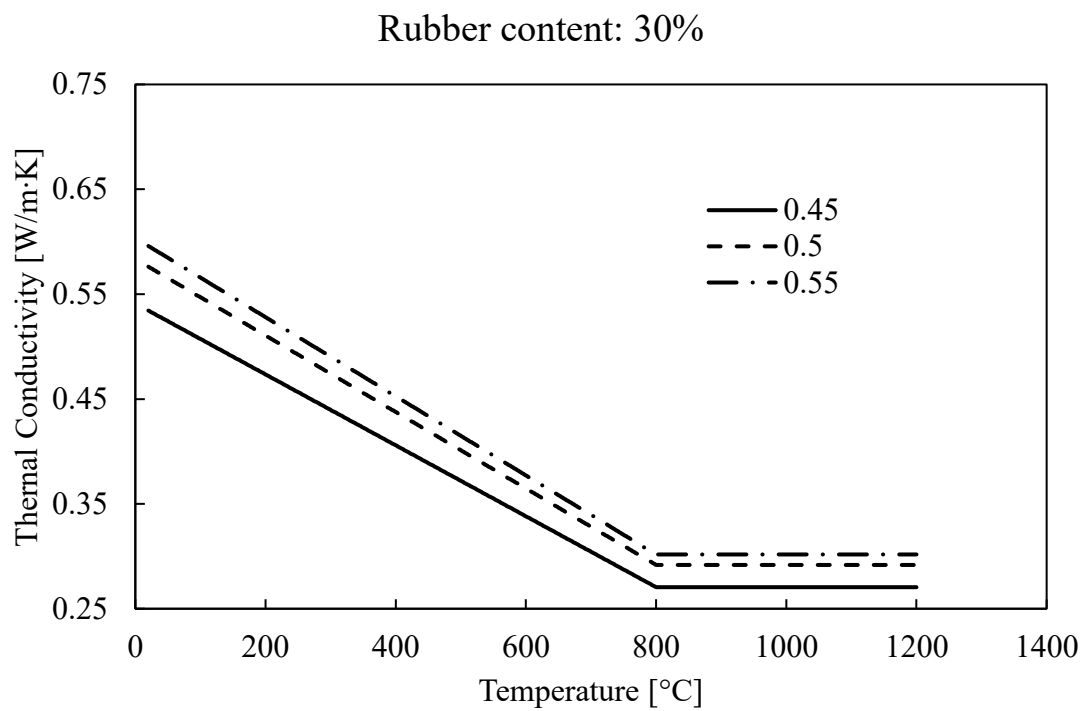


Figure 3-20. Thermal conductivity as function of temperature for 30% of rubber content.



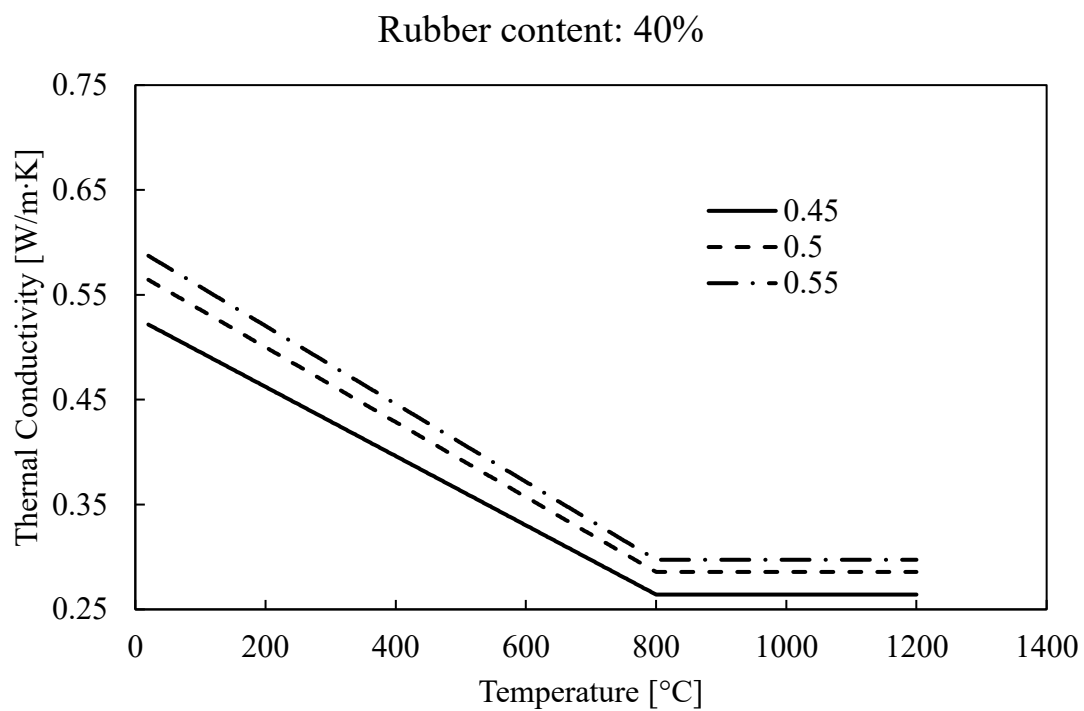


Figure 3-21. Thermal conductivity as function of temperature for 40% of rubber content.

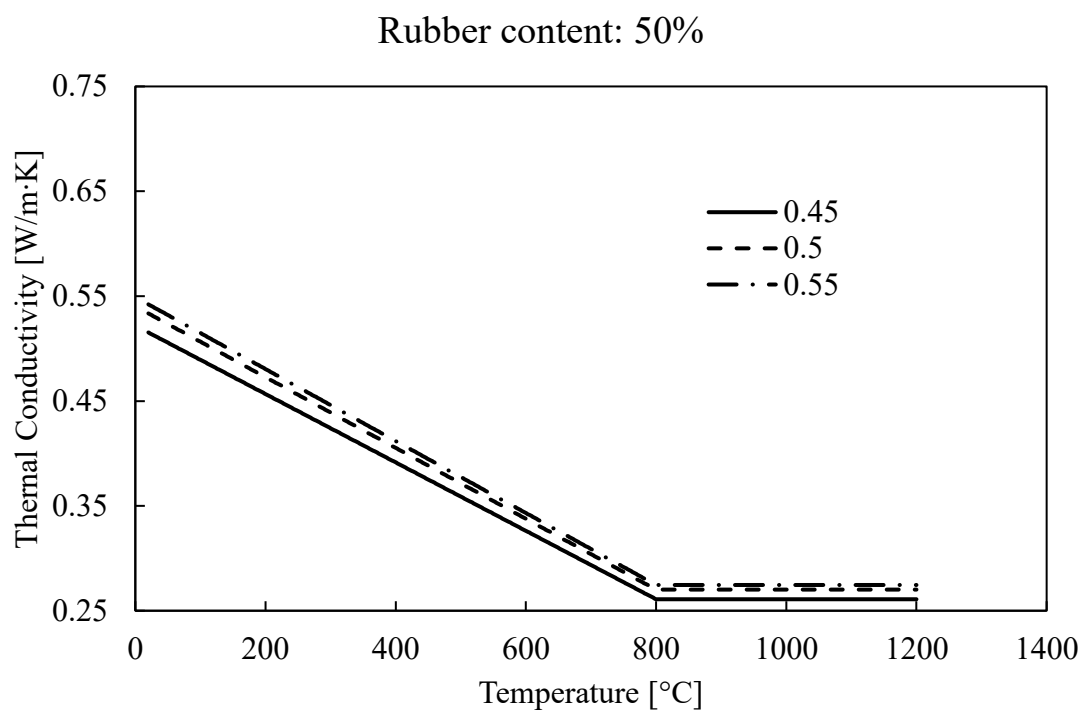


Figure 3-22. Thermal conductivity as function of temperature for 50% of rubber content.

### 3.3.3. Proposed specific heat data

For the specific heat of rubber concrete, two correlated research made by Najim et al. were consulted. In this experimental investigation, some of the final results were the values of density and thermal conductivity of rubber concrete, both in dry and saturated condition.

Three different water/cement ratios were considered (0.55, 0.51 and 0.48) For each one of the water/cement ratios, coarse or fine aggregate were replaced by 10%, 20% and 30% with crumb rubber. Aggregate/cement ratio was fixed with a value of 4.8 for all mixes and coarse aggregate/fine aggregate ratio was fixed with a value of 0.61.

Even though the study considers the replacement in both coarse and fine aggregate, for the matter of the present analysis and considering the conditions in the previous studies taken into account for the proposed data of density and thermal conductivity, just the results obtained for the mixtures where only the fine aggregate was replaced by crumb rubber were considered.

*Table 3-2. Results of density and specific heat for dry and saturated conditions (Najim et al., 2011).*

w/c	Rubber Content	Dry Density [kg/m <sup>3</sup> ]	Saturated Density [kg/m <sup>3</sup> ]	Dry Specific Heat [J/kg.°K]	Saturated Specific Heat [J/kg.°K]
0.55	0%	2288	2372	907	970
	10%	2113	2227	927	1019
	20%	2056	2179	948	1049
	30%	1913	2044	968	1083
0.51	0%	2296	2385	903	970
	10%	2162	2284	924	1020
	20%	2039	2179	944	1060
	30%	1878	2044	965	1112
0.48	0%	2311	2390	901	961
	10%	2179	2292	921	1010
	20%	2081	2217	942	1053
	30%	1934	2100	963	1107

In order to provide a relation between the density and the specific heat, the average values between dry and saturated conditions of both parameters were considered. The trend of the results resembles a linear relationship. The proposed equation for the specific heat as

function of the density, both at room temperature, and its corresponding coefficient of determination are shown in Figure 3-23.

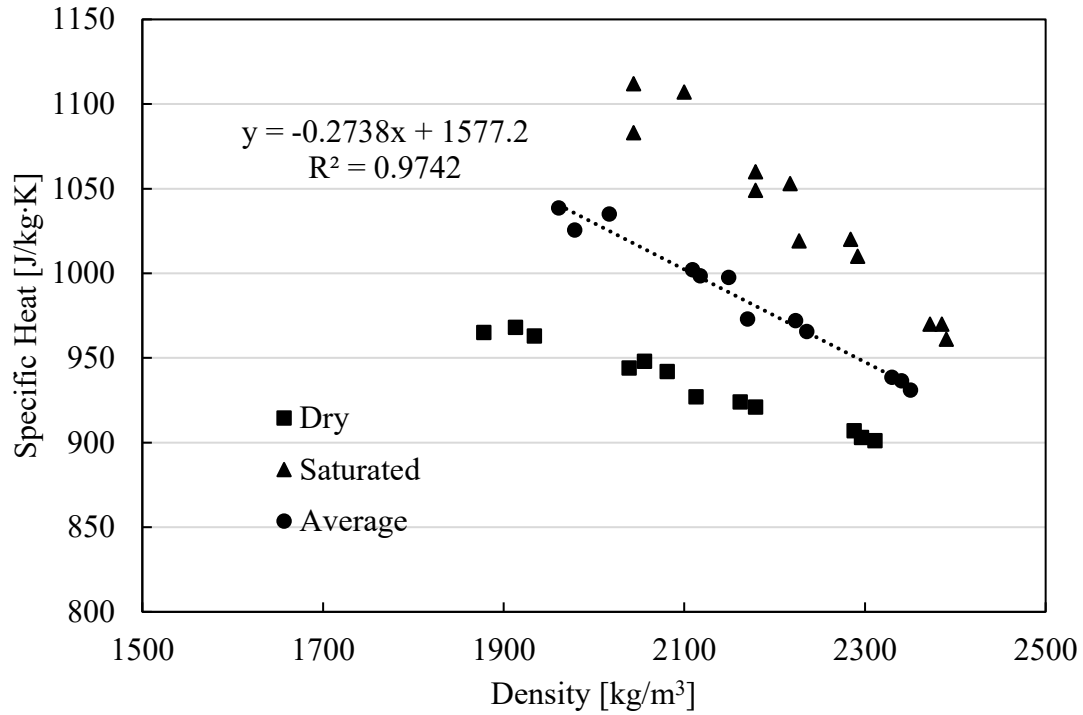


Figure 3-23. Variation of specific heat as a function of density of rubber concrete.

Recapitulating the procedure for the thermal conductivity data, for the variation of the specific heat capacity as function of the temperature, it is proposed the use of the equations given by the Eurocode, considering the specific heat at ambient temperature calculated with the proposed equation as function of the density.

Table 3-3. Specific heat as function of density of various rubber concrete mixes, based on results obtained by Ling.

Rubber content	w/c	Density [kg/m³]	Specific Heat [J/kg·°K]
0%	0.45	2156	986.96
	0.5	2178	980.93
	0.55	2211	971.90
5%	0.45	2137	992.16
	0.5	2164	984.77
	0.55	2183	979.56
10%	0.45	2114	998.45
	0.5	2143	990.52
	0.55	2165	984.49

15%	0.45	2100	1002.29
	0.5	2156	986.96
	0.55	2173	982.30
20%	0.45	2076	1008.86
	0.5	2117	997.63
	0.55	2140	991.34
25%	0.45	2057	1014.06
	0.5	2119	997.09
	0.55	2132	993.53
30%	0.45	2015	1025.56
	0.5	2068	1011.05
	0.55	2093	1004.20
40%	0.45	1999	1029.94
	0.5	2053	1015.15
	0.55	2082	1007.21
50%	0.45	1991	1032.13
	0.5	2014	1025.83
	0.55	2025	1022.82

The variation of specific heat as function of temperature for all different mixes considered for the analysis are plot from Figure 3-24 to Figure 3-32. Even though Eurocode 4 suggests considering constant this parameter, and since there is no information of the test regarding the moisture content nor the pick specific heat for rubber concrete, it is decided to choose an intermediate case in which it is taken into account the variation of the specific heat and considering the peak value ( $C_{pu}$ ) equal to 0.

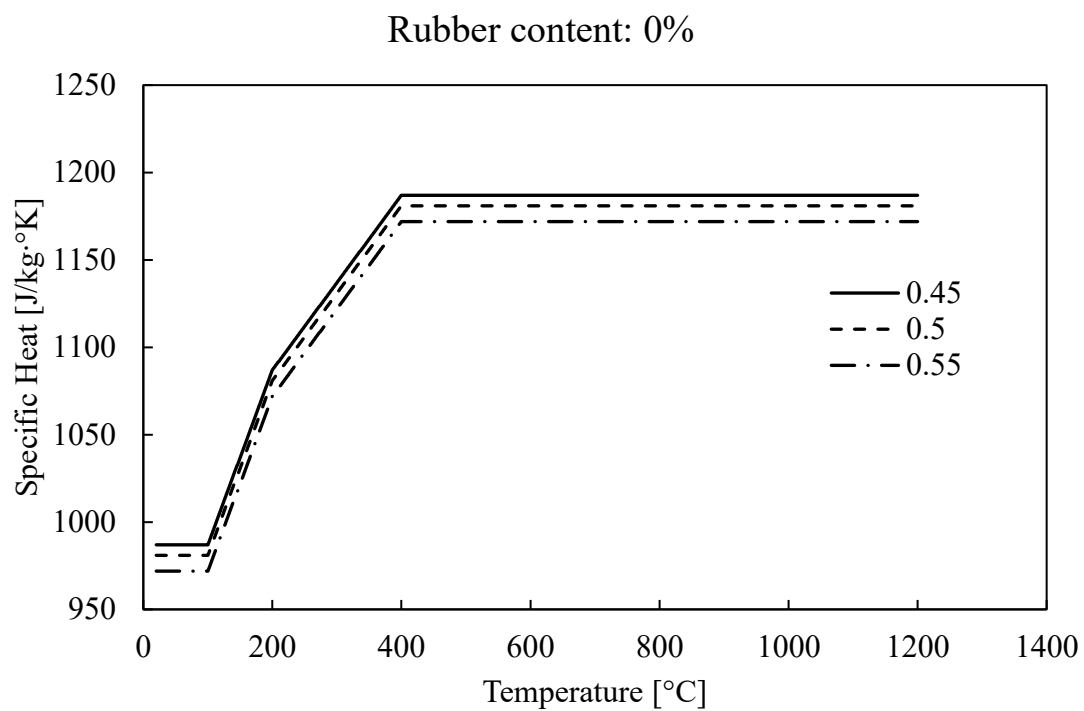


Figure 3-24. Specific heat as function of temperature for 0% of rubber content.

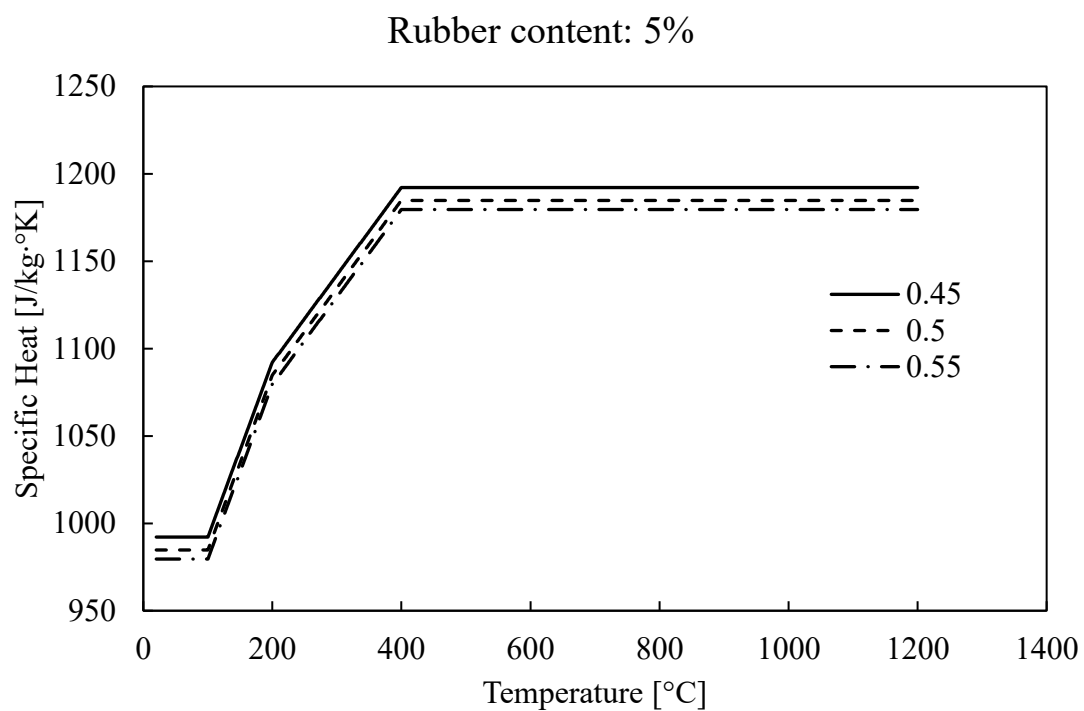


Figure 3-25. Specific heat as function of temperature for 5% of rubber content.

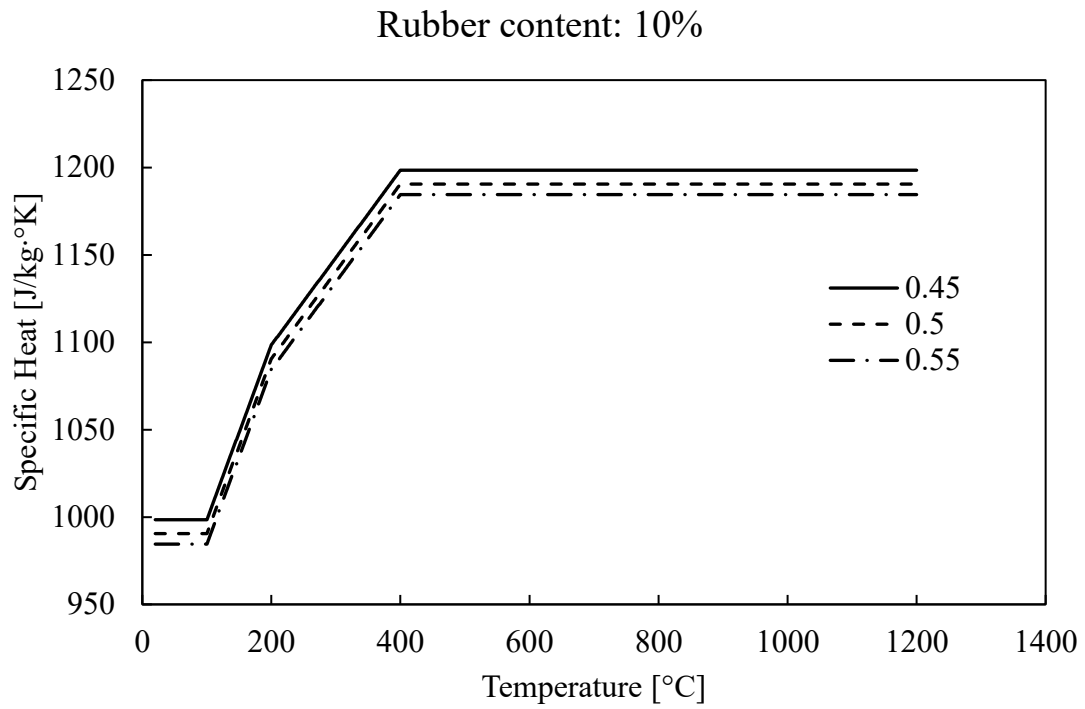


Figure 3-26. Specific heat as function of temperature for 10% of rubber content.

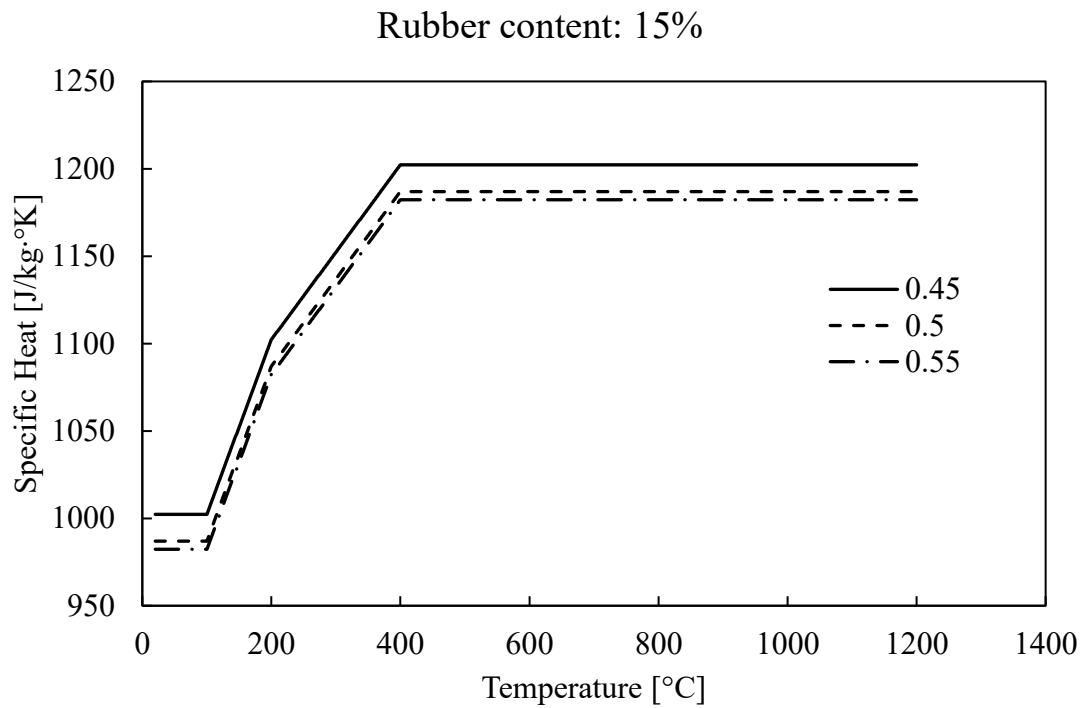


Figure 3-27. Specific heat as function of temperature for 15% of rubber content.

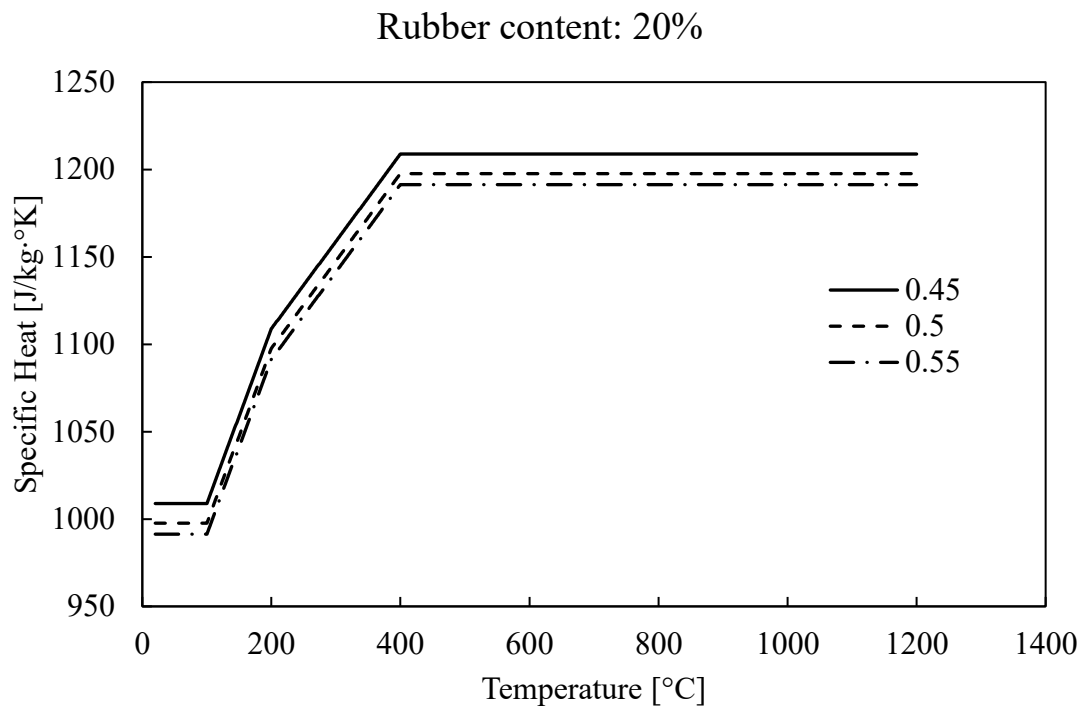


Figure 3-28. Specific heat as function of temperature for 20% of rubber content.

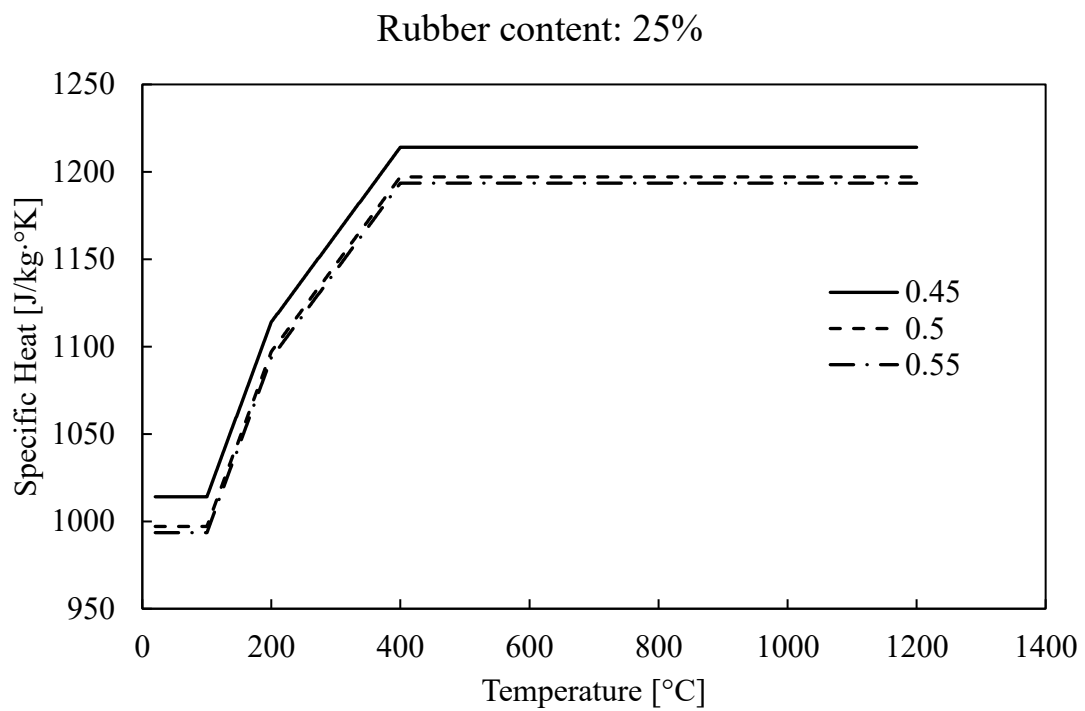


Figure 3-29. Specific heat as function of temperature for 25% of rubber content.

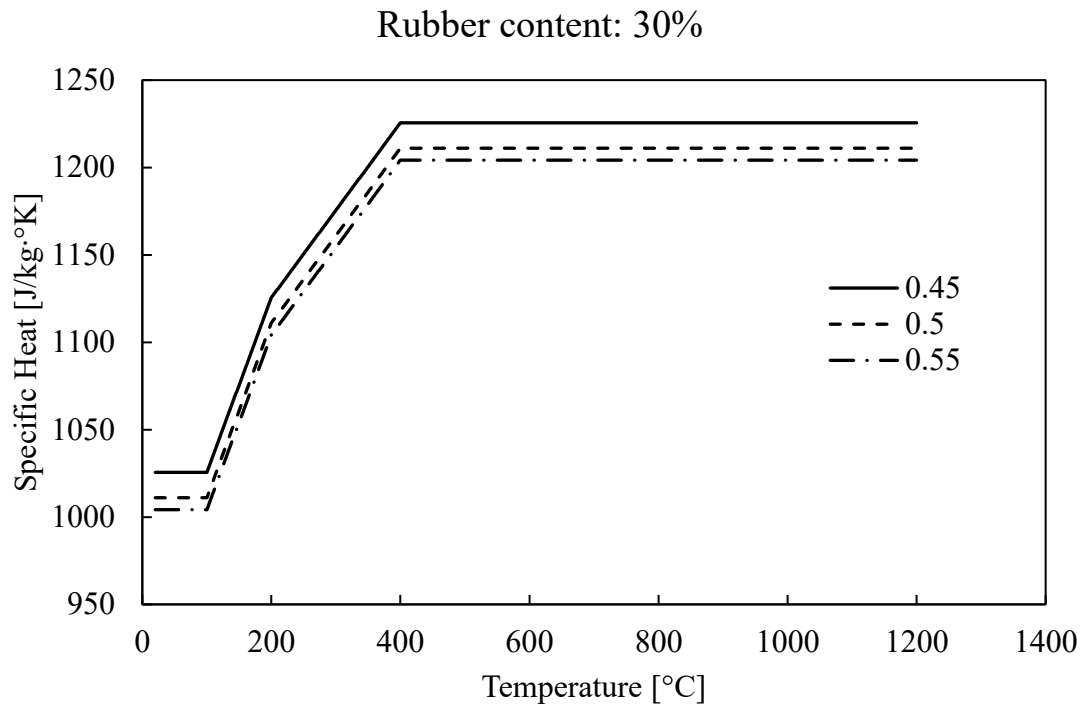


Figure 3-30. Specific heat as function of temperature for 30% of rubber content.

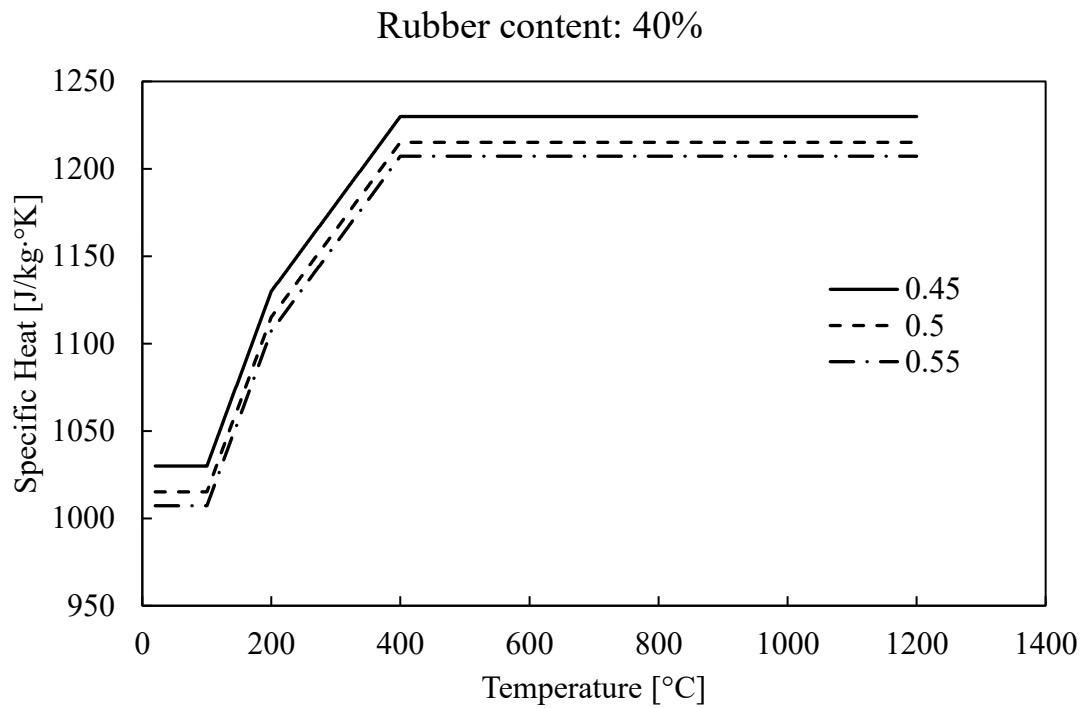


Figure 3-31. Specific heat as function of temperature for 40% of rubber content.



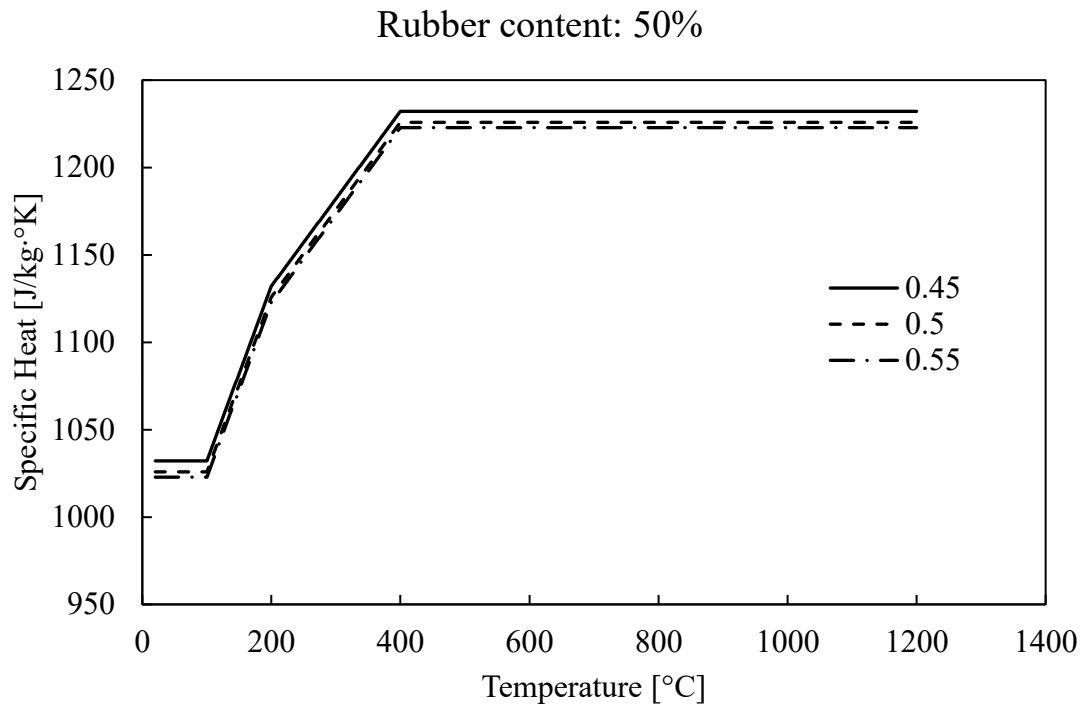


Figure 3-32. Specific heat as function of temperature for 50% of rubber content.

### 3.3.4. Compressive strength data

The compressive strength at ambient temperature employed for the analysis is taken from the same study used for the density data, carried out by Ling and is shown in Table 3-4.

Table 3-4. Compressive strength of different mixtures of rubber concrete by Ling.

Rubber Content	Compressive Strength [MPa]		
	w/c		
	0.45	0.5	0.55
0%	30.8	32.4	42.5
5%	30.1	35.4	35.0
10%	25.0	32.7	31.9
15%	23.3	28.2	29.5
20%	20.4	26.4	26.3
25%	19.9	24.8	22.8
30%	15.8	20.2	20.1
40%	10.5	15.4	16.3
50%	9.5	12.5	12.4

### 3.3.5. Choose data summary and comparison

In order to better understand the different characteristics of the different mixtures used for each one of the papers/investigations considered, Table 3-5 summarizes all

parameters, where column w/c refers to the water-cement ratio, agg./c to the aggregate-cement ratio, coarse/fine to the coarse-fine ratio, and replacement % to the percentage of fine aggregate replaced by crumb rubber.

*Table 3-5. Summary of reference literature for input data.*

Paper	Authors	Property	w/c	agg./ c	Coarse/ Fine	Replacement %
Prediction of density and compressive strength for rubberized concrete blocks	Tung-Chai Ling	Density and compressive strength	0.45 0.50 0.55	5.6	0.5	5 - 10 - 15 - 20 - 25 - 30 - 40 - 50
Enhancing Physical/Mechanical and Thermal Properties of Rubberized Concrete	Khan / Raja Bilal Nasar / Khitab / Anwar	Thermal conductivity	0.45	4.7	0.5	5 - 10 - 15
Transient thermal behaviour of crumb rubber-modified concrete and implications for thermal response and energy efficiency in buildings	Matthew R. Hall / Khalid B. Najim / Christina J. Hopfeb	Specific heat	0.48 0.51 0.55	4.8	0.61	10 - 20 - 30

For a further analysis between the different results obtained across the different research, as the density is the main parameter considered for the purposed data for the analysis, the results from Ling paper with the others is presented.

The percentage of variation of the density and the compressive strength between Ling and Bilal Nasar et al. papers is shown in Table 3-6. For both parameters, the maximum variation was for the control mix with 0% replacement of fine aggregate with crumb rubber, with a 13.5% variation for the density and an 8.8% variation for the compressive strength.

Table 3-6. Variation of density and compressive strength of rubber concrete, between Ling and Bilal Nasar et al. papers.

Rubber Content [%]	Density (Ling) [kg/m <sup>3</sup> ]	Density (Khan et. al.) [kg/m <sup>3</sup> ]	Compressive strength (Ling) [MPa]	Compressive strength (Khan et. al.) [MPa]	Density variation	Compressive strength variation
0	2156	2448	30.8	28.1	13.5%	8.8%
5	2137	2404	30.1	29.6	12.5%	1.7%
10	2114	2278	25	26.3	7.8%	5.2%
15	2100	2098	23.3	22.5	0.1%	3.4%

For the comparison with Najim et al. paper, it is just possible to contrast the values of the densities since this research does not perform compressive strength test and just focused on the thermal behaviour. Table 3-7 presents the comparison of both papers and the percentage of variation of the density, being 5.4% and 5.5% the two highest corresponding to the control mix and the one with 30% of fine aggregate replacement with crumb rubber.

Table 3-7. Variation of density of rubber concrete, between Ling and Najim et al. papers.

Rubber Content [%]	Density (Ling) [kg/m <sup>3</sup> ]	Density (Najim et. al.) [kg/m <sup>3</sup> ]	Density variation
0	2211	2330	5.4%
10	2165	2170	0.2%
20	2140	2117.5	1.1%
30	2093	1978.5	5.5%

### 3.4. Model definition

Using the software “IS Fuoco” developed by the company CDM Dolmen Srl, the analysis of the cross-section subjected to a fire scenario is performed, since the algorithm is based on the thermal and mechanical analysis described in the present chapter, as well as the required regulations. The definition of the model considers the geometry, the material, the type of exposure and the thermal properties.

#### 3.4.1. Materials

First of all, the mechanic and thermal material are defined. Regarding the mechanic materials, the value of the characteristic compressive strength is required by the program.

The other parameters have default values from the most recent Eurocode, for “cold” and “fire” conditions.

**Materiali Meccanici**

Caratteristiche Meccaniche | Analisi "a caldo"

Nome: RUB5\_45 - 30.1 MPa

f<sub>ck</sub>: 30.1

Gamma c: 1.5

Alfa cc: 0.85

Alfa ct: 1

Eurocodici + NTC18 ☒ Norma predefinita

Calcestruzzo

Altro ☐ Classe predefinita

Visualizza diagramma OK ☐ Salva i parametri come predefiniti per il lavoro corrente ☐ Salva i parametri come predefiniti in Custom Annulla

## Proprietà meccaniche RUB5\_45 - 30.1 MPa.

### Descrizione materiale.

Materiale: RUB5\_45 - 30.1 MPa. Normativa: Eurocodici + NTC18 - EN 1992-1-2 mar 2004.

La seguente tabella riassume le caratteristiche meccaniche.

f <sub>ck</sub> [N/mm <sup>2</sup> ]	30.1
ε <sub>c2</sub> [%]	0.2

Figure 3-33. Example of mechanic properties for mixture with 5% rubber content with  $w/c=0.45$ , CDM DOLMEN Srl.

**Materiali Meccanici**

Caratteristiche Meccaniche | Analisi "a caldo"

☐ EN 1992-1-2 gen 1998 (metodo semplificato) <

Gamma c,fi: 1 Alfa cc,fi: 1

Aggregato

☒ Siliceo ☐ Calcareo ☐ Leggero

☒ EN 1992-1-2 mar 2004 (metodo semplificato) <

Gamma c,fi: 1 Alfa cc,fi: 1

Aggregato

☒ Siliceo ☐ Calcareo

Eurocodici + NTC18 ☒ Norma predefinita

Calcestruzzo

Altro ☐ Classe predefinita

Visualizza diagramma OK ☐ Salva i parametri come predefiniti per il lavoro corrente ☒ Salva i parametri come predefiniti in Custom Annulla

## Proprietà meccaniche RUB5\_45 - 30.1 MPa.

### Descrizione materiale.

Materiale: RUB5\_45 - 30.1 MPa. Normativa: Eurocodici + NTC18 - EN 1992-1-2 mar 2004.

La seguente tabella riassume le caratteristiche meccaniche.

f <sub>ck</sub> [N/mm <sup>2</sup> ]	30.1
ε <sub>c2</sub> [%]	0.2

Figure 3-34. Example for thermal analysis parameters for mixture with 5% rubber content with  $w/c=0.45$ , CDM DOLMEN Srl.

Regarding the thermal materials, there must be introduced the values of the density, thermal conductivity, and specific heat as function of the temperature and established in section 3.3. The corresponding values can be found in Appendix B to Appendix D for each one of the different mixtures taken into account for the present analysis.

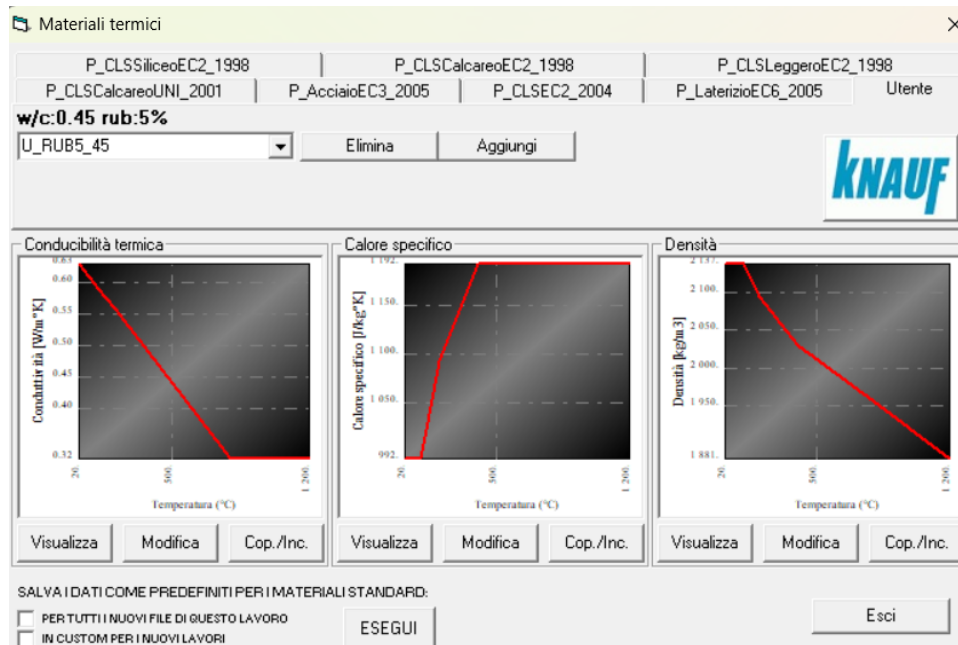


Figure 3-35. Example of thermal properties settings for mixture with 5% rubber content with  $w/c=0.45$ , CDM DOLMEN Srl.

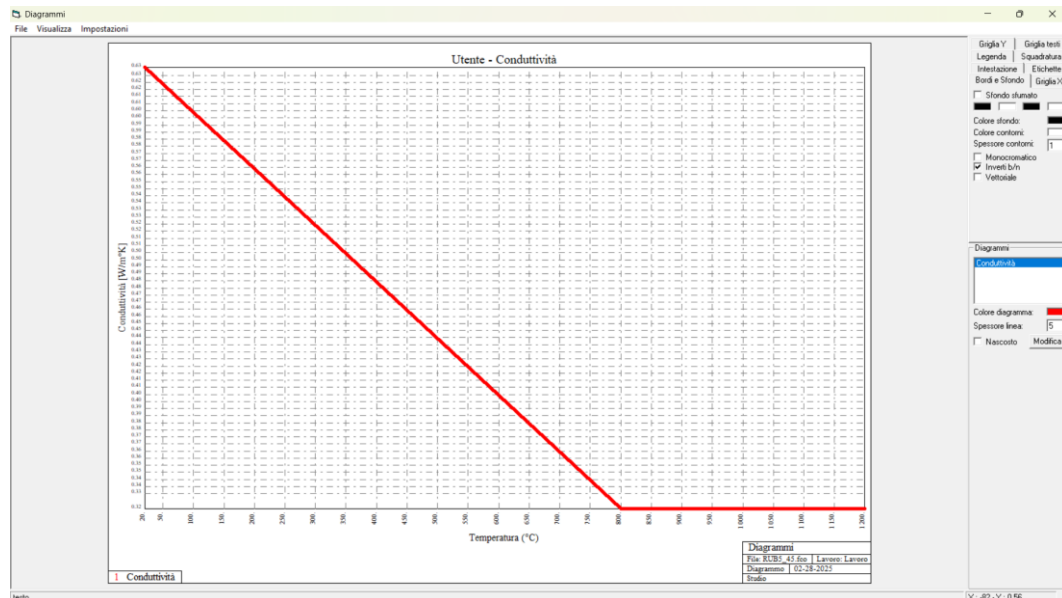


Figure 3-36. Example thermal conductivity graphic for mixture with 5% rubber content with  $w/c=0.45$ , CDM DOLMEN Srl.

### 3.4.2. Geometry

Once the materials are defined, the geometry is introduced in the program. When defining the geometry, it must be chosen the mechanic and thermal material composing the cross section. Then, introducing the dimensions of the cross section in the boxes for the desire geometry, the element is defined.

**SEZIONI STANDARD**

SEZIONE : 1 ANNULLA

**Descrizione Sezione :** Sez. 1 - Rettangolare

**Normativa :** Eurocodici + NTC16

**Materiale meccanico :** Calcestruzzo

**Classe materiale :** Altro

**Materiale termico :** Utente

**Materiale utente :** U\_RUB5\_45

**RETTANGOLARE DA INERZIA**

Jz = 1000000 OK

50 25

OK

Figure 3-37. Example of definition of the cross-section, CDM DOLMEN Srl.

Now, by setting the concrete cover, the diameter and the amount of longitudinal reinforcement, the complete cross section is defined.

**DATI FERRI** X

**AREE PUNTUALI (FERRI, CAVI, ECC...)**

E Numero Ferri: 8

	Z	Y	Ø	T	Area	Tipo materiale	Classe materiale	T	ε	T	N
1	22	22	14		1.539	Acciaio Barre	B450C		0		
2	7.333	22	14		1.539	Acciaio Barre	B450C		0		
3	-7.333	22	14		1.539	Acciaio Barre	B450C		0		
4	-22	22	14		1.539	Acciaio Barre	B450C		0		
5	22	3	16		2.011	Acciaio Barre	B450C		0		
6	7.333	3	16		2.011	Acciaio Barre	B450C		0		
7	-7.333	3	16		2.011	Acciaio Barre	B450C		0		
8	-22	3	16		2.011	Acciaio Barre	B450C		0		

AGGIUNGI AGG. MASCH. ELIM. ULT. ☐ Freccie

Figure 3-38. Example of definition of longitudinal reinforcement, CDM DOLMEN Srl.

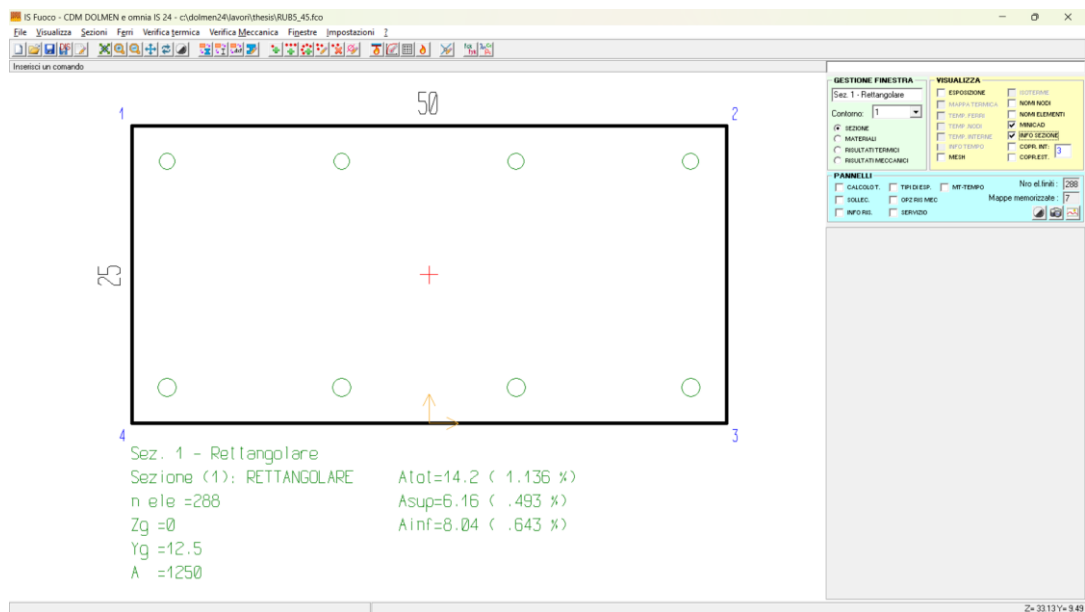


Figure 3-39. Example of cross-section with dimensions 50x25cm with reinforcement, CDM DOLMEN Srl.

### 3.4.3. Exposure

The software contains different types of exposure that can be assign to each one of the contours of the geometry. For the present analysis, as it was established before, the chosen exposure is the standard temperature-time curve from Eurocode and just to bottom surface of the element will be subjected to it. The top surface of the element will be exposed to the air at ambient temperature equal to 20°C.

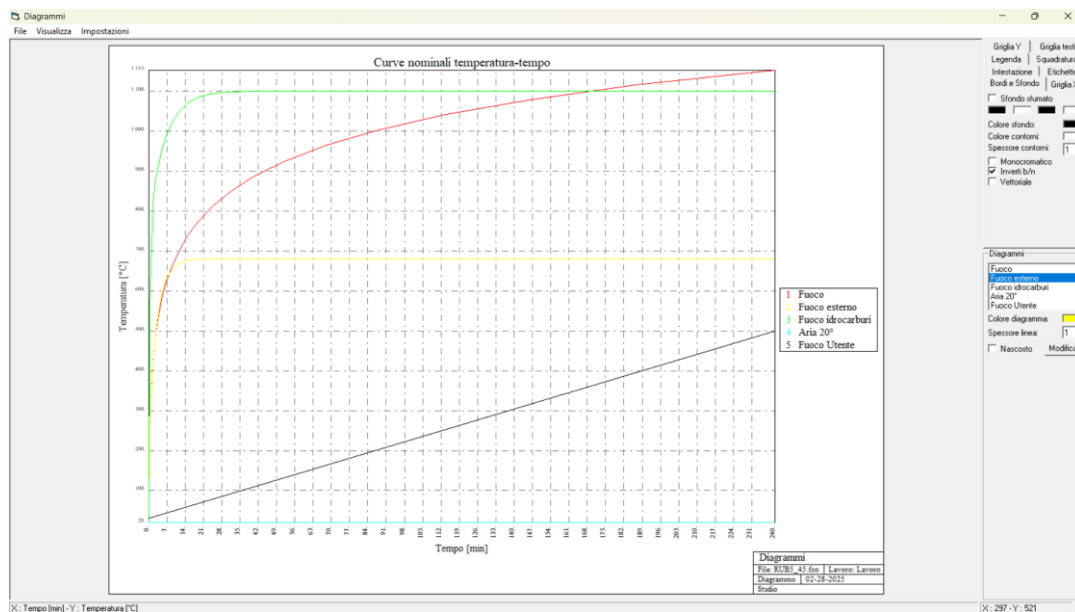


Figure 3-40. Types of exposure present in the software "IS Fuoco", CDM DOLMEN Srl.

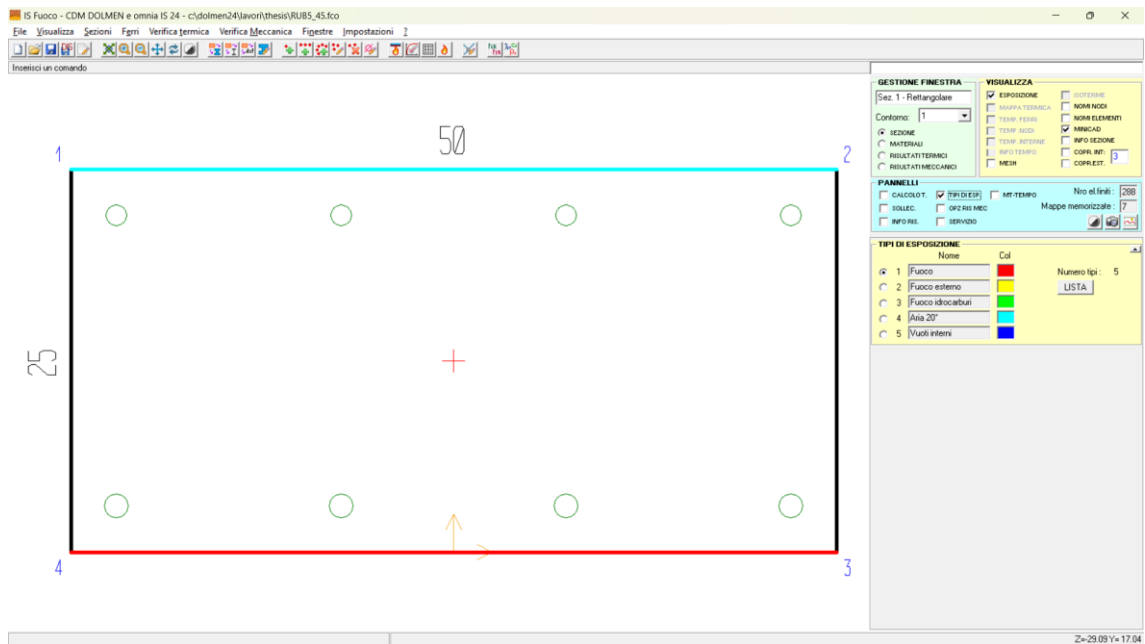


Figure 3-41. Assigned exposure to each surface of the cross-section, CDM DOLMEN Srl.

#### 3.4.4. Space-time discretization

The last thing before running the analysis is defining the mesh of the cross-section, which subdivides the member in finite elements. The program has different options for subdividing the cross-section. It is chosen a generic mesh, which creates a discretization with regular elements.

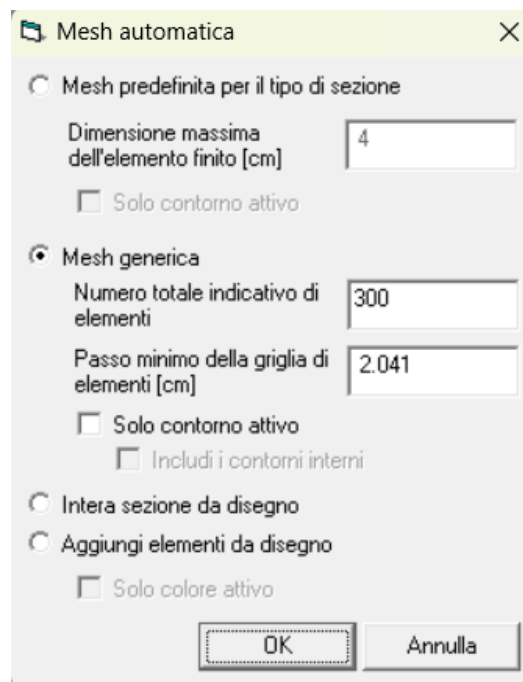


Figure 3-42. Mesh definition, CDM DOLMEN Srl.



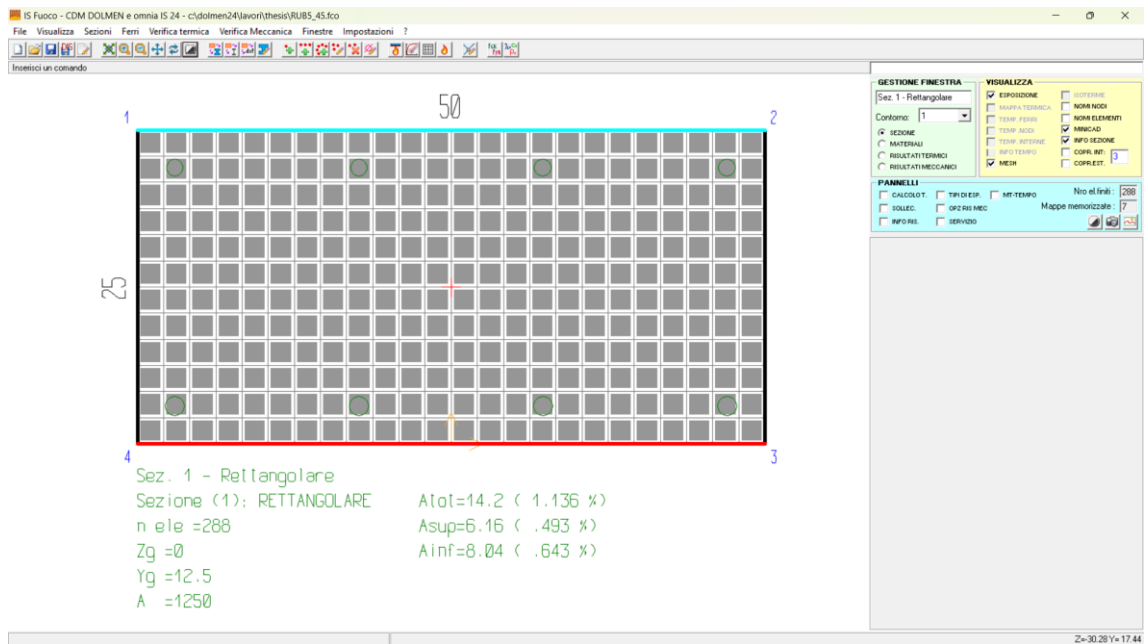


Figure 3-43. Complete cross-section defined, CDM DOLMEN Srl.

It must be defined the number of thermal maps (containing the isotherms), and the time interval between each one of them. For a fire with duration of 180 minutes it could be set a total of 6 thermal maps every 30 minutes (see Figure 3-44).

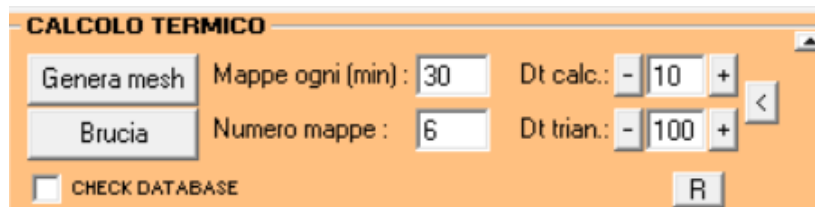


Figure 3-44. Time discretization for thermal maps of the cross-section, CDM DOLMEN Srl.

Once the member is completely defined, it is possible to proceed with the thermal and mechanical analysis.

### 3.4.5. Models resume

For each different mixture, a numerical model is done. Water-cement ratios of 0.45, 0.5 and 0.55 are analysed, having a control or reference mixture without any rubber content, and other 8 models varying the rubber content as 5%, 10%, 15%, 20%, 25%, 30%, 40% and 50% of fine aggregate replacement, for a total of 27 models.

*Table 3-8. Summary of models developed.*

Rubber content	Water-cement ratio		
	0.45	0.5	0.55
0%	REF_45	REF_50	REF_55
5%	RUB5_45	RUB5_50	RUB5_55
10%	RUB10_45	RUB10_50	RUB10_55
15%	RUB15_45	RUB15_50	RUB15_55
20%	RUB20_45	RUB20_50	RUB20_55
25%	RUB25_45	RUB25_50	RUB25_55
30%	RUB30_45	RUB30_50	RUB30_55
40%	RUB40_45	RUB40_50	RUB40_55
50%	RUB50_45	RUB50_50	RUB50_55

# 4. Results and Analysis

## 4.1. Case of study

In order to study the performance of rubber concrete at high temperatures, a cross section with dimensions of 50cm x 25cm is going to be analysed, with longitudinal reinforcement of 14 mm diameter at the top and 16 mm diameter at the bottom, with a concrete cover of 3 cm.

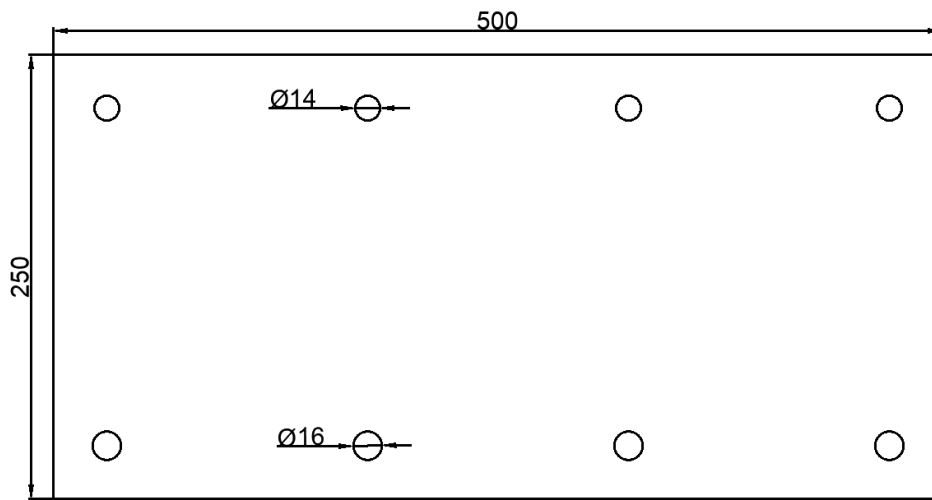


Figure 4-1. Cross section under analysis (dimensions in mm).

This cross section was selected due to the fact that a previous numerical analysis was performed to this section by the software company CDM Dolmen Srl and the results are available for comparison.

For different mixtures of rubber concrete, varying water-cement ratio and different rubber content, it is aimed to obtain the different isotherms across the transverse cross section of the element at different instants when subjected to a fire scenario following the standard temperature-time curve (see Figure 1-2), as well as its resistance to axial force and bending moment.

With the use of the program “IS FUOCO” provided by CDM Dolmen Srl, the thermal and mechanical analysis of the cross section is performed. The computation executed by this software is based on the Final Element Method (FEM), a numerical method for

solving differential equations, subdividing the element in smaller ones and denominated finite elements. This subdivision is called discretization and for this thesis, time discretization and space discretization in two dimensions is done.

#### 4.2. *Base analysis from CDM Dolmen Srl. comparison*

The analysis performed by CDM Dolmen Srl, was based on the paper “Numerical analysis of the thermomechanical behaviour of rubber concrete at high temperatures” by Karim Serroukh et al. This paper provides the characteristics and properties for a control mix without any rubber content, and 3 mixtures with rubber replacement of 10%, 20% and 30%, keeping a water-cement ratio of 0.49.

The properties for the thermal analysis (density, thermal conductivity, and specific heat) were considered constant, without any variation with the temperature. Table 4-1 summarises the values of the required properties used for the model.

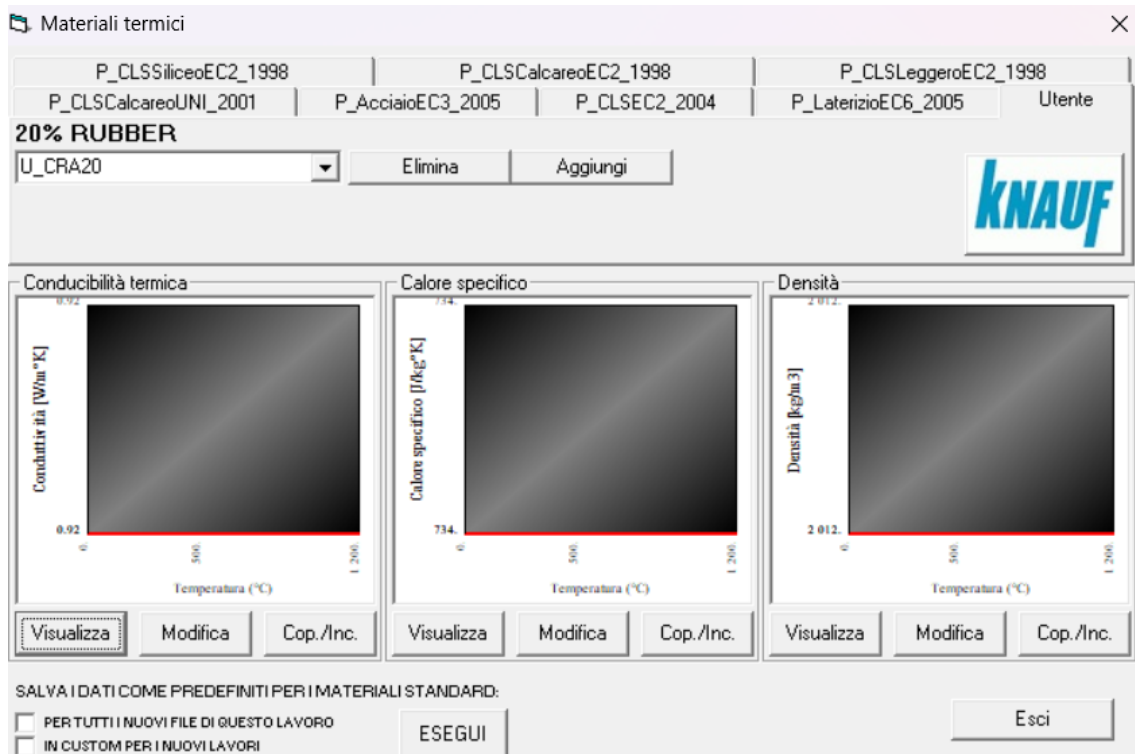


Figure 4-2. Thermal properties of CDM Dolmen analysis.

Table 4-1. Input properties from CDM Dolmen Srl analysis (Karim Serroukh et al., 2023c).

Rubber Content	Compressive Strength [MPa]	Thermal Cond. [W/m·°K]	Specific Heat [J/kg·°K]	Density [kg/m <sup>3</sup> ]
0%	63.4	1.680	653.34	2330

10%	49.5	1.270	706.23	2212
20%	35.7	0.920	734.05	2012
30%	22.5	0.510	752.45	1887

The results of the analysis were for the standard temperature-time curve, up to the first 90 minutes of the fire scenario.

*Table 4-2. Resistance to bending moment. Taken from “Analisi di Resistenza al Fuoco di Elementi in C.A. in Funzione di Diverse Percentuali di Aggregati in Gomma Utilizzando il Programma IS Fuoco” (Formica, 2023).*

	<b>M. Res.</b>	<b>M. Res.</b>	<b>M. Res.</b>	<b>M. Res.</b>	<b>M. Res.</b>
	(kNm)	(kNm)	(kNm)	(kNm)	(kNm)
	<b>Freddo</b>	<b>0'</b>	<b>30'</b>	<b>60'</b>	<b>90'</b>
<b>TR_CNA</b>	69.85	84.34	71.24	33.42	15.16
<b>TR_CRA10</b>	67.47	83.91	77.41	39.96	17.83
<b>TR_CRA20</b>	67.34	80.73	79.51	43.48	22.02
<b>TR_CRA30</b>	64.99	77.12	77.12	55.62	34.57

Since this analysis just considered mixtures with a water-cement ratio of 0.49, these results are compared only with the proposed models with water-cement ratio of 0.50 and for the corresponding percentage of rubber content.

*Table 4-3. Resistance to bending moment, in kN·m, from proposed models with w/c=0.50.*

<b>Rubber Content</b>	<b>Temperature</b>				
	<b>Cold</b>	<b>0</b>	<b>30</b>	<b>60</b>	<b>90</b>
0%	66.79	79.90	79.90	79.90	65.75
10%	66.84	79.97	79.97	79.97	66.84
20%	65.73	78.27	78.27	78.27	66.08
30%	64.54	76.42	76.42	76.42	65.94

As it can be seen from both analyses, at the beginning of the fire, the bending moment resistance of the section increases. However, for the proposed models, a reduction on this resistance is only noticeable after 90 minutes (see section 4.3.2. ). Therefore, it is difficult to make a proper comparison between both analyses. This difference could be explained by two main factors, the aggregate-cement ratio, and the thermal properties.

First of all, the aggregate-cement ratio from the models performed by Dolmen was 3.37 for all mixtures, which is significantly lower than the ratios from the chosen papers for the proposed models. As mentioned throughout the present document, the thermal and mechanical behaviour of any concrete is highly influenced by its composition, therefore,

having different aggregate-cement ratios might have caused a change in the properties of the analysed elements and consequently, in the resistance. This argument is strongly supported by the second factor, which is the actual values of the thermal properties.

From the paper made by Karim Serroukh et al., the thermal conductivity of the control concrete is  $1.68 \text{ W/m}\cdot\text{K}$  and the specific heat is  $653.34 \text{ J/kg}\cdot\text{K}$ , while for the paper by Bilal Nasar et al., the thermal conductivity has a value of  $1.02 \text{ W/m}\cdot\text{K}$  and from Najim et al. paper the specific heat in dry condition is  $907 \text{ J/kg}\cdot\text{K}$  and for saturated condition  $970 \text{ J/kg}\cdot\text{K}$ .

It is noticeable that the difference between the concrete parameters used for Dolmen analysis and the base papers for the proposed models of the present thesis is considerable. The thermal conductivity is the property that defines how the heat flows through a material, while the specific heat indicates the amount of energy required to rise its temperature. From Dolmen models the thermal conductivity is higher and the specific heat is lower in comparison with the ones from the chosen research therefore, the heat flows through the section easily and it requires much lower energy to increase its temperature, explaining why a reduction in the bending moment resistance is just noticeable after 90 minutes, in the case of the proposed models. This effect can be easily appreciated with the thermal maps, indicating different isotherms and the temperature of the reinforcement.

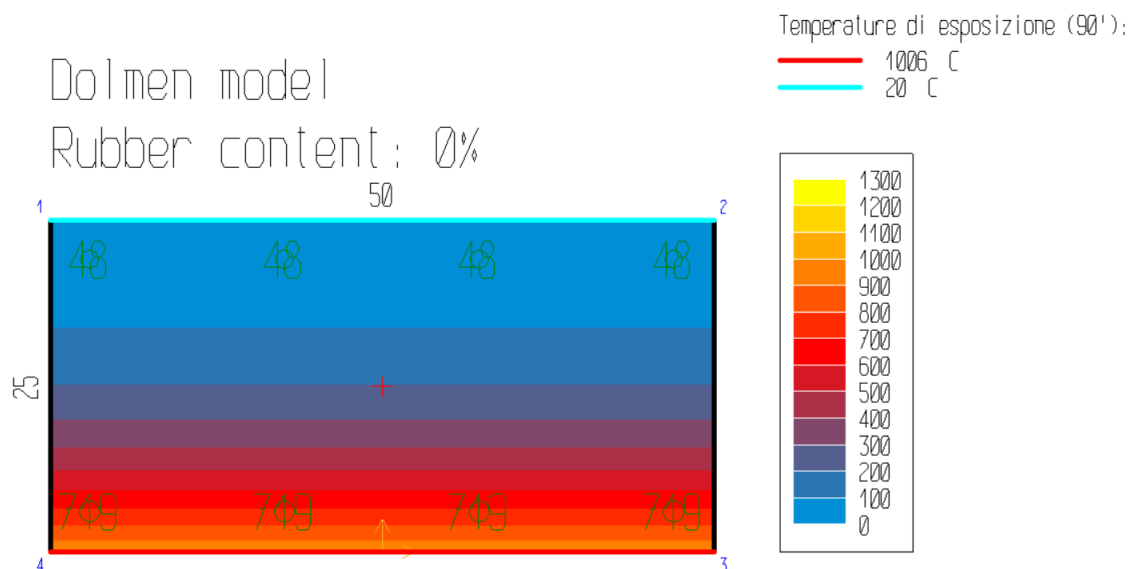


Figure 4-3. Thermal map from CDM Dolmen model without rubber content.

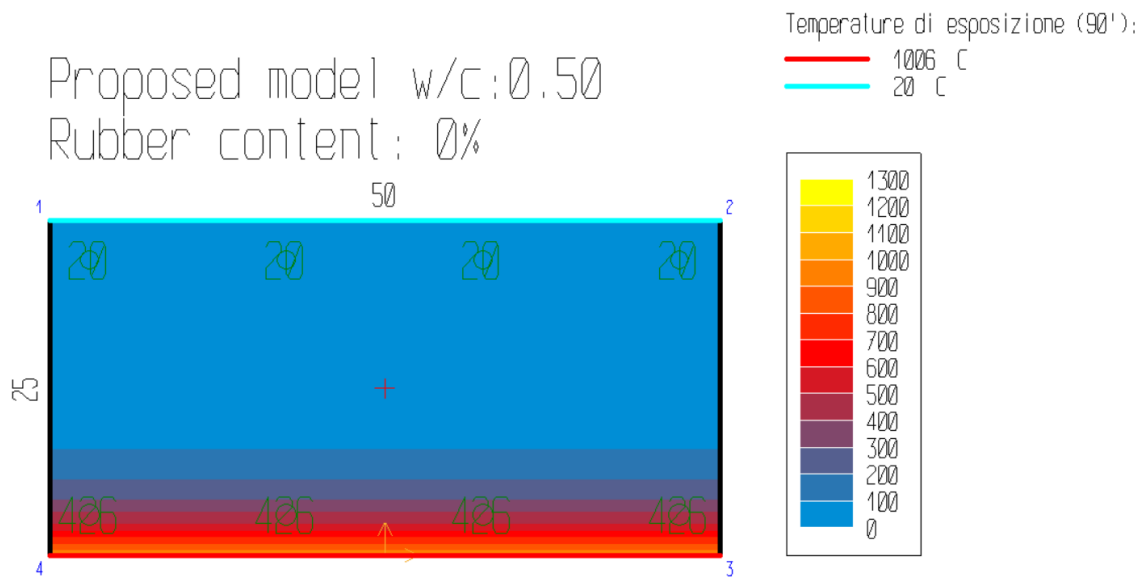


Figure 4-4. Thermal map from proposed model with w/c=0.5 without rubber content.

As it can be seen from Figure 4-3 and Figure 4-4, for the CDM Dolmen model, isotherms are more distributed along the cross section while in the proposed model the isotherms are concentrated near the exposed surface. Additionally, the bottom reinforcement reached a temperature of 719°C for the first case, while for the second case a temperature of 426°C, for a 90-minute exposure. In general, this trend of the results between both analyses is the same for different rubber content. Dolmen models have a more extended distribution of the temperature, and the reinforcement reaches higher temperatures in comparison with the proposed models. Additionally, the top reinforcement reached a temperature of 48°C in the Dolmen model, while in the proposed model, it remained at ambient temperature.

Regarding the variation in rubber content, for both models, when it increases, heat flows with more difficulty and rubber concrete reaches lower temperatures at specific moments during the fire scenario. As an example, for a 90-minute exposure and a rubber content of 30%, longitudinal reinforcement reached temperatures of 581°C in CDM Dolmen model and 408°C in proposed models (see Figure 4-5 and Figure 4-6).

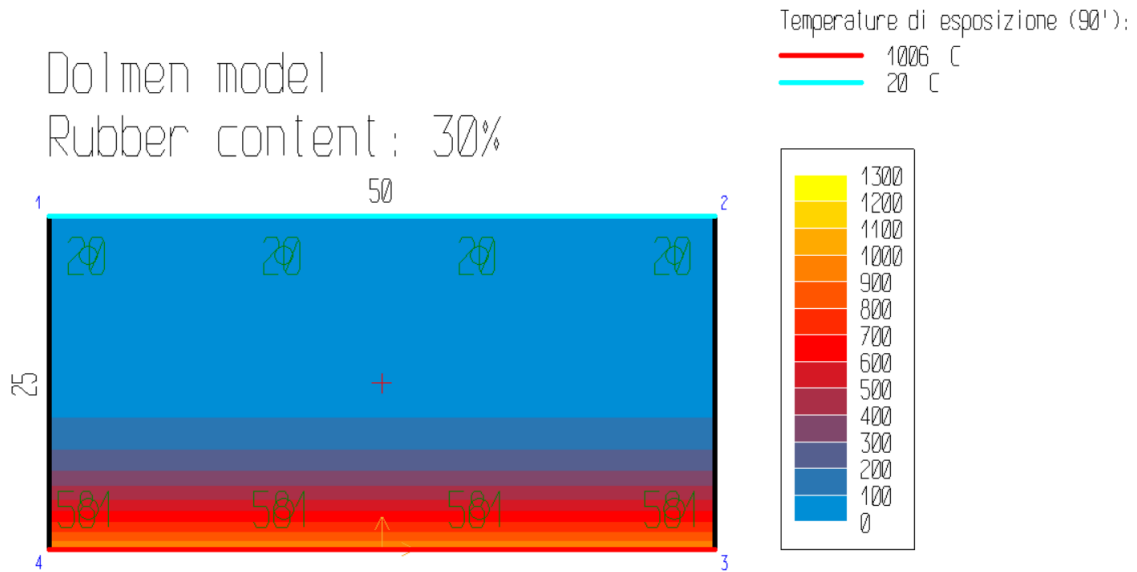


Figure 4-5. Thermal map from CDM Dolmen model with 30% of rubber content.

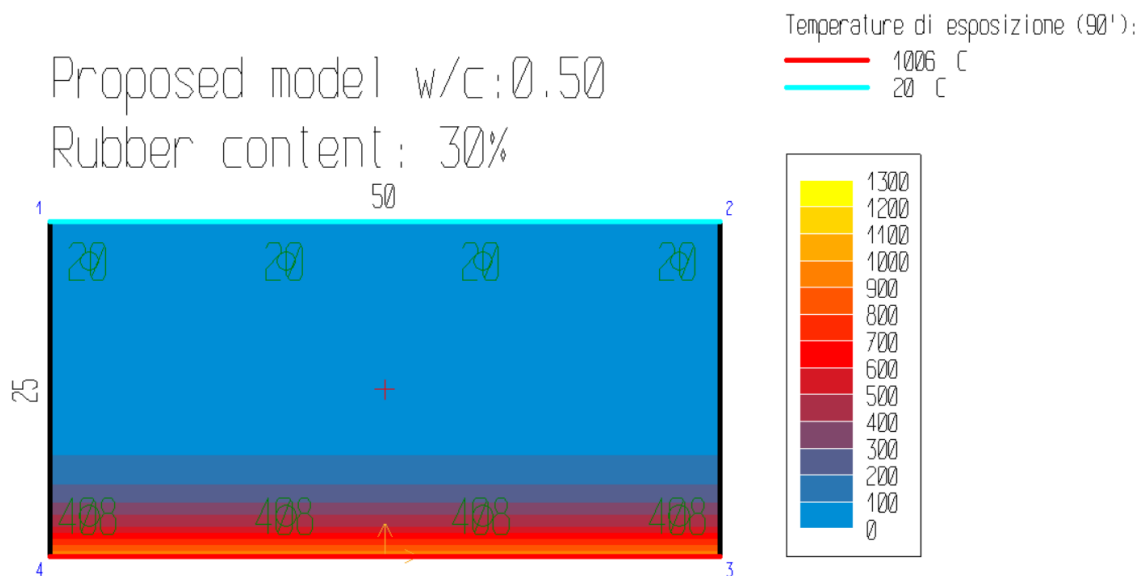


Figure 4-6. Thermal map from proposed model with w/c=0.5 with 30% rubber content.

From this comparison, it is possible to see the effect of the initial parameters taken into account for the analysis and it is also evident the influence of the composition of the concrete mixture when determining its mechanical and thermal properties.

For a more detailed analysis of the effect of rubber content in concrete, a longer exposure to fire is required for the proposed models. Therefore, a 180-minute exposure is chosen for a more complete analysis.



### 4.3. Proposed models

Three main values were considered for the analysis of rubber concrete with different compositions: bending moment resistance, axial resistance, and temperature of reinforcement.

#### 4.3.1. Temperature of reinforcement

From Figure 4-7 to Figure 4-10, the results of the temperature of the bottom reinforcement are plotted (for results in detail, see Table E-5, Table E-6, Table E-7 and Table E-8). In general, the temperature of the bottom reinforcement, which is the one closer to the fire exposure, always increases. Additionally, the rate in which the temperature of the reinforcement increases, is lower when the content of rubber increases.

This trend indicates that rubber has an insulating effect on the concrete, providing more protection for the reinforcement, against elevated temperatures.

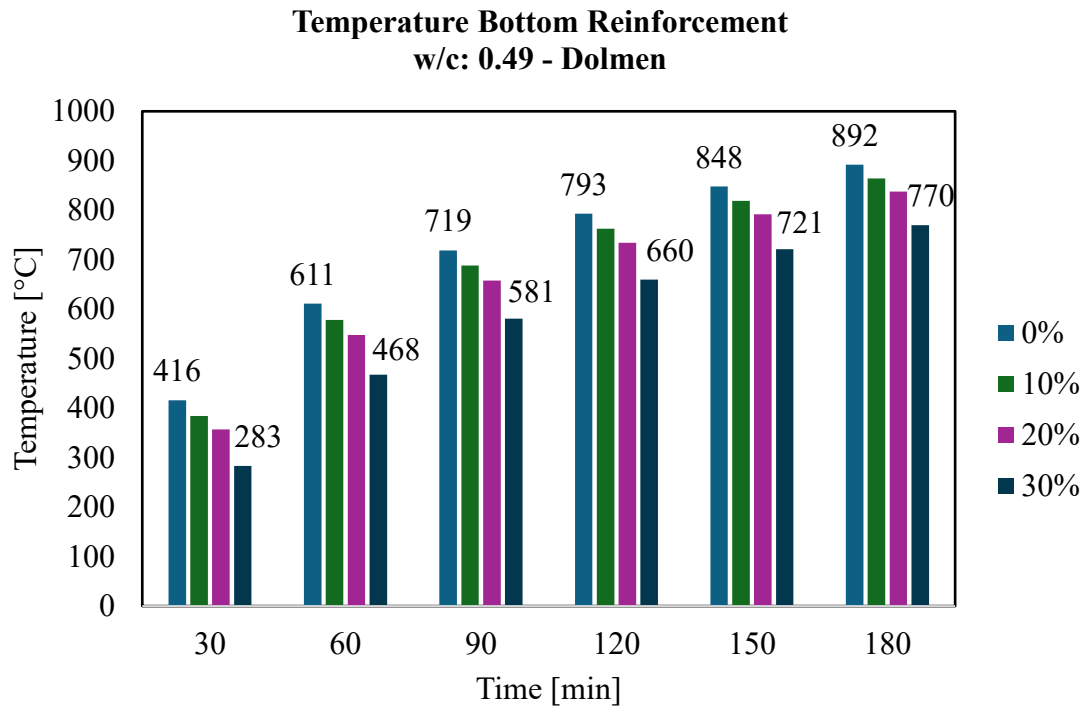


Figure 4-7. Temperature of reinforcement in rubber concrete with different rubber content, Dolmen Models.

Now, comparing the effect of different water-cement ratios, when it increases, the temperature of the reinforcement slightly increases, but its barely noticeable. As an example, for the control concretes (without rubber content) with water-cement ratios of

0.45, 0.50 and 0.55 the bottom reinforcement reached temperatures equal to 423°C, 426°C and 431°C respectively, for a 90-minute exposure; while for the concretes with higher rubber content (50%) the corresponding temperatures were 394°C, 398°C and 400°C. Even though the water content of the initial mixtures influences on the final temperature of the reinforcement, rubber content effect is more dominant. Table 4-4, shows in detail, for two representative exposures (90 and 180 minutes) the percentage of reduction of temperature of the reinforcement when replacing fine aggregate with crumb rubber. For a 50% of rubber content, the mean reduction of the temperature was 6.9% and 5.6% for a 90-minute and 180-minute exposure, respectively.

*Table 4-4. Percentage of temperature reduction of bottom reinforcement in comparison with control concrete (without rubber content).*

Rubber Content	0.45		0.5		0.55		Mean value	
Time	90	180	90	180	90	180	90	180
5%	0.7%	0.7%	0.5%	0.5%	0.9%	0.8%	0.7%	0.7%
10%	1.7%	1.3%	1.2%	1.2%	1.6%	1.3%	1.5%	1.3%
15%	2.1%	1.9%	0.7%	0.7%	1.2%	1.0%	1.3%	1.2%
20%	3.1%	2.5%	2.1%	1.8%	2.6%	2.0%	2.6%	2.1%
25%	4.0%	3.2%	2.1%	1.8%	2.8%	2.3%	3.0%	2.5%
30%	5.9%	4.7%	4.2%	3.5%	4.2%	3.5%	4.8%	3.9%
40%	6.6%	5.4%	4.7%	4.0%	4.6%	3.8%	5.3%	4.4%
50%	6.9%	5.6%	6.6%	5.4%	7.2%	5.8%	6.9%	5.6%

Since the reinforcement reaches lower temperatures with higher content ratios, this means that it remains structurally effective for a longer time, preserving its mechanical properties.

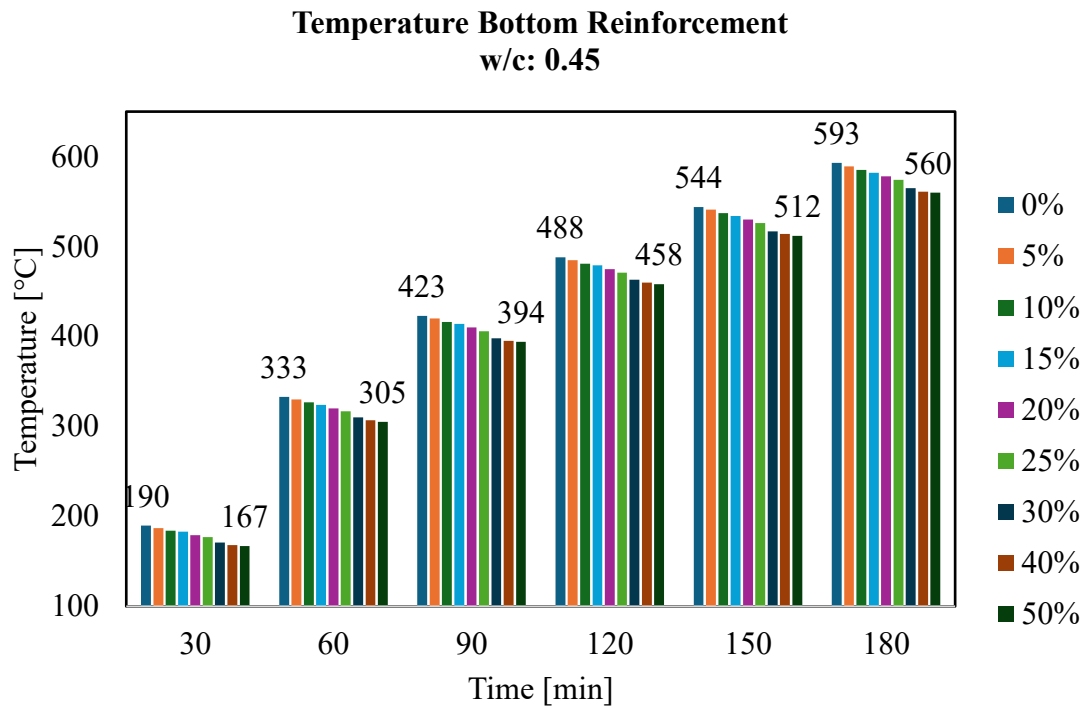


Figure 4-8. Temperature of reinforcement in rubber concrete with different rubber content, proposed models with w/c=0.45.

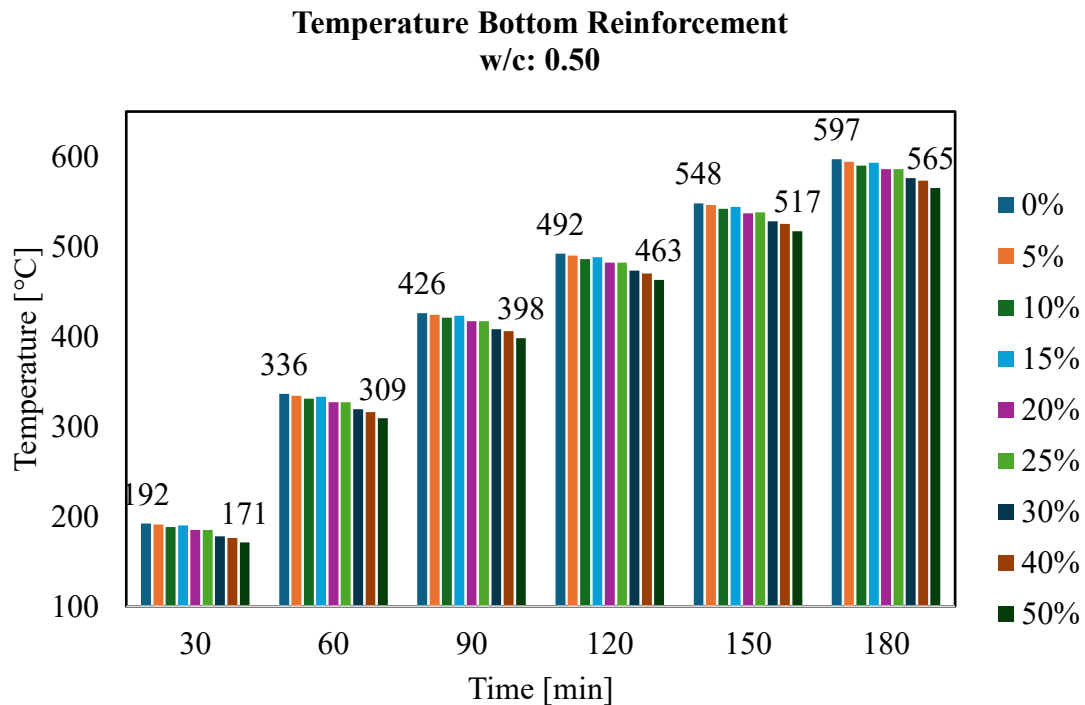


Figure 4-9. Temperature of reinforcement in rubber concrete with different rubber content, proposed models with w/c=0.50.

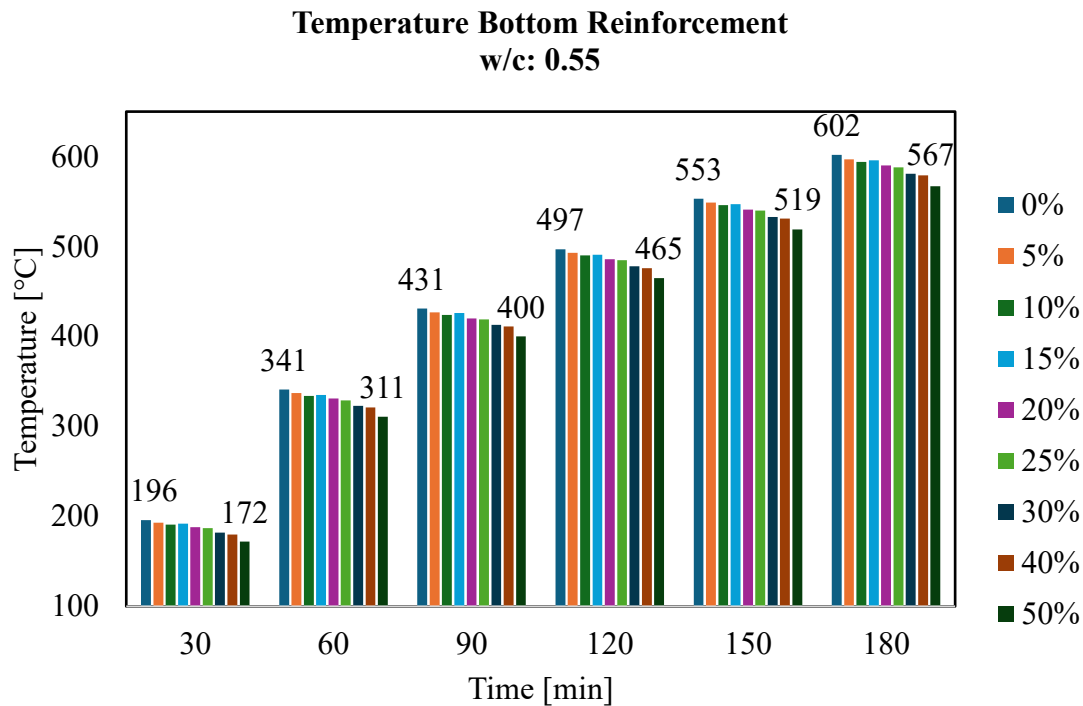


Figure 4-10. Temperature of reinforcement in rubber concrete with different rubber content, proposed models with w/c=0.55.

#### 4.3.2. Bending moment resistance

From Figure 4-11 to Figure 4-17, the results of the bending moment resistance are plotted (for detailed results, see Table F-9, Table F-10, Table F-11 and Table F-12). Generally speaking, the bending moment resistance of the analysed cross-section reduces when the temperature increases. The main reason for this effect, as has been mentioned in the present thesis, is that concrete losses strength when is heated. However, at the beginning of the analysis, the resistance increases. This increment is explained by the fact that the safety factors for fire conditions are set equal to 1, according to the Eurocode. Therefore, in the computation of the resistance, the characteristic strength of concrete is equal to the design strength.

Another aspect to consider is that, at ambient temperature, the characteristic strength of control concrete is higher than the one of concretes with rubber, therefore leading to a lower resistance to bending moment.

In contrast, when concrete is exposed to fire, rubber concrete has better performance since its reduction on bending resistance is lower than the reduction on the control concrete.

Additionally, it is extremely noticeable that, in the case of the proposed models, a reduction on the bending resistance during the first 60 minutes of exposure does not take place in any of the proposed models, while from the model analysed by CDM Dolmen, immediately after 30 minutes, the bending moment resistance decreases. This difference could be explained by the difference between the values of the thermal properties, which in the case of the proposed models, lead to a lower transfer of heat across the element. It also reinforces the fact that, a direct comparison of the values between the CDM Dolmen analysis and the proposed ones, is not feasible.

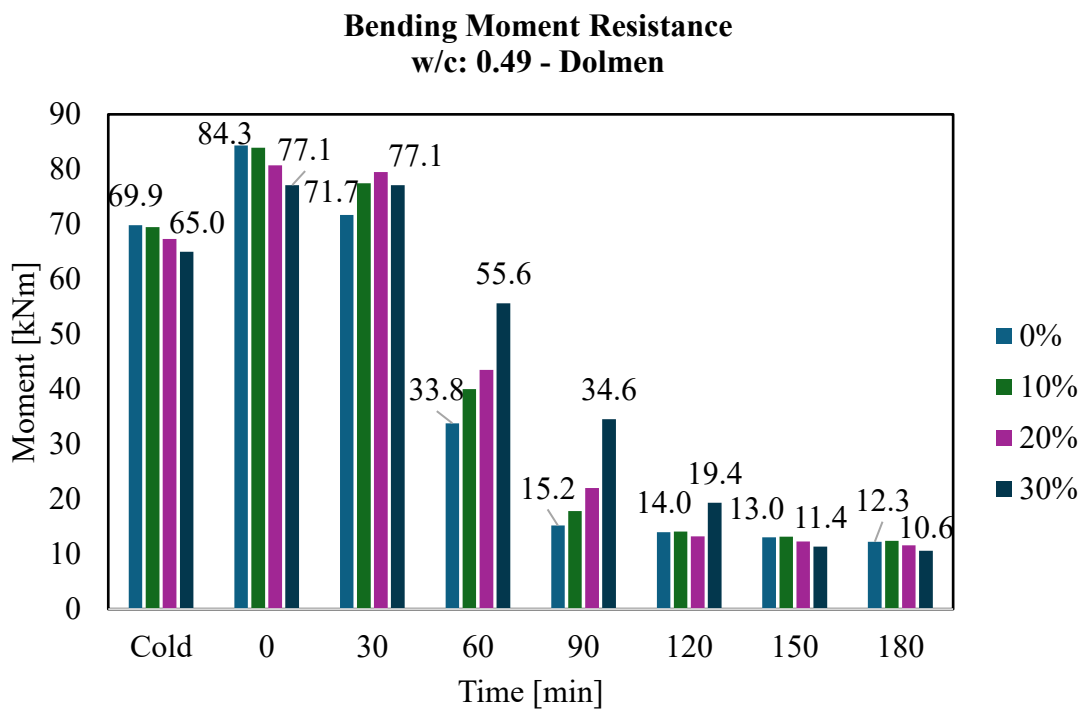


*Figure 4-11. Bending moment resistance of rubber concrete with different rubber content, Dolmen Models.*

Since the reduction of the resistance takes place after 90 minutes of exposure, the analysis of the proposed models just considers the resistance at cold scenario, at the beginning of the fire and its development from minute 90 to 180.

Figure 4-13, Figure 4-15 and Figure 4-17 plot the percentage of reduction of the bending resistance. For all water-cement ratios, the initial reduction of the bending resistance (at 90 minutes exposure) is between 10% to 20%. From there, the reduction keeps increasing, reaching values up to 59%. For all three water-cement ratios, the control concrete has the highest percentage of reduction with maximum value of 58.6% of loss for a 180-minute

exposure, while rubber concrete with 50% of rubber content the lowest with a maximum reduction of 52.8% for the same time of exposure.

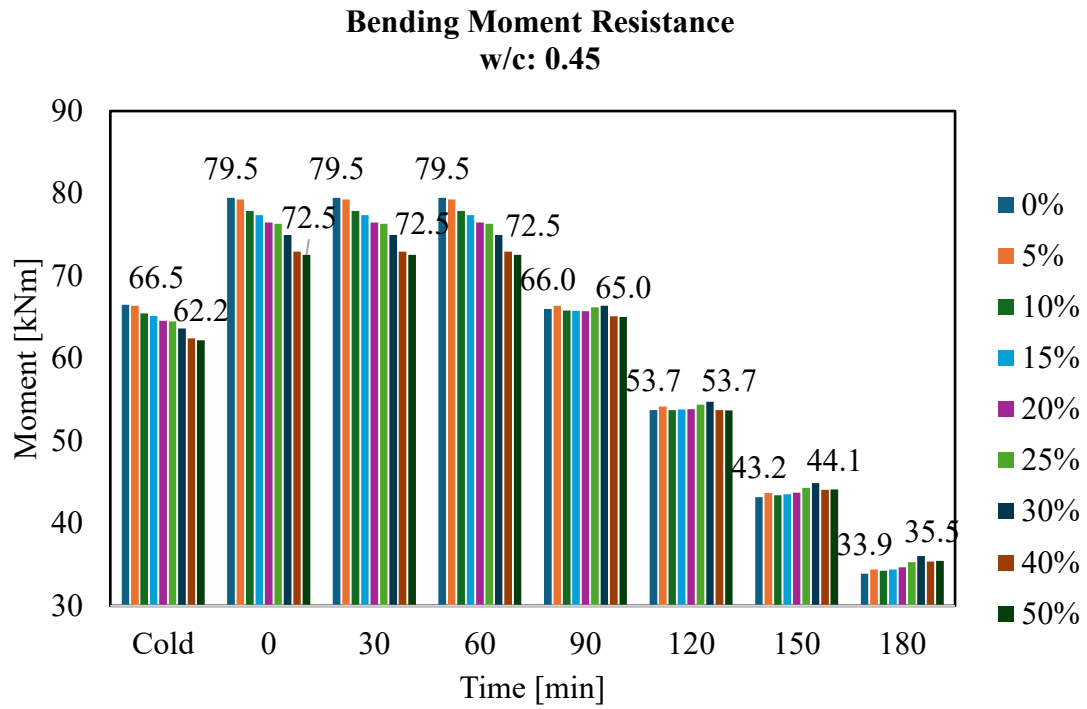
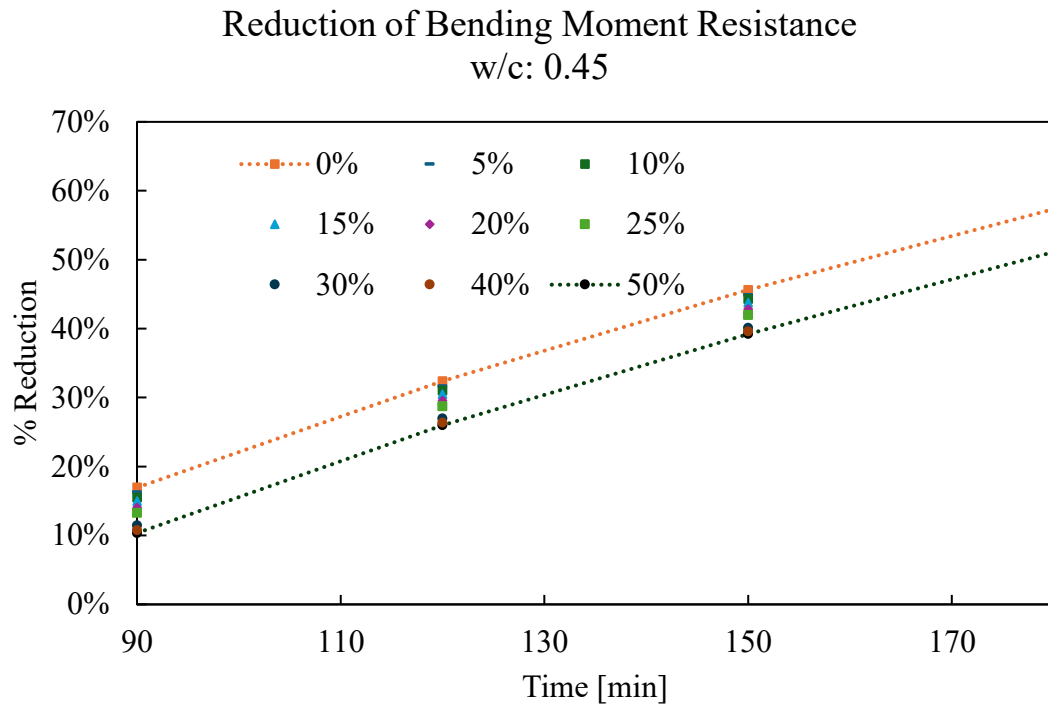


Figure 4-12. Bending moment resistance of rubber concrete with different rubber content, proposed models with w/c=0.45.



*Figure 4-13. Percentage of reduction of bending moment resistance from proposed models with  $w/c=0.45$ .*

It is the great importance to highlight the fact that, even though the general trend is a reduction in strength by adding crumb rubber in concrete, for a water-cement ratio of 0.5 and a rubber content equal to 5% and 10%, the resistance is higher than the control concrete. A probable reason for this is the fact that from the base results used as input data for the analysis, the compressive strength of the samples with these characteristics exhibited a higher characteristic strength. Therefore, the numerical analysis led to higher resistances.

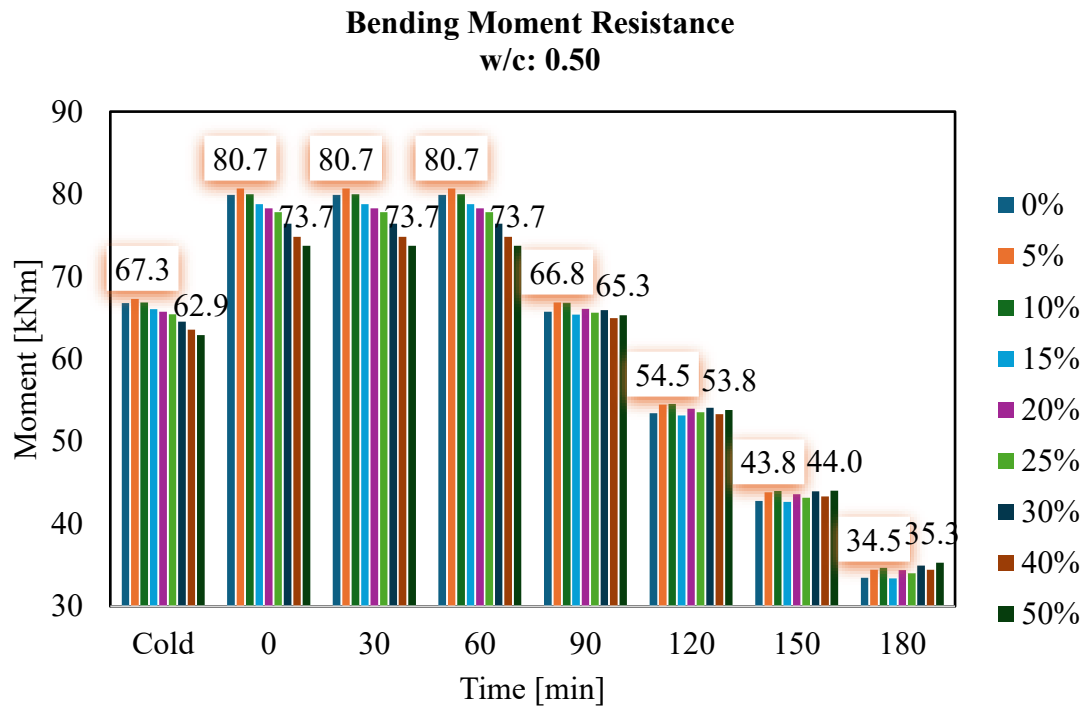


Figure 4-14. Bending moment resistance of rubber concrete with different rubber content, proposed models with w/c=0.50.

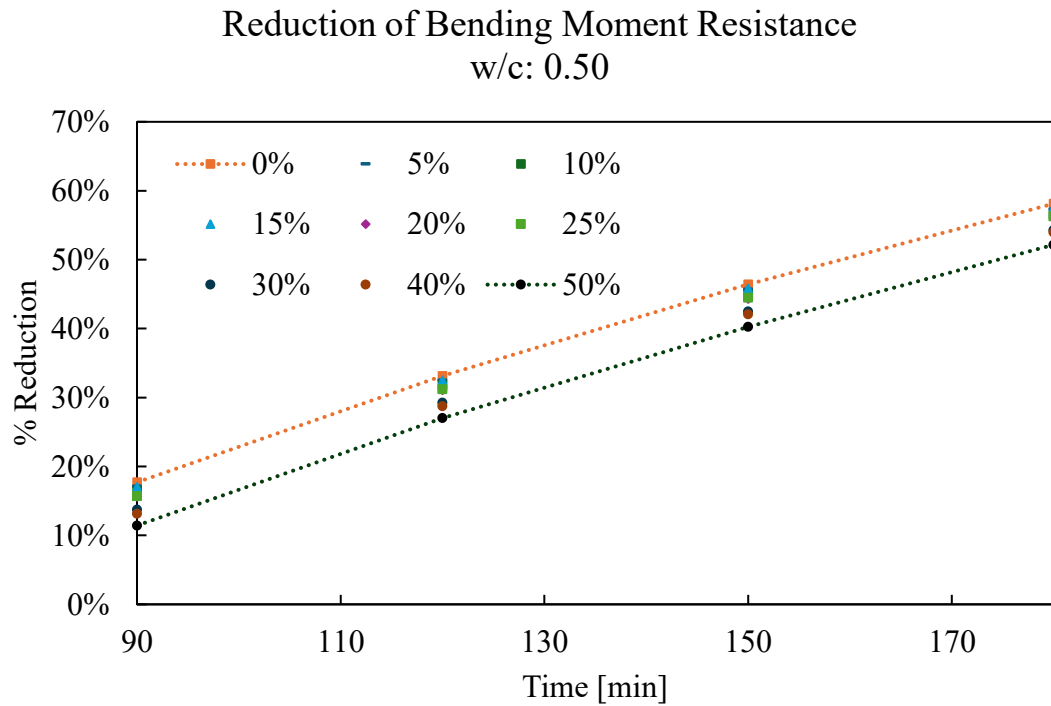


Figure 4-15. Percentage of reduction of bending moment resistance from proposed models with w/c=0.50.



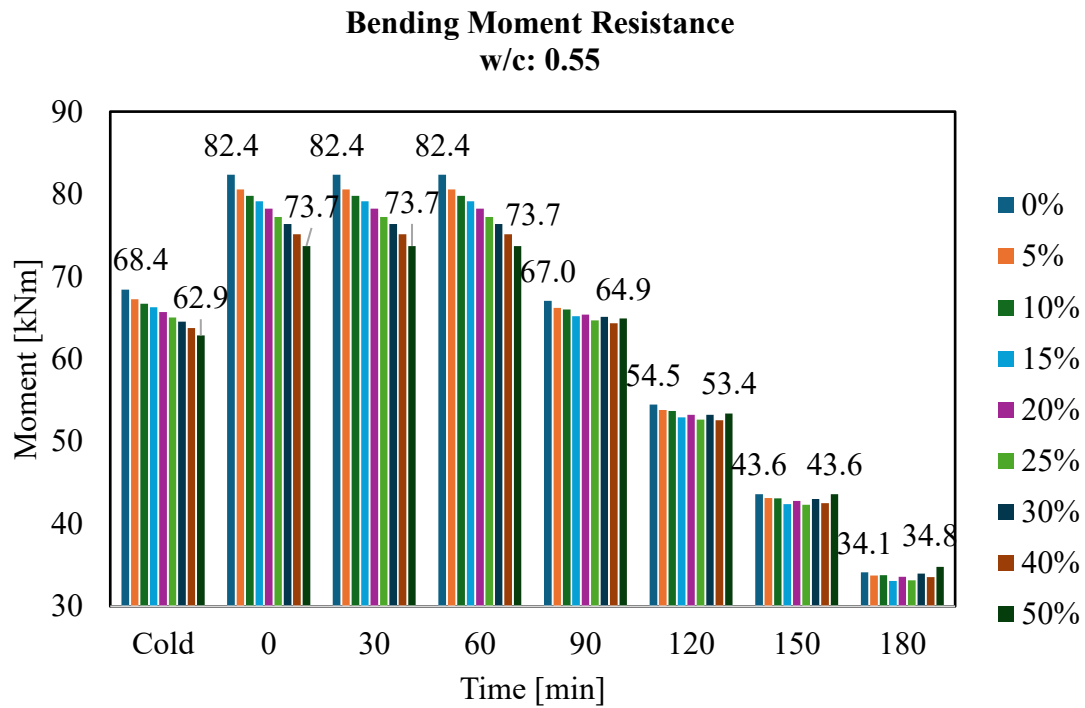


Figure 4-16. Bending moment resistance of rubber concrete with different rubber content, proposed models with w/c=0.55.

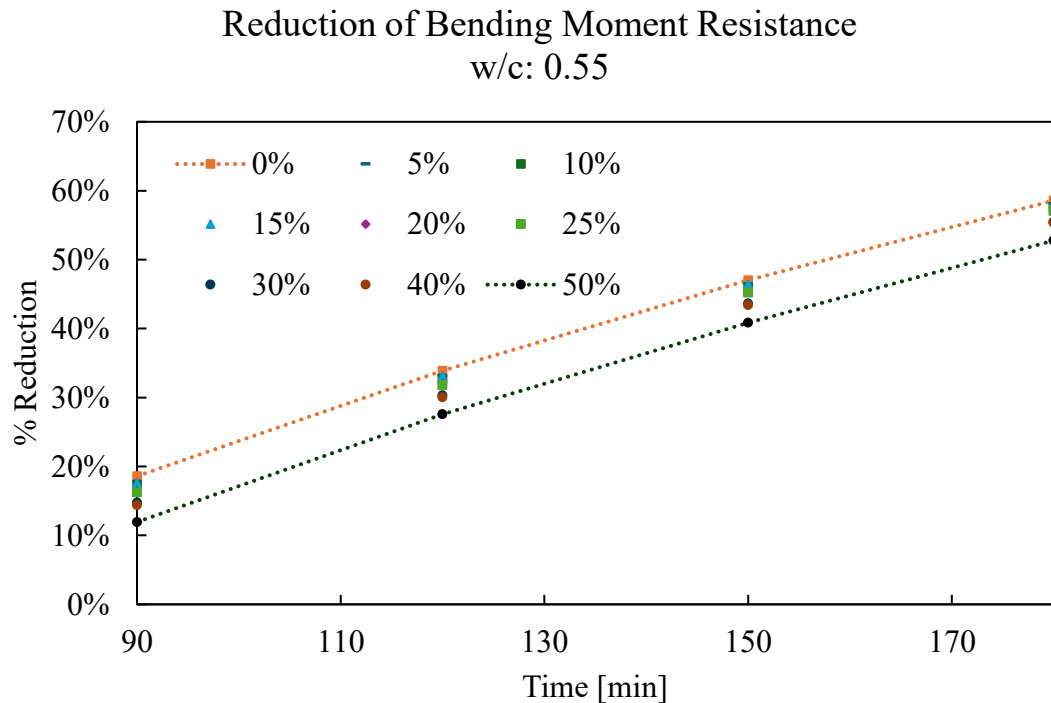


Figure 4-17. Percentage of reduction of bending moment resistance from proposed models with w/c=0.55.

From Figure 4-18 to Figure 4-20, it is possible to analyse the effect of crumb rubber content in the concrete mix. It is possible to see that for the models with a water-cement ratios of 0.45 and 0.50, after 90 minutes of exposure to fire, rubber concrete starts to exhibit a better performance than the control concrete, which correspond to positive values of percentage of variation. On the other hand, the models with a water-cement ratio equal to 0.55 have a negative variation of the resistance for different exposures and for all the different rubber contents considered, except for a rubber content equal to 50% and for 180-minute exposure. In general, considering the trend of the graphics, rubber concrete starts showing a better performance at high temperatures in comparison with normal concrete.

Additionally, it is apparent some sort of peak-like behaviour in all three graphics for a rubber content equal to 30%, where the variation of the bending resistance between the control concrete and the rubber concretes are the highest for some models. As an example, for a water-cement ratio of 0.45 and a 180-minute exposure, the rubber concrete with a 30% of rubber content has a bending resistance 6.8% higher than the control concrete. A possible explanation for this behaviour is the insulation properties of rubber. Since the computation of the bending resistance neglects the part of concrete in tension, it depends on the concrete in compression and the reinforcement. At higher rubber content, the reinforcement subjected to tension has less degradation of its mechanical properties, thanks to the insulation provided by rubber concrete, and leading to higher bending resistance when exposed to fire, in comparison with control concretes.

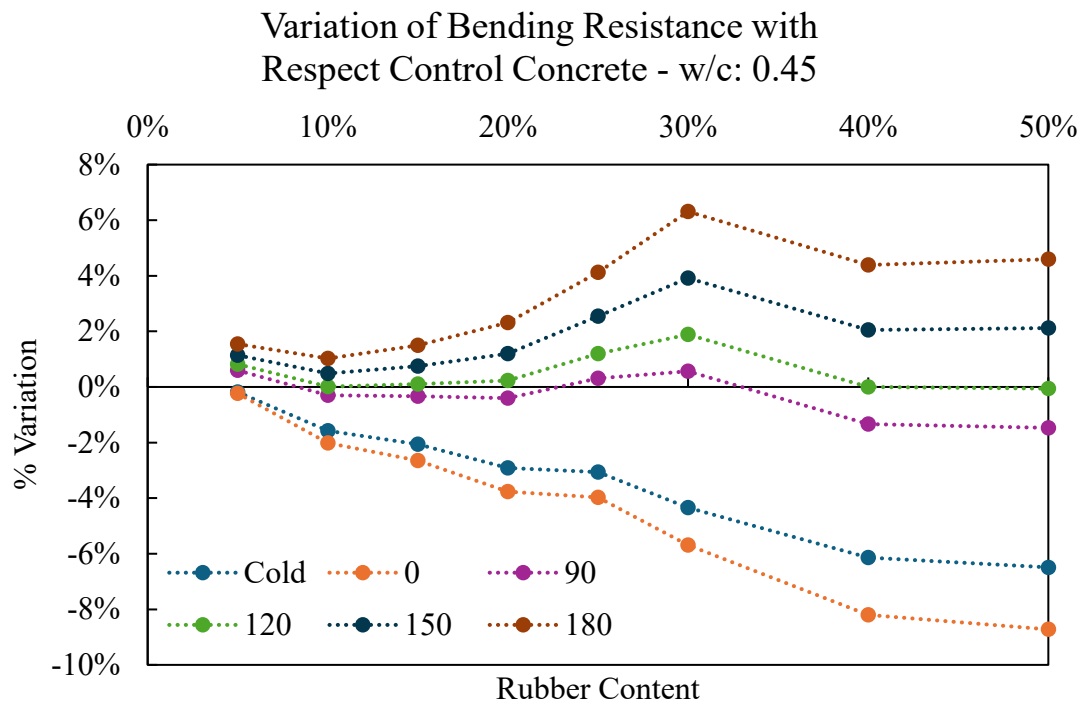


Figure 4-18. Variation of bending moment resistance with respect control concrete for models with w/c: 0.45.

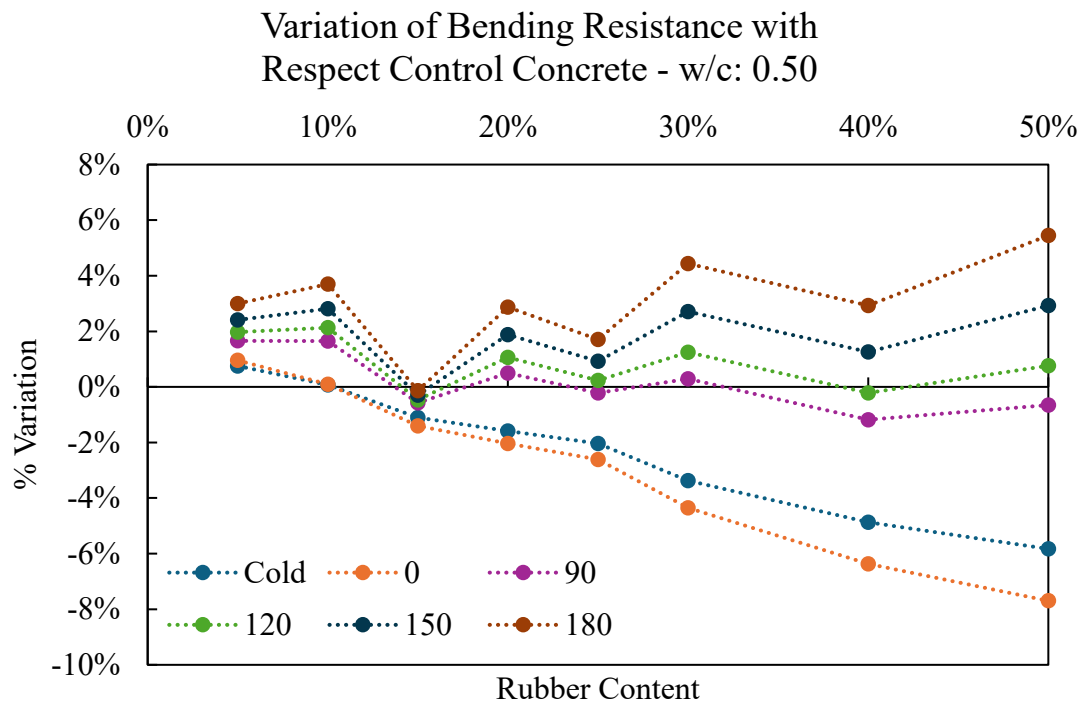
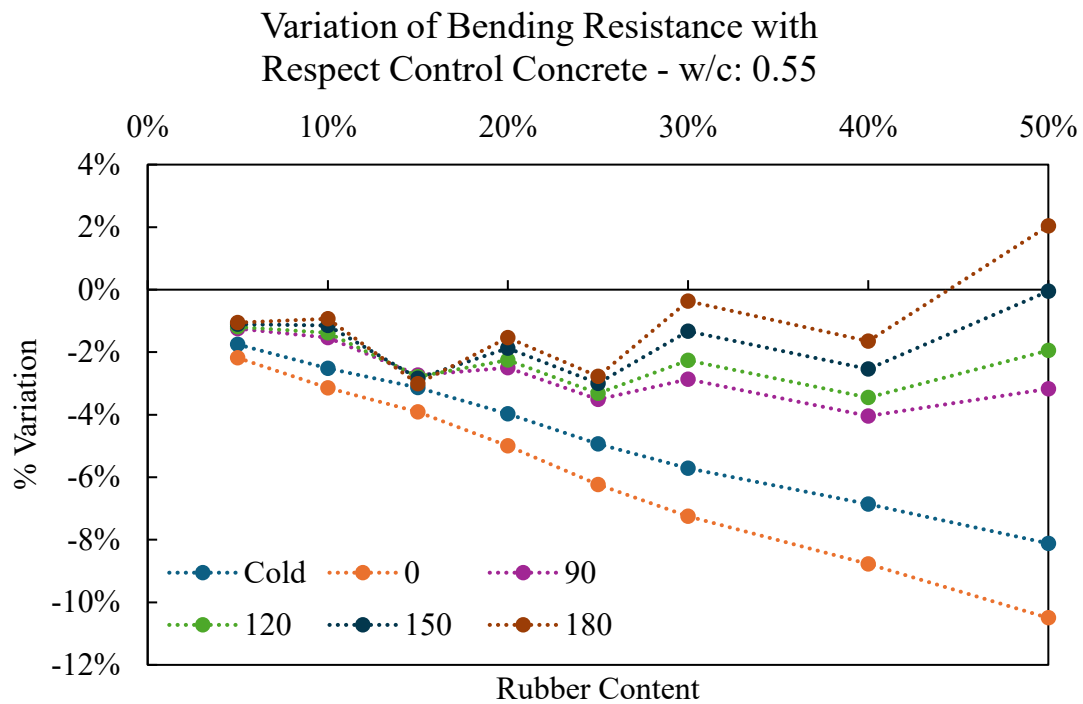


Figure 4-19. Variation of bending moment resistance with respect control concrete for models with w/c: 0.50.



*Figure 4-20. Variation of bending moment resistance with respect control concrete for models with w/c: 0.55.*

#### 4.3.3. Axial resistance

From Figure 4-21 to Figure 4-26, the results of the bending moment resistance are plotted (for detailed results, see Table G-13, Table G-14, Table G-15 and Table G-16). As for the bending moment, the axial resistance also decreases when temperature of concrete raises. Additionally, as expected, the general behaviour is that control concrete has a higher axial strength at ambient temperature than rubber concretes.

Regarding the percentage of reduction, as well as the bending moment resistance, control concrete has higher reduction of its axial resistance, in contrast with rubber concretes. By increasing the percentage of rubber content, the reduction of the strength is lower for a given time of exposure to fire. However, it is noticeable that at 30 and 60 minutes of exposure, there are some negative values of the percentage of reduction indicating that the axial resistance actually slightly increased. This initial increment in the axial strength is explained by the fact that the safety factors for a fire scenario are set equal to 1, just as for the bending resistance.

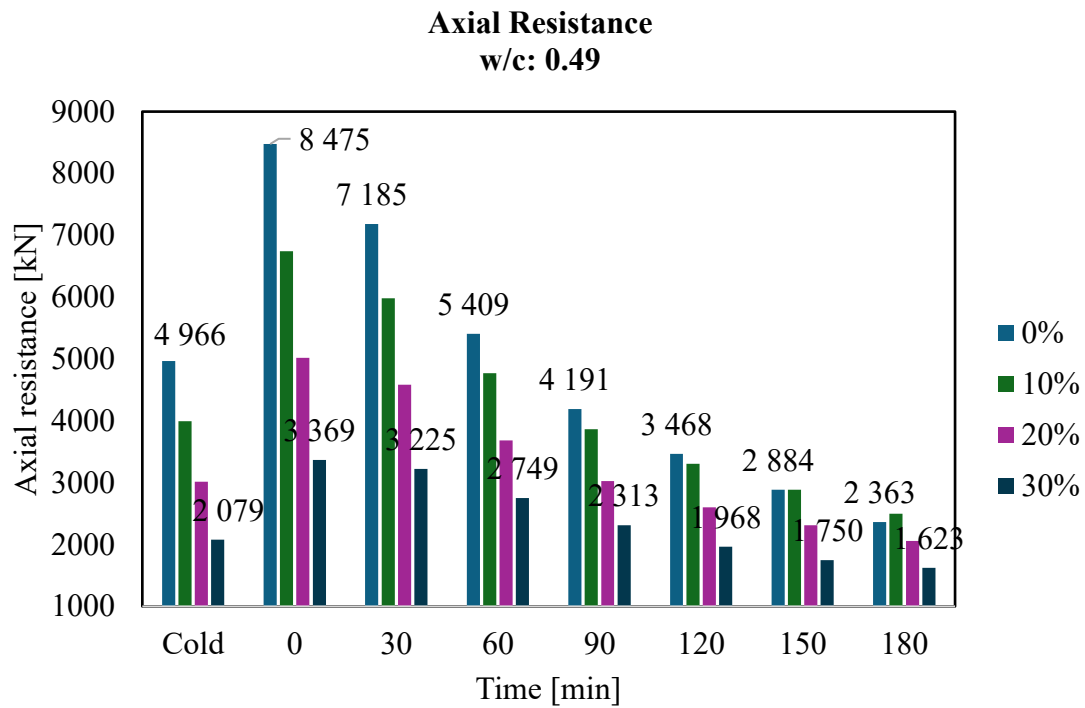


Figure 4-21. Axial resistance of rubber concrete with different rubber content, Dolmen Models.

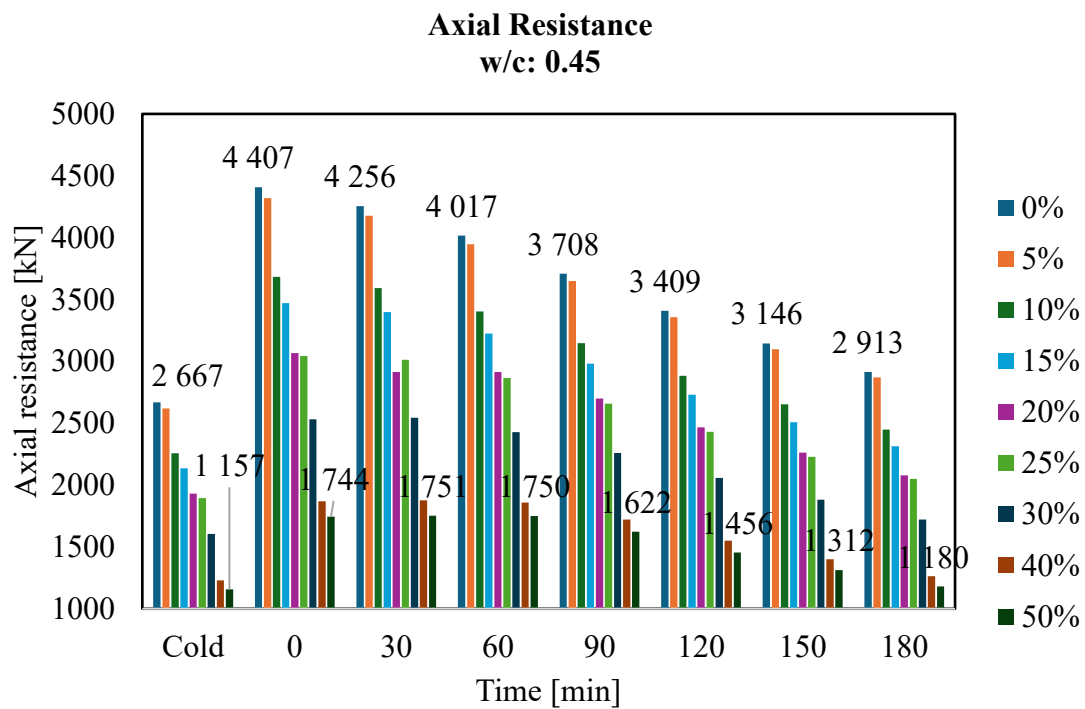


Figure 4-22. Axial resistance of rubber concrete with different rubber content, proposed models with w/c=0.45.

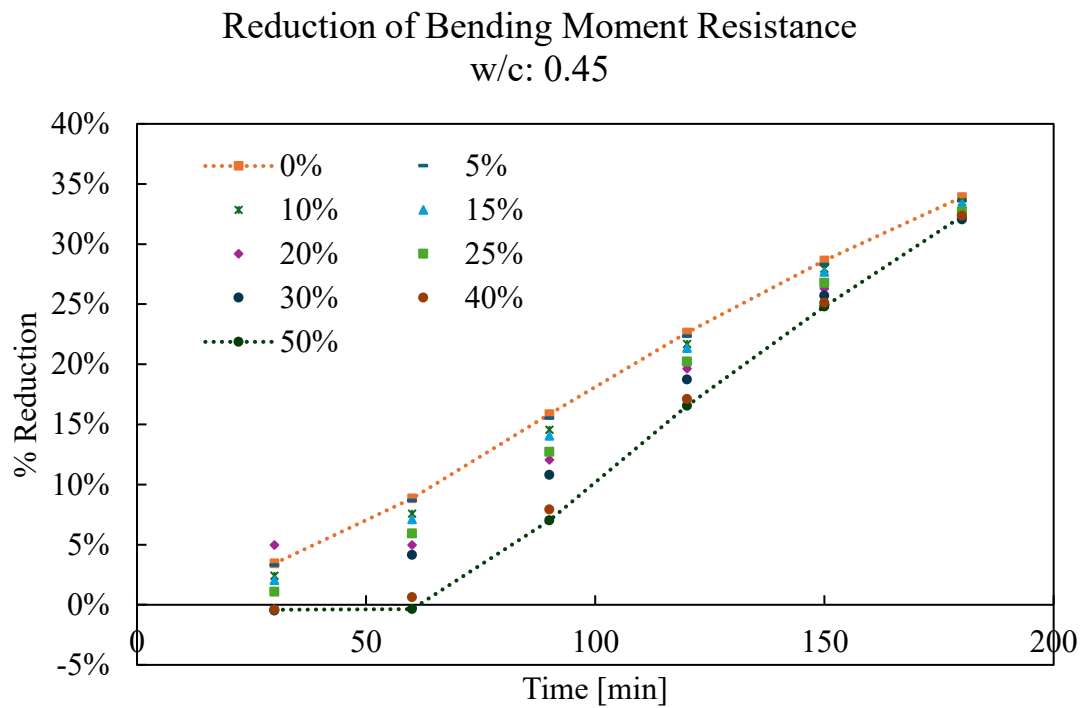


Figure 4-23. Percentage of reduction of axial resistance from proposed models with w/c=0.45.

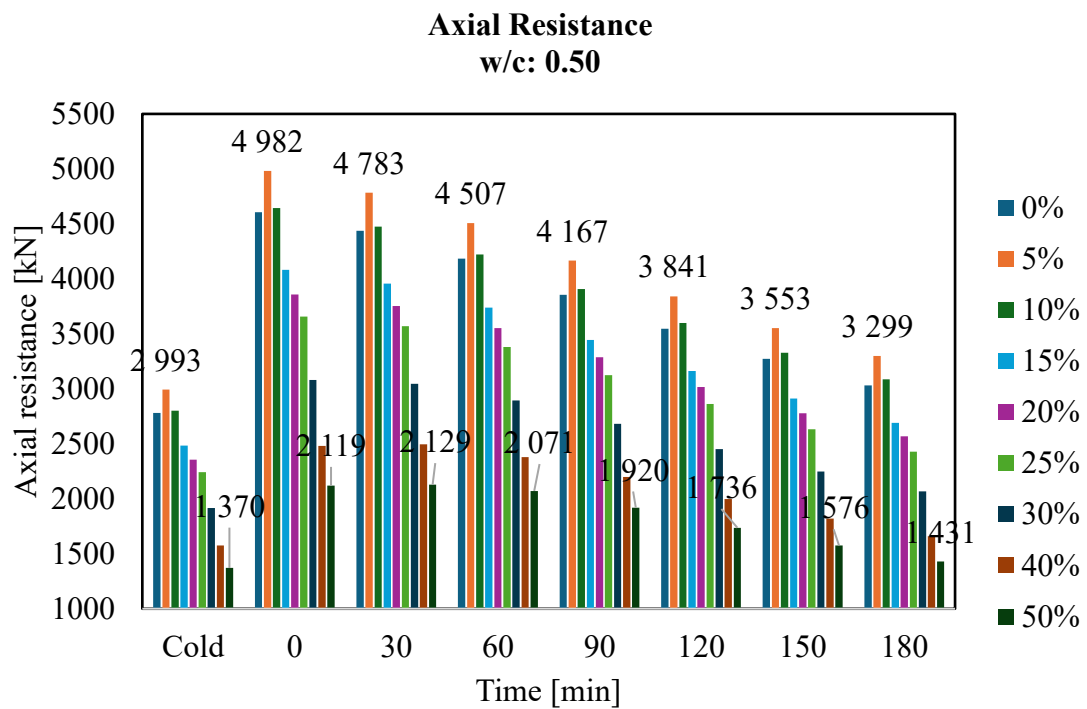


Figure 4-24. Axial resistance of rubber concrete with different rubber content, proposed models with w/c=0.50.

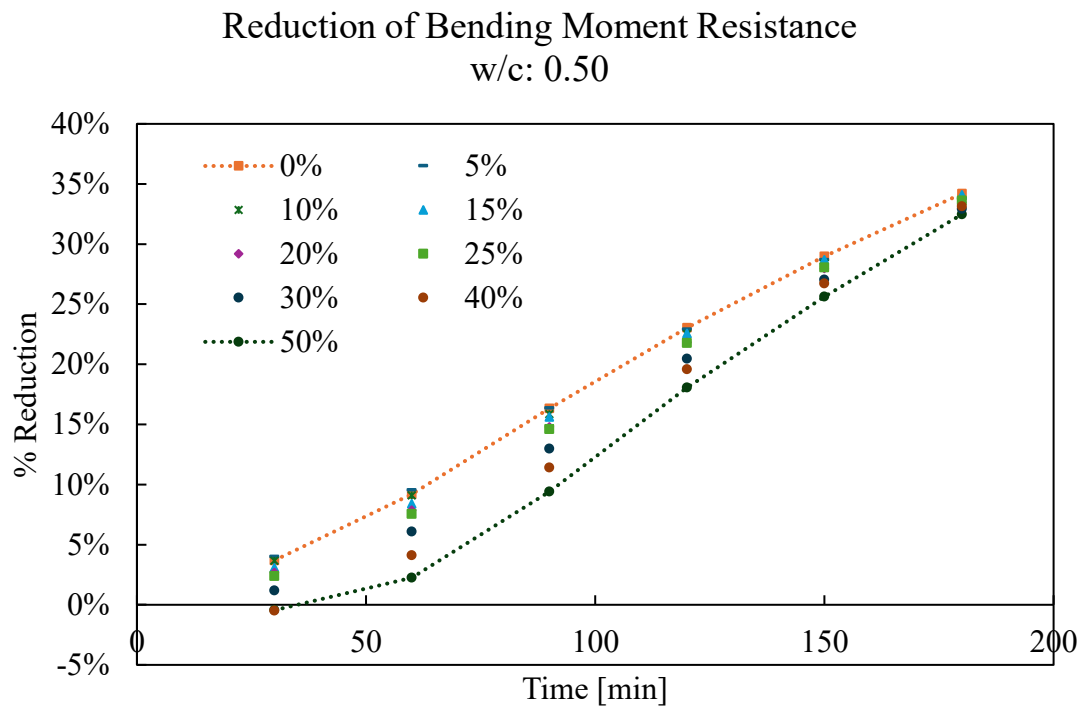


Figure 4-25. Percentage of reduction of axial resistance from proposed models with w/c=0.50.

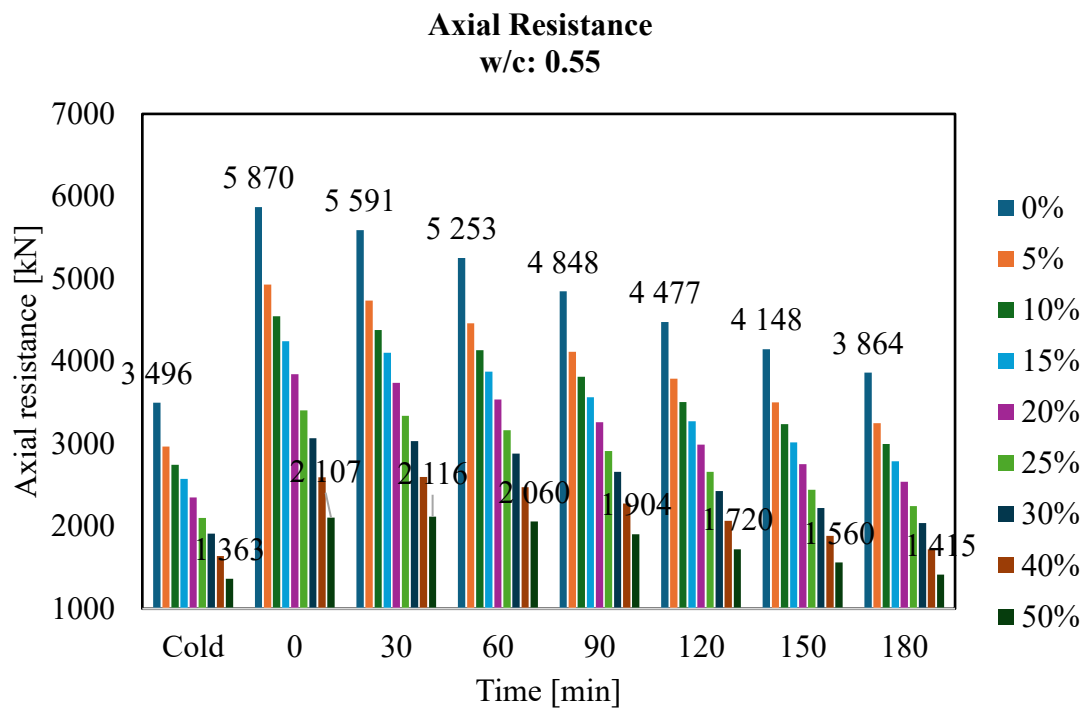


Figure 4-26. Axial resistance of rubber concrete with different rubber content, proposed models with w/c=0.55.

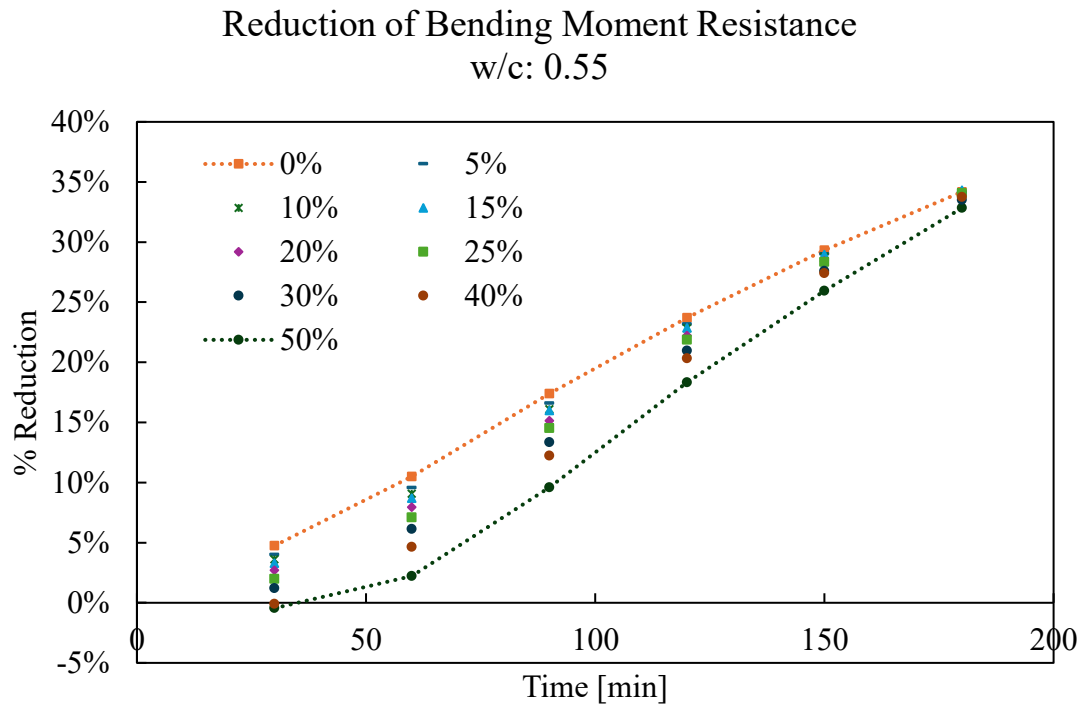


Figure 4-27. Percentage of reduction of axial resistance from proposed models with w/c=0.55.

From Figure 4-28 to Figure 4-30, the variation of the axial resistance with respect to the control concrete is plotted for different times of exposure to fire. Except for the models with water-cement ratio equal to 0.55 and with rubber content of 5% and 10%, all other models present a negative variation of the axial resistance. The only models presenting higher axial resistance were the ones in which the characteristic strength of the concrete was higher than the control concrete.

In contrast with the bending moment resistance, where some of the models had a positive variation of its resistance with respect to the control concrete (see Figure 4-18 to Figure 4-20), just 2 models presented higher axial resistance (the ones with higher initial strength). The main reason for this is that, for the bending resistance, the part of concrete subjected to compression is considered while the part of concrete subjected to tension is neglected therefore, the tension in the cross section depends on the reinforcement and its temperature. On the other hand, for the axial resistance to compression, all concrete is considered and consequently, a variation on its characteristic strength would have a considerable impact on its resistance.



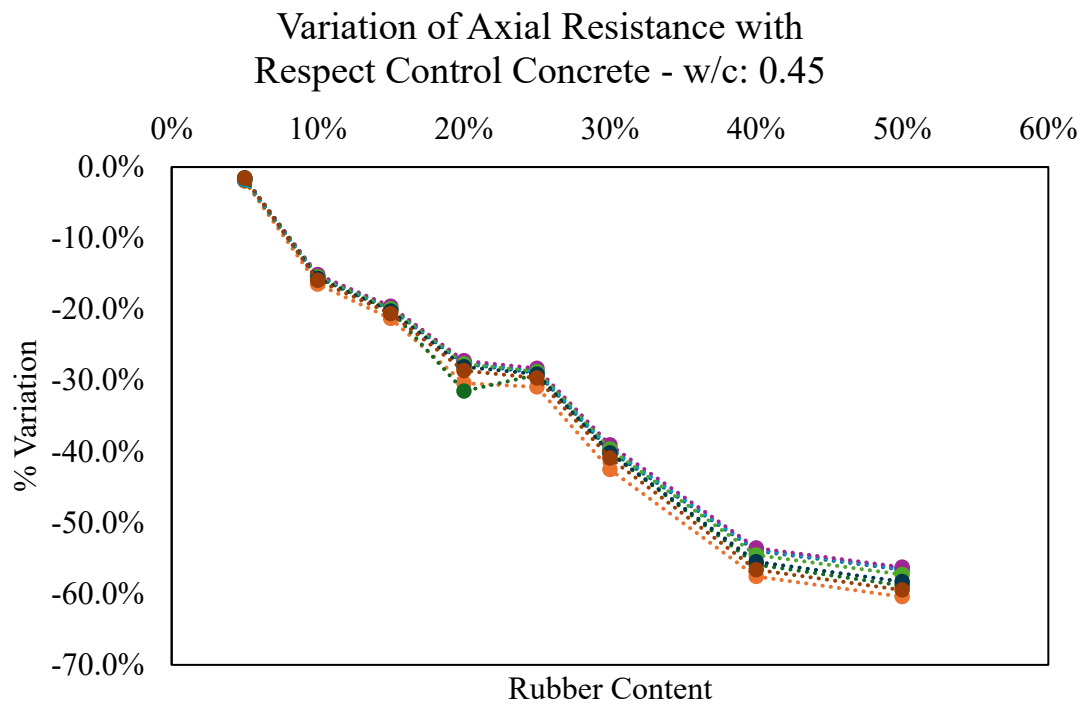


Figure 4-28. Variation of axial resistance with respect control concrete for models with w/c: 0.45.

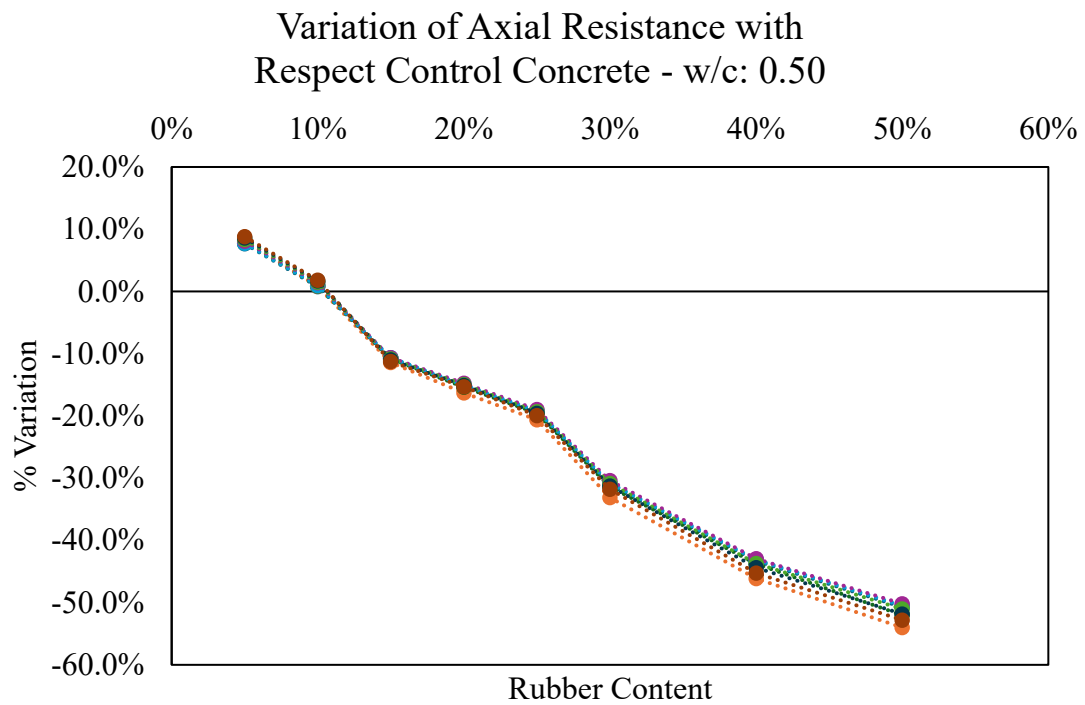


Figure 4-29. Variation of axial resistance with respect control concrete for models with w/c: 0.50.

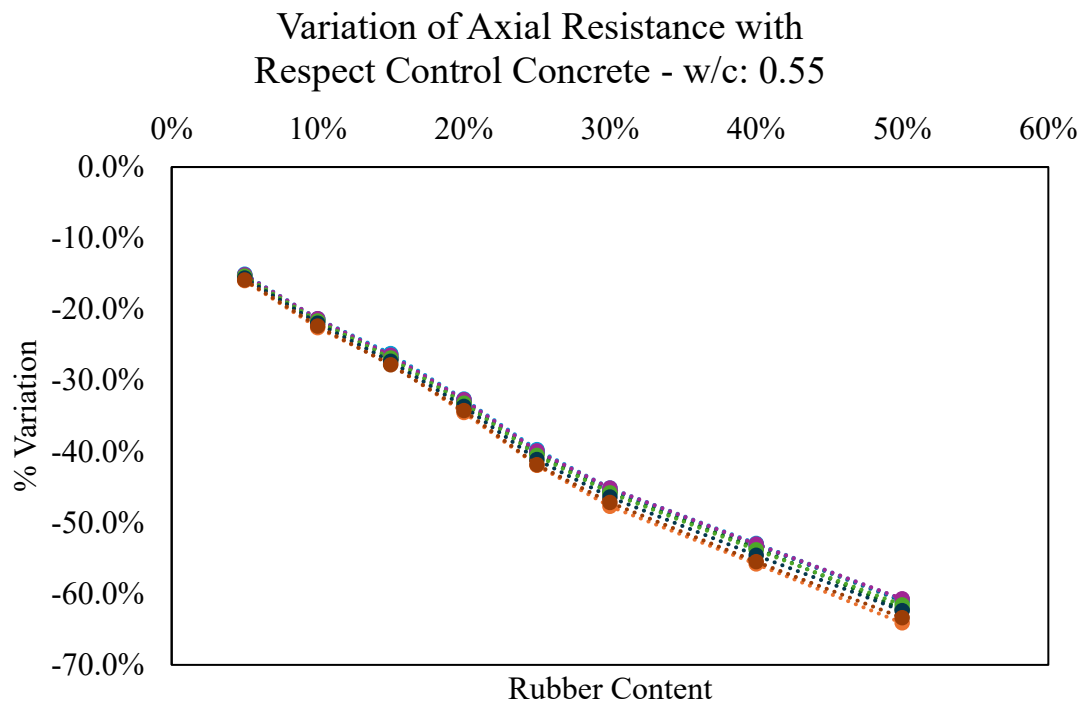


Figure 4-30. Variation of axial resistance with respect control concrete for models with w/c: 0.55.

#### 4.3.4. Bending moment – axial diagram (M-N interaction domain)

In this section the different graphics of the M-N interaction domain are illustrated for the various times of exposure to fire for the models with water-cement ratio equal to 0.45. Figure 4-31 shows the M-N interaction domains at different times of exposures for the control concrete with water-cement ratio of 0.45. The trend of the domain is the same for all models. Cold analysis, nominated as “*I (A freddo)*”, has the smallest domain. Then, once the fire starts, the domain increases due to the change of the safety factors. At higher fire exposures, the domains start to reduce, both for axial and bending due to the degradation of concrete and the reinforcement. As this trend remains the same for all models, the next figures just show the domains at cold analysis and for 0, 60, 120 and 180 minutes exposure, in order to get clearer graphics.

Analysing the influence of the rubber content, from the M-N interaction domains it can be seen that it decreases when the rubber content increases, being the control concrete the widest, while the rubber concrete with 50% of rubber content, the smallest.

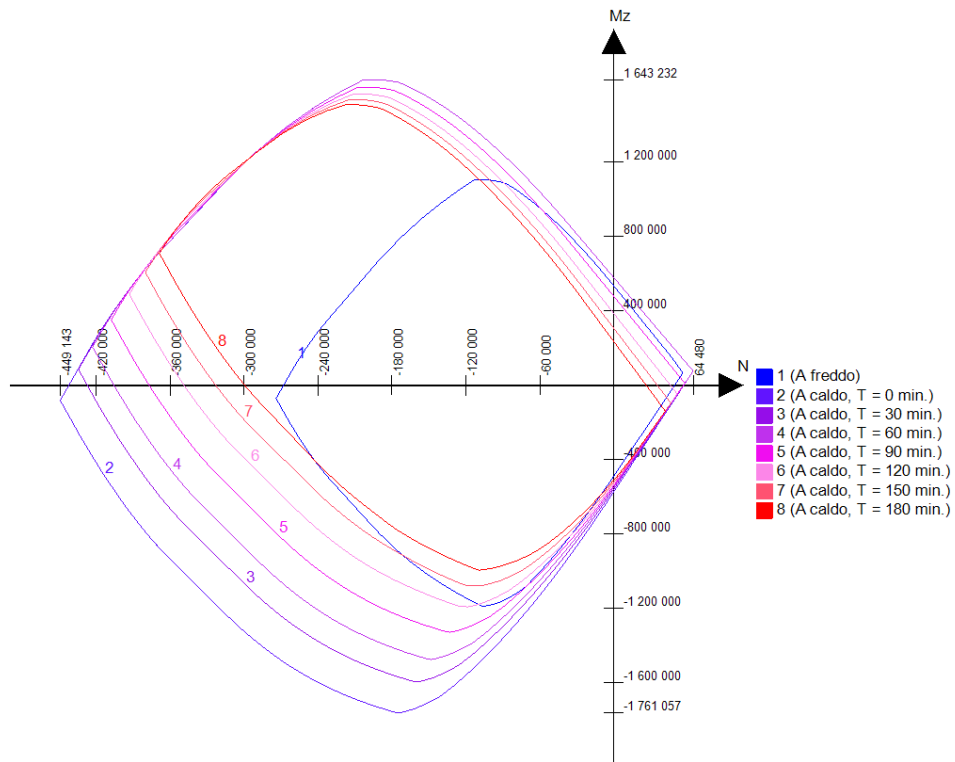


Figure 4-31. M-N interaction domain for control concrete with  $w/c$ : 0.45.

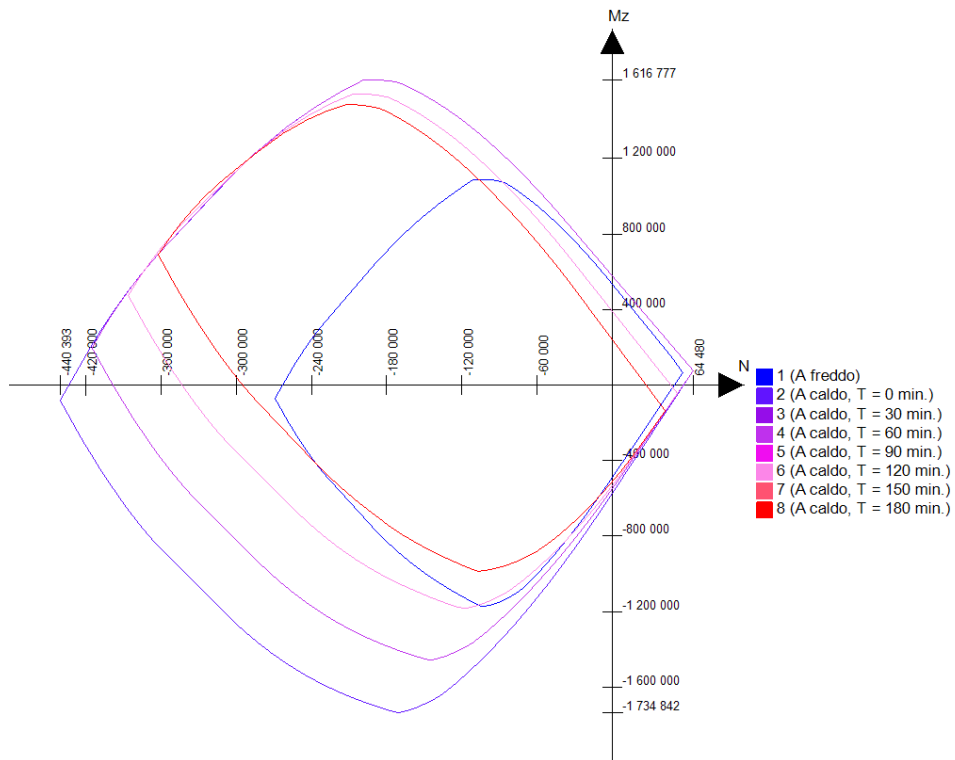


Figure 4-32. M-N interaction domain for concrete rubber content of 5% and  $w/c$ : 0.45.

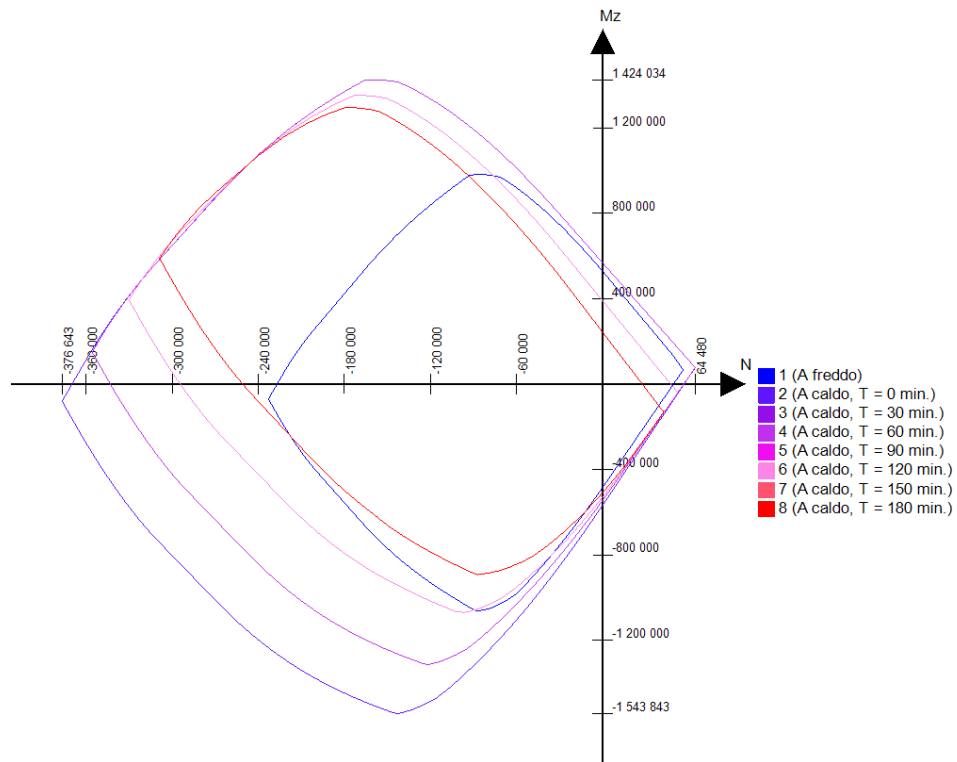


Figure 4-33. M-N interaction domain for concrete rubber content of 10% and w/c: 0.45.

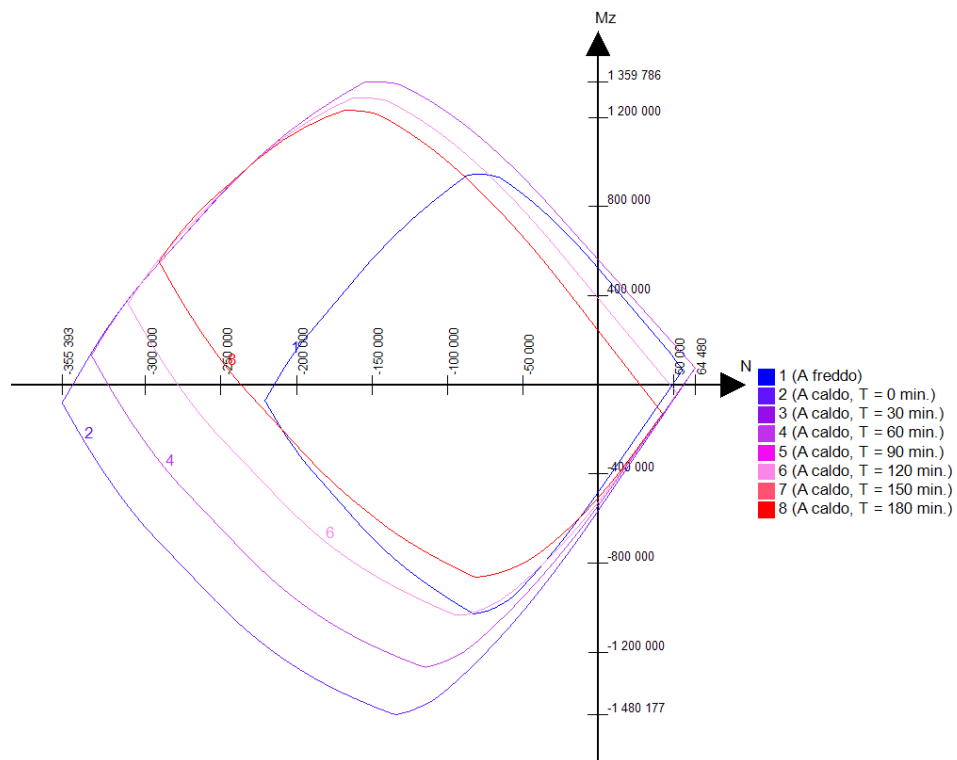


Figure 4-34. M-N interaction domain for concrete rubber content of 15% and w/c: 0.45.

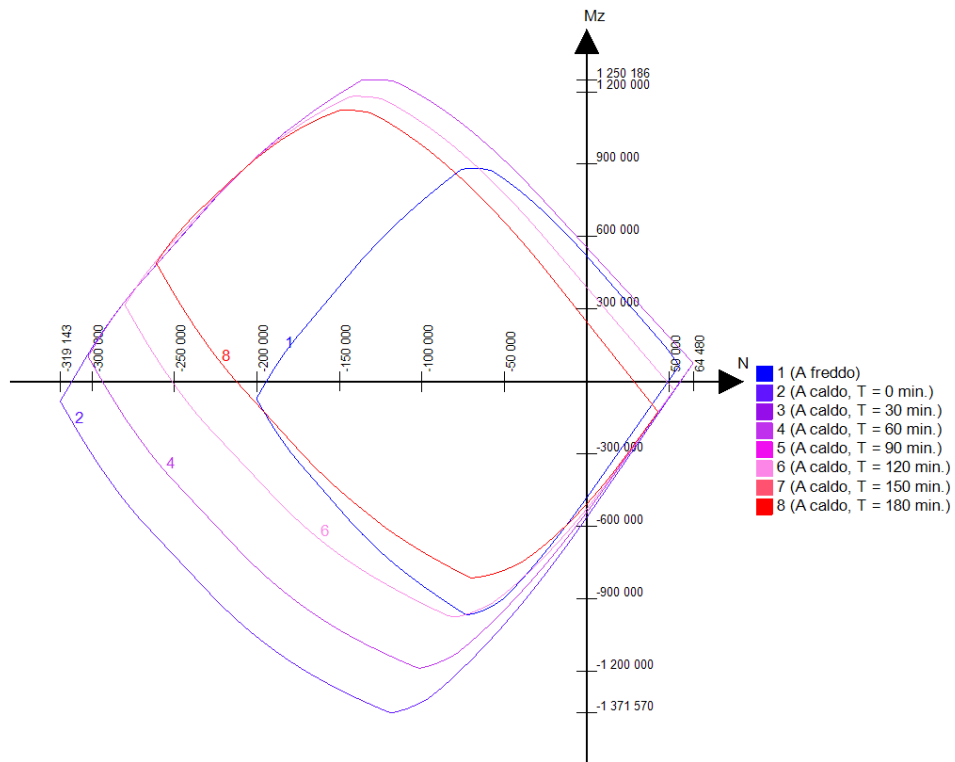


Figure 4-35. M-N interaction domain for concrete rubber content of 20% and w/c: 0.45.

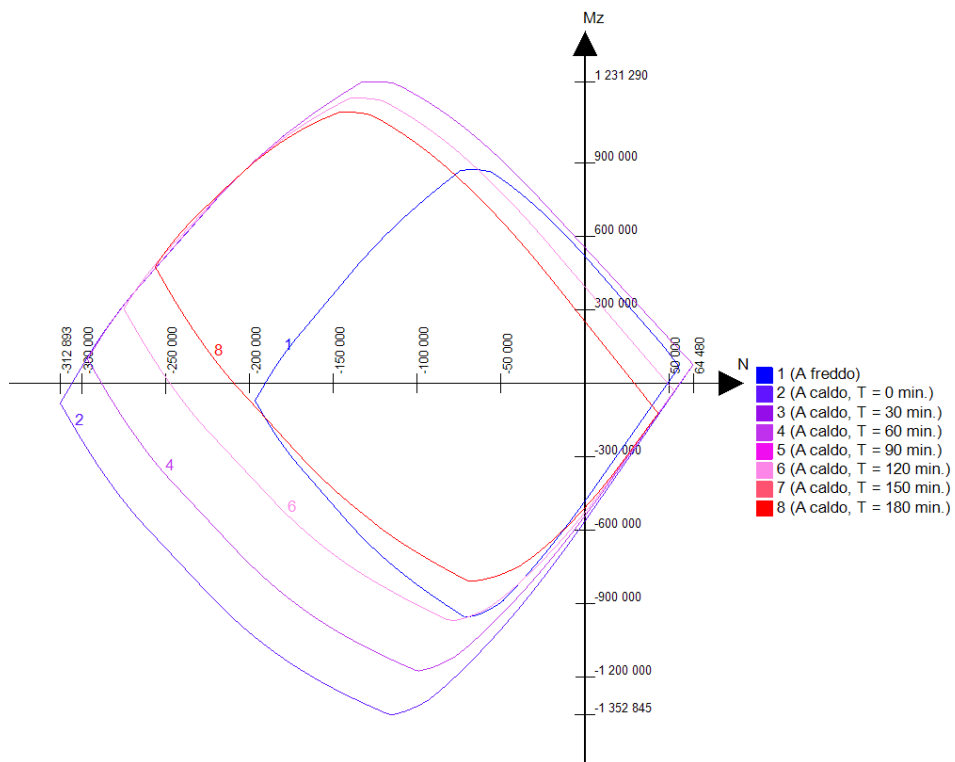


Figure 4-36. M-N interaction domain for concrete rubber content of 25% and w/c: 0.45.

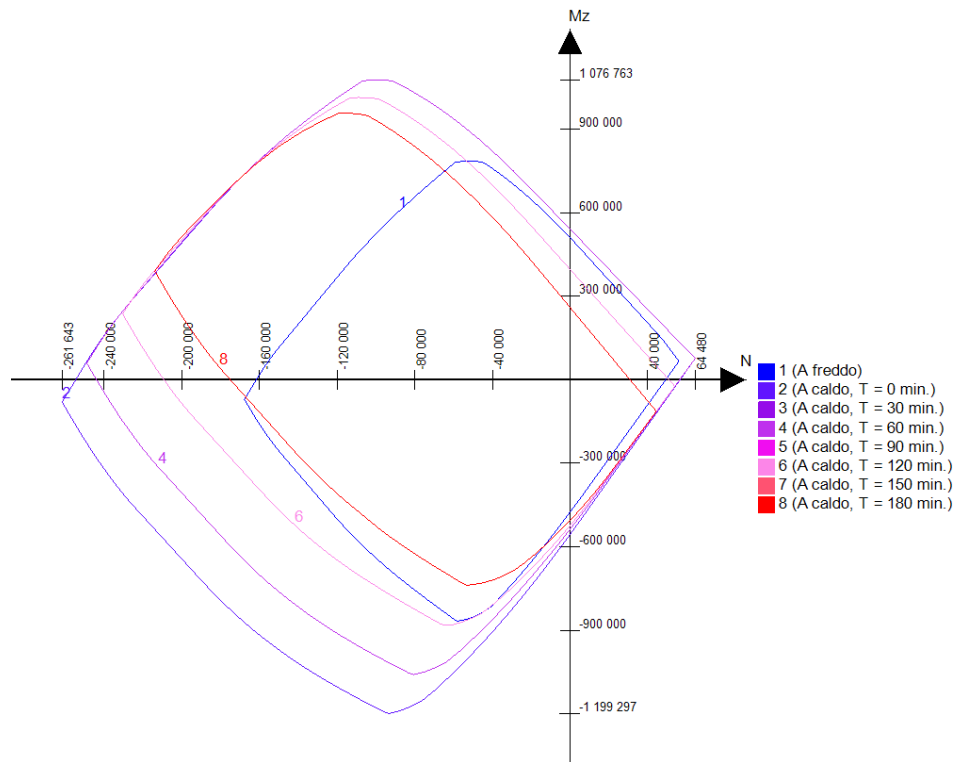


Figure 4-37. M-N interaction domain for concrete rubber content of 30% and w/c: 0.45.

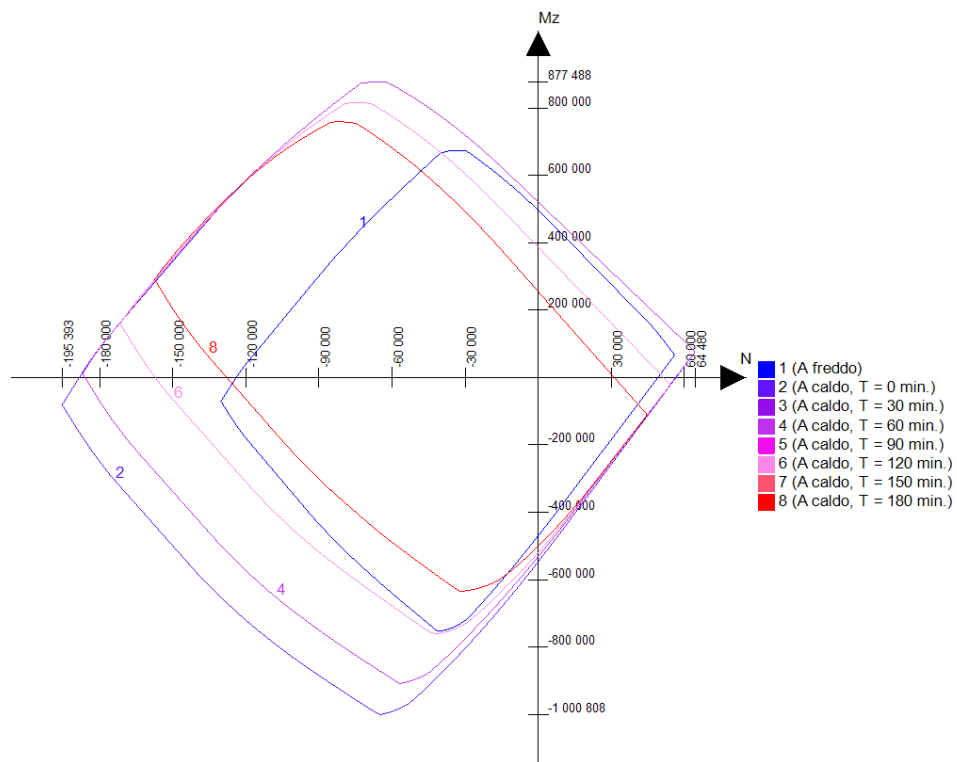


Figure 4-38. M-N interaction domain for concrete rubber content of 40% and w/c: 0.45.

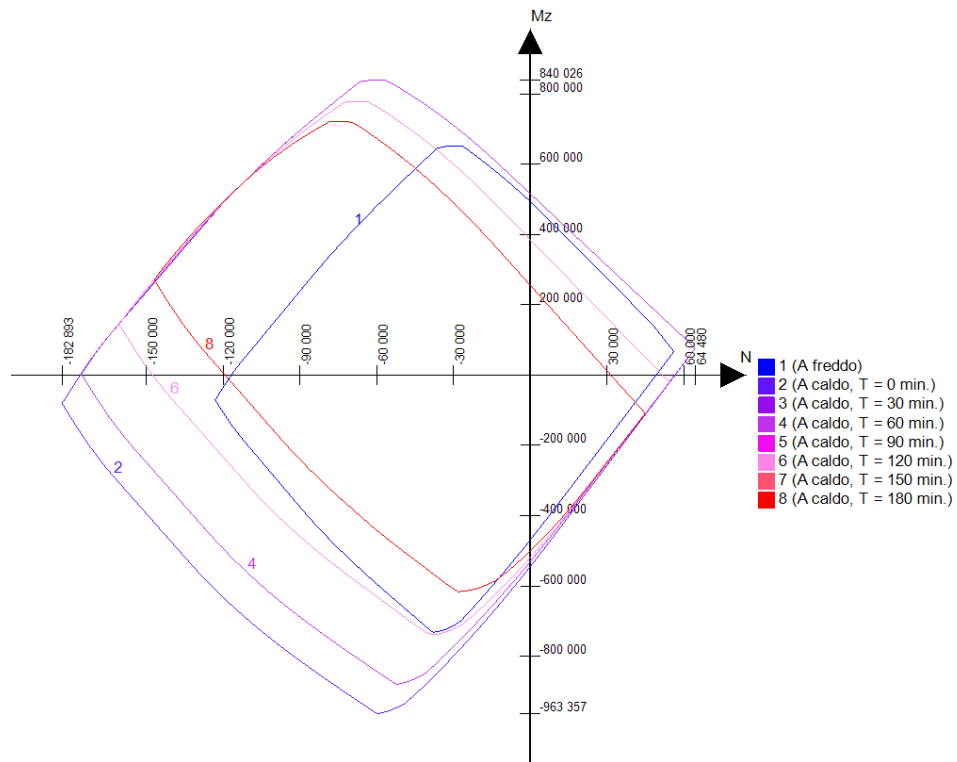


Figure 4-39. M-N interaction domain for concrete rubber content of 50% and w/c: 0.45.





# 5. Conclusions

This thesis has provided an analysis regarding the fire resistance of rubber concrete structures, making special emphasis on the thermal and mechanical behaviour of different mixtures exposed to fire. Through numerical modeling, key parameters such as the reinforcement temperature, the bending moment resistance, the axial resistance, and the M-N interaction domain, it is assessed the influence of rubber content in concrete mixtures.

One of the most important findings is that rubber concrete show higher insulation properties in comparison with standard concrete. This effect is demonstrated by the lower temperatures of the reinforcement. The lower values of the thermal conductivity and the higher values of the specific heat, cause a lower rate in which the temperature of the element increases, showing a better performance under fire scenarios.

Regarding the mechanical performance, the numerical analysis shows that, even if rubber concrete shows a lower initial compressive and bending strengths in comparison with normal concrete, it keeps a greater percentage of its initial resistance under prolonged fire exposure. The reduction in axial and bending moment resistance is less severe in rubber concrete, specially at moderated percentage of replacement. This shows that rubber concrete could be a viable alternative, with a relatively good structural behaviour and being environmentally friendly by introducing products of waste tyres.

The M-N interaction domain analysis supports the advantages of rubber concrete. However, the effectiveness is extremely dependent on the percentage of rubber replacement.

Considering the overall behaviour of rubber concrete in the present analysis, it is suggested for future investigations to consider the viability of rubber concrete as an alternative for intervention of existing structures which require an improvement of its fire resistance.

Despite of the advantages, the optimization of the mixture of rubber concrete is still a challenge. The trade-off between the mechanical performance and the fire resistance must be carefully balanced in design applications. According to the results, a 30% of fine

aggregate can be replaced by rubber content in order to enhance and take advantage of the benefits of rubber crumbs in concrete without affecting in a great matter its mechanical properties.

Since the analysis performed in this thesis was completely numerical and there was a lack of experimental data regarding the variation of the thermal properties with the temperature, further experimental validation is required in order to make a comparison with the results obtained in the present thesis and to properly see the effect of some parameters such as the water-cement, aggregate-cement and coarse/fine aggregate ratios. One suggested test is bending test of a rubber concrete beam that has been subjected to elevated temperatures in order to properly assess its resistances.

## 6. References

- Azunna, S. U., Aziz, F. N. A. A., Rashid, R. S. M., & Bakar, N. B. A. (2024). Review on the characteristic properties of crumb rubber concrete. In *Cleaner Materials* (Vol. 12). Elsevier Ltd. <https://doi.org/10.1016/j.clema.2024.100237>
- Benýšek, M. (2021). *Analysis of Fire Resistance of Concrete Structures Based on Different Fire Models*.
- Bilal Nasar, R., Bilal Nasar Khan, R., & Khitab, A. (2020a). Enhancing Physical, Mechanical and Thermal Properties of Rubberized Concrete. *The Asian Institute of Research Engineering and Technology Quarterly Reviews*, 3(1), 33–45.
- Bilal Nasar, R., Bilal Nasar Khan, R., & Khitab, A. (2020b). Enhancing Physical, Mechanical and Thermal Properties of Rubberized Concrete. *The Asian Institute of Research Engineering and Technology Quarterly Reviews*, 3(1), 33–45.
- CDM DOLMEN Srl. (n.d.-a). *Validazione del Codice di Calcolo IS Fuoco*. CDM DOLMEN Srl. [www.cdmdolmen.it](http://www.cdmdolmen.it)
- CDM DOLMEN Srl. (n.d.-b). *Validazione del Codice di Calcolo IS Fuoco*. CDM DOLMEN Srl. [www.cdmdolmen.it](http://www.cdmdolmen.it)
- Correia, J. R., Marques, A. M., Pereira, C. M. C., & De Brito, J. (2012). Fire reaction properties of concrete made with recycled rubber aggregate. *Fire and Materials*, 36(2), 139–152. <https://doi.org/10.1002/fam.1094>
- El Marzak, M., Aicha, M. Ben, Lamrani, B., & Alaoui, A. H. (2022). Analysis of the heat transfer time in rubber aggregate concrete as a function of humidity percentage at very high temperature. *Materials Today: Proceedings*, 57, 786–792. <https://doi.org/10.1016/j.matpr.2022.02.354>
- European Commission, J. R. C. (2002a). *EN 1991-1-2: Eurocode 1: Actions on structures - Part 1-2: General actions - Actions on structures exposed to fire*. <https://data.europa.eu/doi/10.2788/91658>
- European Commission, J. R. C. (2002b). *EN 1992-1-2: Eurocode 2: Design of concrete structures - Part 1-2: General rules - Structural fire design*.

- European Commission, J. R. C. (2005). *EN 1994-1-2: Eurocode 4: Design of composite steel and concrete structures – Part 1-2: General rules - Structural fire design*.
- Fadiel, A. A. M., Abu-Lebdeh, T., Munteanu, I. S., Niculae, E., & Petrescu, F. I. T. (2023a). Mechanical Properties of Rubberized Concrete at Elevated Temperatures. *Journal of Composites Science*, 7(7). <https://doi.org/10.3390/jcs7070283>
- Fadiel, A. A. M., Abu-Lebdeh, T., Munteanu, I. S., Niculae, E., & Petrescu, F. I. T. (2023b). Mechanical Properties of Rubberized Concrete at Elevated Temperatures. *Journal of Composites Science*, 7(7). <https://doi.org/10.3390/jcs7070283>
- Formica, F. (2023). *Analisi di Resistenza al Fuoco di Elementi in C.A. in Funzione di Diverse Percentuali di Aggregati in Gomma Utilizzando il Programma IS Fuoco*.
- Karim Serroukh, H., El Marzak, M., Benaicha, M., Li, W., Zhu, J., & Hafidi Alaoui, A. (2023a). Numerical analysis of the thermomechanical behavior of rubber concrete at high temperatures. *Structural Concrete*, 24(3), 3236–3250. <https://doi.org/10.1002/suco.202300150>
- Karim Serroukh, H., El Marzak, M., Benaicha, M., Li, W., Zhu, J., & Hafidi Alaoui, A. (2023b). Numerical analysis of the thermomechanical behavior of rubber concrete at high temperatures. *Structural Concrete*, 24(3), 3236–3250. <https://doi.org/10.1002/suco.202300150>
- Karim Serroukh, H., El Marzak, M., Benaicha, M., Li, W., Zhu, J., & Hafidi Alaoui, A. (2023c). Numerical analysis of the thermomechanical behavior of rubber concrete at high temperatures. *Structural Concrete*, 24(3), 3236–3250. <https://doi.org/10.1002/suco.202300150>
- Khoury, G. A. (2000). Effect of fire on concrete and concrete structures. *Progress in Structural Engineering and Materials*, 2(4), 429–447. <https://doi.org/10.1002/pse.51>
- Ling, T. C. (2011a). Prediction of density and compressive strength for rubberized concrete blocks. *Construction and Building Materials*, 25(11), 4303–4306. <https://doi.org/10.1016/j.conbuildmat.2011.04.074>

- Ling, T. C. (2011b). Prediction of density and compressive strength for rubberized concrete blocks. *Construction and Building Materials*, 25(11), 4303–4306. <https://doi.org/10.1016/j.conbuildmat.2011.04.074>
- Mhaya, A. M., Baghban, M. H., Faridmehr, I., Huseien, G. F., Abidin, A. R. Z., & Ismail, M. (2021a). Performance evaluation of modified rubberized concrete exposed to aggressive environments. *Materials*, 14(8). <https://doi.org/10.3390/ma14081900>
- Mhaya, A. M., Baghban, M. H., Faridmehr, I., Huseien, G. F., Abidin, A. R. Z., & Ismail, M. (2021b). Performance evaluation of modified rubberized concrete exposed to aggressive environments. *Materials*, 14(8). <https://doi.org/10.3390/ma14081900>
- Ministero delle Infrastrutture e dei Trasporti. (2018). Capitolo 3. Azioni sulle Costruzioni. In *Norme Tecniche per le Costruzioni*.
- Najim, K. B., & Hall, M. R. (2012). Workability and mechanical properties of crumb-rubber concrete. *Proceedings of Institution of Civil Engineers: Construction Materials*, 166, 7–17. <https://doi.org/10.1680/coma.11.00036>
- Najim, K. B., Hall, M. R., & Hopfe, C. J. (2011). Transient thermal behaviour of crumb rubber-modified concrete and implications for thermal response and energy efficiency in buildings. *Applied Thermal Engineering*, 33–34(1), 77–85. <https://doi.org/10.1016/j.applthermaleng.2011.09.015>

## Appendix A. Density Values for Different Rubber Concrete Mixtures

*Table A-1. Density values for different rubber concrete mixtures, extracted from "Prediction of density and compressive strength for rubberized concrete blocks" by Ling.*

<b>w/c</b>	<b>Rubber Content [%]</b>	<b>Density [kg/m<sup>3</sup>]</b>
0.45	0	2156
	5	2137
	10	2114
	15	2100
	20	2076
	25	2057
	30	2015
	40	1999
	50	1991
0.5	0	2178
	5	2164
	10	2143
	15	2156
	20	2117
	25	2119
	30	2068
	40	2053
	50	2014
0.55	0	2211
	5	2183
	10	2165
	15	2173
	20	2140
	25	2132
	30	2093
	40	2082
	50	2025

## Appendix B. Input Data for Model with 0.45 Water-Cement Ratio

*Table B-2. Input data for models with w/c: 0.45.*

Rubber Content	Compressive Strength [MPa]	Temperature [°C]	Thermal Conductivity [W/m·°K]	Specific Heat [J/kg·°K]	Density [kg/m <sup>3</sup> ]
0%	30.80	20	0.6457	986.96	2156.00
		100	0.6130	986.96	2156.00
		115	0.6069	1001.96	2156.00
		200	0.5722	1086.96	2112.88
		400	0.4904	1186.96	2048.20
		800	0.3270	1186.96	1972.74
		1200	0.3270	1186.96	1897.28
5%	30.10	20	0.6307	992.16	2137.00
		100	0.5988	992.16	2137.00
		115	0.5928	1007.16	2137.00
		200	0.5589	1092.16	2094.26
		400	0.4790	1192.16	2030.15
		800	0.3194	1192.16	1955.36
		1200	0.3194	1192.16	1880.56
10%	25.00	20	0.6125	998.45	2114.00
		100	0.5815	998.45	2114.00
		115	0.5757	1013.45	2114.00
		200	0.5428	1098.45	2071.72
		400	0.4652	1198.45	2008.30
		800	0.3102	1198.45	1934.31
		1200	0.3102	1198.45	1860.32
15%	23.30	20	0.6015	1002.29	2100.00
		100	0.5710	1002.29	2100.00
		115	0.5653	1017.29	2100.00
		200	0.5330	1102.29	2058.00
		400	0.4568	1202.29	1995.00
		800	0.3046	1202.29	1921.50
		1200	0.3046	1202.29	1848.00
20%	20.40	20	0.5825	1008.86	2076.00
		100	0.5530	1008.86	2076.00
		115	0.5475	1023.86	2076.00
		200	0.5162	1108.86	2034.48
		400	0.4424	1208.86	1972.20
		800	0.2950	1208.86	1899.54
		1200	0.2950	1208.86	1826.88
25%	19.90	20	0.5675	1014.06	2057.00

<b>Rubber Content</b>	<b>Compressive Strength [MPa]</b>	<b>Temperature [°C]</b>	<b>Thermal Conductivity [W/m·°K]</b>	<b>Specific Heat [J/kg·°K]</b>	<b>Density [kg/m³]</b>
		100	0.5388	1014.06	2057.00
		115	0.5334	1029.06	2057.00
		200	0.5029	1114.06	2015.86
		400	0.4310	1214.06	1954.15
		800	0.2874	1214.06	1882.16
		1200	0.2874	1214.06	1810.16
30%	15.80	20	0.5343	1025.56	2015.00
		100	0.5073	1025.56	2015.00
		115	0.5022	1040.56	2015.00
		200	0.4735	1125.56	1974.70
		400	0.4058	1225.56	1914.25
		800	0.2706	1225.56	1843.73
		1200	0.2706	1225.56	1773.20
40%	10.50	20	0.5217	1029.94	1999.00
		100	0.4953	1029.94	1999.00
		115	0.4903	1044.94	1999.00
		200	0.4623	1129.94	1959.02
		400	0.3962	1229.94	1899.05
		800	0.2642	1229.94	1829.09
		1200	0.2642	1229.94	1759.12
50%	9.50	20	0.5154	1032.13	1991.00
		100	0.4893	1032.13	1991.00
		115	0.4844	1047.13	1991.00
		200	0.4567	1132.13	1951.18
		400	0.3914	1232.13	1891.45
		800	0.2610	1232.13	1821.77
		1200	0.2610	1232.13	1752.08



## Appendix C. Input Data for Model with 0.50 Water-Cement Ratio

*Table C-3. Input data for models with w/c: 0.50.*

Rubber Content	Compressive Strength [MPa]	Temperature [°C]	Thermal Conductivity [W/m·°K]	Specific Heat [J/kg·°K]	Density [kg/m <sup>3</sup> ]
0%	32.40	20	0.6631	980.93	2178.00
		100	0.6295	980.93	2178.00
		115	0.6232	995.93	2178.00
		200	0.5876	1080.93	2134.44
		400	0.5036	1180.93	2069.10
		800	0.3358	1180.93	1992.87
		1200	0.3358	1180.93	1916.64
5%	35.40	20	0.6520	984.77	2164.00
		100	0.6190	984.77	2164.00
		115	0.6128	999.77	2164.00
		200	0.5778	1084.77	2120.72
		400	0.4952	1184.77	2055.80
		800	0.3302	1184.77	1980.06
		1200	0.3302	1184.77	1904.32
10%	32.70	20	0.6355	990.52	2143.00
		100	0.6033	990.52	2143.00
		115	0.5972	1005.52	2143.00
		200	0.5631	1090.52	2100.14
		400	0.4826	1190.52	2035.85
		800	0.3218	1190.52	1960.85
		1200	0.3218	1190.52	1885.84
15%	28.20	20	0.6457	986.96	2156.00
		100	0.6130	986.96	2156.00
		115	0.6069	1001.96	2156.00
		200	0.5722	1086.96	2112.88
		400	0.4904	1186.96	2048.20
		800	0.3270	1186.96	1972.74
		1200	0.3270	1186.96	1897.28
20%	26.40	20	0.6149	997.63	2117.00
		100	0.5838	997.63	2117.00
		115	0.5779	1012.63	2117.00
		200	0.5449	1097.63	2074.66
		400	0.4670	1197.63	2011.15
		800	0.3114	1197.63	1937.06
		1200	0.3114	1197.63	1862.96
25%	24.80	20	0.6165	997.09	2119.00

<b>Rubber Content</b>	<b>Compressive Strength [MPa]</b>	<b>Temperature [°C]</b>	<b>Thermal Conductivity [W/m·°K]</b>	<b>Specific Heat [J/kg·°K]</b>	<b>Density [kg/m3]</b>
		100	0.5853	997.09	2119.00
		115	0.5794	1012.09	2119.00
		200	0.5463	1097.09	2076.62
		400	0.4682	1197.09	2013.05
		800	0.3122	1197.09	1938.89
		1200	0.3122	1197.09	1864.72
30%	20.20	20	0.5762	1011.05	2068.00
		100	0.5470	1011.05	2068.00
		115	0.5416	1026.05	2068.00
		200	0.5106	1111.05	2026.64
		400	0.4376	1211.05	1964.60
		800	0.2918	1211.05	1892.22
		1200	0.2918	1211.05	1819.84
40%	15.40	20	0.5644	1015.15	2053.00
		100	0.5358	1015.15	2053.00
		115	0.5304	1030.15	2053.00
		200	0.5001	1115.15	2011.94
		400	0.4286	1215.15	1950.35
		800	0.2858	1215.15	1878.50
		1200	0.2858	1215.15	1806.64
50%	12.50	20	0.5335	1025.83	2014.00
		100	0.5065	1025.83	2014.00
		115	0.5015	1040.83	2014.00
		200	0.4728	1125.83	1973.72
		400	0.4052	1225.83	1913.30
		800	0.2702	1225.83	1842.81
		1200	0.2702	1225.83	1772.32

## Appendix D. Input Data for Model with 0.55 Water-Cement Ratio

*Table D-4. Input data for models with w/c: 0.55.*

Rubber Content	Compressive Strength [MPa]	Temperature [°C]	Thermal Conductivity [W/m·°K]	Specific Heat [J/kg·°K]	Density [kg/m <sup>3</sup> ]
0%	42.50	20	0.6892	971.90	2211.00
		100	0.6543	971.90	2211.00
		115	0.6477	986.90	2211.00
		200	0.6107	1071.90	2166.78
		400	0.5234	1171.90	2100.45
		800	0.3490	1171.90	2023.07
		1200	0.3490	1171.90	1945.68
5%	35.00	20	0.6671	979.56	2183.00
		100	0.6333	979.56	2183.00
		115	0.6269	994.56	2183.00
		200	0.5911	1079.56	2139.34
		400	0.5066	1179.56	2073.85
		800	0.3378	1179.56	1997.45
		1200	0.3378	1179.56	1921.04
10%	31.90	20	0.6528	984.49	2165.00
		100	0.6198	984.49	2165.00
		115	0.6136	999.49	2165.00
		200	0.5785	1084.49	2121.70
		400	0.4958	1184.49	2056.75
		800	0.3306	1184.49	1980.98
		1200	0.3306	1184.49	1905.20
15%	29.50	20	0.6592	982.30	2173.00
		100	0.6258	982.30	2173.00
		115	0.6195	997.30	2173.00
		200	0.5841	1082.30	2129.54
		400	0.5006	1182.30	2064.35
		800	0.3338	1182.30	1988.30
		1200	0.3338	1182.30	1912.24
20%	26.30	20	0.6331	991.34	2140.00
		100	0.6010	991.34	2140.00
		115	0.5950	1006.34	2140.00
		200	0.5610	1091.34	2097.20
		400	0.4808	1191.34	2033.00
		800	0.3206	1191.34	1958.10
		1200	0.3206	1191.34	1883.20
25%	22.80	20	0.6268	993.53	2132.00

<b>Rubber Content</b>	<b>Compressive Strength [MPa]</b>	<b>Temperature [°C]</b>	<b>Thermal Conductivity [W/m·°K]</b>	<b>Specific Heat [J/kg·°K]</b>	<b>Density [kg/m3]</b>
		100	0.5950	993.53	2132.00
		115	0.5891	1008.53	2132.00
		200	0.5554	1093.53	2089.36
		400	0.4760	1193.53	2025.40
		800	0.3174	1193.53	1950.78
		1200	0.3174	1193.53	1876.16
30%	20.10	20	0.5960	1004.20	2093.00
		100	0.5658	1004.20	2093.00
		115	0.5601	1019.20	2093.00
		200	0.5281	1104.20	2051.14
		400	0.4526	1204.20	1988.35
		800	0.3018	1204.20	1915.10
		1200	0.3018	1204.20	1841.84
40%	16.30	20	0.5873	1007.21	2082.00
		100	0.5575	1007.21	2082.00
		115	0.5520	1022.21	2082.00
		200	0.5204	1107.21	2040.36
		400	0.4460	1207.21	1977.90
		800	0.2974	1207.21	1905.03
		1200	0.2974	1207.21	1832.16
50%	12.40	20	0.5422	1022.82	2025.00
		100	0.5148	1022.82	2025.00
		115	0.5096	1037.82	2025.00
		200	0.4805	1122.82	1984.50
		400	0.4118	1222.82	1923.75
		800	0.2746	1222.82	1852.88
		1200	0.2746	1222.82	1782.00

## Appendix E. Results of Temperature of Bottom Reinforcement

*Table E-5. Temperature in °C of bottom reinforcement from Dolmen model.*

<b>Rubber Content</b>	<b>DOLMEN - w/c: 0.49</b>							
<b>Time</b>	<b>Cold</b>	<b>0</b>	<b>30</b>	<b>60</b>	<b>90</b>	<b>120</b>	<b>150</b>	<b>180</b>
0%	20	20	416	611	719	793	848	892
5%	-	-	-	-	-	-	-	-
10%	20	20	384	578	688	763	819	864
15%	-	-	-	-	-	-	-	-
20%	20	20	357	548	658	734	792	838
25%	-	-	-	-	-	-	-	-
30%	20	20	283	468	581	660	721	770
40%	-	-	-	-	-	-	-	-
50%	-	-	-	-	-	-	-	-

*Table E-6. Temperature in °C of bottom reinforcement from proposed model with w/c: 0.45.*

<b>Rubber Content</b>	<b>w/c: 0.45</b>							
<b>Time</b>	<b>Cold</b>	<b>0</b>	<b>30</b>	<b>60</b>	<b>90</b>	<b>120</b>	<b>150</b>	<b>180</b>
0%	20	20	190	333	423	488	544	593
5%	20	20	187	330	420	485	541	589
10%	20	20	184	327	416	481	537	585
15%	20	20	183	324	414	479	534	582
20%	20	20	179	320	410	475	530	578
25%	20	20	177	317	406	471	526	574
30%	20	20	171	310	398	463	517	565
40%	20	20	168	307	395	460	514	561
50%	20	20	167	305	394	458	512	560

*Table E-7. Temperature in °C of bottom reinforcement from proposed model with w/c: 0.50.*

<b>Rubber Content</b>	<b>w/c: 0.50</b>							
<b>Time</b>	<b>Cold</b>	<b>0</b>	<b>30</b>	<b>60</b>	<b>90</b>	<b>120</b>	<b>150</b>	<b>180</b>
0%	20	20	192	336	426	492	548	597
5%	20	20	191	334	424	490	546	594
10%	20	20	188	331	421	486	542	590
15%	20	20	190	333	423	488	544	593
20%	20	20	185	327	417	482	537	586
25%	20	20	185	327	417	482	538	586

<b>Rubber Content</b>	<b>w/c: 0.50</b>							
<b>Time</b>	<b>Cold</b>	<b>0</b>	<b>30</b>	<b>60</b>	<b>90</b>	<b>120</b>	<b>150</b>	<b>180</b>
30%	20	20	178	319	408	473	528	576
40%	20	20	176	316	406	470	525	573
50%	20	20	171	309	398	463	517	565

*Table E-8. Temperature in °C of bottom reinforcement from proposed model with w/c: 0.55.*

<b>Rubber Content</b>	<b>w/c: 0.55</b>							
<b>Time</b>	<b>Cold</b>	<b>0</b>	<b>30</b>	<b>60</b>	<b>90</b>	<b>120</b>	<b>150</b>	<b>180</b>
0%	20	20	196	341	431	497	553	602
5%	20	20	193	337	427	493	549	597
10%	20	20	191	334	424	490	546	594
15%	20	20	192	335	426	491	547	596
20%	20	20	188	331	420	486	541	590
25%	20	20	187	329	419	485	540	588
30%	20	20	182	323	413	478	533	581
40%	20	20	180	321	411	476	531	579
50%	20	20	172	311	400	465	519	567

## Appendix F. Results of Bending Moment Resistance

*Table F-9. Bending Moment Resistance in kN·m from Dolmen model.*

<b>Rubber Content</b>	<b>DOLMEN - w/c: 0.49</b>							
<b>Time</b>	<b>Cold</b>	<b>0</b>	<b>30</b>	<b>60</b>	<b>90</b>	<b>120</b>	<b>150</b>	<b>180</b>
0%	69.9	84.3	71.7	33.8	15.2	14.0	13.0	12.3
5%	-	-	-	-	-	-	-	-
10%	69.5	83.9	77.5	40.0	17.9	14.1	13.2	12.4
15%	-	-	-	-	-	-	-	-
20%	67.3	80.7	79.5	43.5	22.0	13.2	12.3	11.6
25%	-	-	-	-	-	-	-	-
30%	65.0	77.1	77.1	55.6	34.6	19.4	11.4	10.6
40%	-	-	-	-	-	-	-	-
50%	-	-	-	-	-	-	-	-

*Table F-10. Bending moment resistance in kN·m from proposed model with w/c: 0.45.*

<b>Rubber Content</b>	<b>w/c: 0.45</b>							
<b>Time</b>	<b>Cold</b>	<b>0</b>	<b>30</b>	<b>60</b>	<b>90</b>	<b>120</b>	<b>150</b>	<b>180</b>
0%	66.5	79.5	79.5	79.5	66.0	53.7	43.2	33.9
5%	66.4	79.3	79.3	79.3	66.4	54.2	43.7	34.4
10%	65.5	77.9	77.9	77.9	65.8	53.8	43.4	34.2
15%	65.1	77.4	77.4	77.4	65.8	53.8	43.5	34.4
20%	64.6	76.5	76.5	76.5	65.7	53.9	43.7	34.7
25%	64.5	76.3	76.3	76.3	66.2	54.4	44.3	35.3
30%	63.6	75.0	75.0	75.0	66.4	54.8	44.9	36.0
40%	62.4	73.0	73.0	73.0	65.1	53.7	44.1	35.4
50%	62.2	72.5	72.5	72.5	65.0	53.7	44.1	35.5

*Table F-11. Bending moment resistance in kN·m from proposed model with w/c: 0.50.*

<b>Rubber Content</b>	<b>w/c: 0.5</b>							
<b>Time</b>	<b>Cold</b>	<b>0</b>	<b>30</b>	<b>60</b>	<b>90</b>	<b>120</b>	<b>150</b>	<b>180</b>
0%	66.8	79.9	79.9	79.9	65.7	53.4	42.8	33.5
5%	67.3	80.7	80.7	80.7	66.8	54.5	43.8	34.5
10%	66.8	80.0	80.0	80.0	66.8	54.6	44.0	34.7

<b>Rubber Content</b>	<b>w/c: 0.5</b>							
<b>Time</b>	<b>Cold</b>	<b>0</b>	<b>30</b>	<b>60</b>	<b>90</b>	<b>120</b>	<b>150</b>	<b>180</b>
15%	66.1	78.8	78.8	78.8	65.4	53.2	42.7	33.4
20%	65.7	78.3	78.3	78.3	66.1	54.0	43.6	34.4
25%	65.4	77.8	77.8	77.8	65.6	53.5	43.2	34.0
30%	64.5	76.4	76.4	76.4	65.9	54.1	44.0	34.9
40%	63.5	74.8	74.8	74.8	65.0	53.3	43.3	34.4
50%	62.9	73.7	73.7	73.7	65.3	53.8	44.0	35.3

*Table F-12. Bending moment resistance in kN-m from proposed model with w/c: 0.55.*

<b>Rubber Content</b>	<b>w/c: 0.55</b>							
<b>Time</b>	<b>Cold</b>	<b>0</b>	<b>30</b>	<b>60</b>	<b>90</b>	<b>120</b>	<b>150</b>	<b>180</b>
0%	68.4	82.4	82.4	82.4	67.0	54.5	43.6	34.1
5%	67.2	80.6	80.6	80.6	66.2	53.8	43.1	33.8
10%	66.7	79.8	79.8	79.8	66.0	53.7	43.1	33.8
15%	66.3	79.1	79.1	79.1	65.2	52.9	42.4	33.1
20%	65.7	78.2	78.2	78.2	65.4	53.2	42.8	33.6
25%	65.1	77.2	77.2	77.2	64.7	52.7	42.3	33.2
30%	64.5	76.4	76.4	76.4	65.1	53.2	43.0	34.0
40%	63.7	75.1	75.1	75.1	64.3	52.6	42.5	33.6
50%	62.9	73.7	73.7	73.7	64.9	53.4	43.6	34.8



## Appendix G. Results of Axial Resistance

Table G-13. Axial Resistance in kN from Dolmen model.

Rubber Content	DOLMEN - w/c: 0.49							
Time	Cold	0	30	60	90	120	150	180
0%	4966.30	8474.73	7184.87	5409.08	4191.04	3468.35	2884.27	2363.29
5%	-	-	-	-	-	-	-	-
10%	3992.46	6744.50	5980.37	4768.70	3864.89	3305.69	2884.68	2497.55
15%	-	-	-	-	-	-	-	-
20%	3014.57	5019.53	4583.95	3683.50	3027.70	2600.17	2312.33	2060.45
25%	-	-	-	-	-	-	-	-
30%	2079.04	3369.38	3224.88	2749.46	2312.85	1967.55	1749.86	1623.03
40%	-	-	-	-	-	-	-	-
50%	-	-	-	-	-	-	-	-

Table G-14. Axial resistance in kN from proposed model with w/c: 0.45.

Rubber Content	w/c: 0.45							
Time	Cold	0	30	60	90	120	150	180
0%	2667.3	4407.0	4255.5	4017.2	3707.8	3409.1	3145.5	2912.9
5%	2617.7	4319.5	4177.0	3945.8	3649.2	3355.5	3097.3	2868.9
10%	2256.2	3681.9	3593.3	3403.5	3146.5	2883.2	2653.1	2448.5
15%	2135.7	3469.4	3399.1	3223.3	2981.8	2729.2	2508.9	2312.4
20%	1930.2	3067.8	2915.2	2915.2	2698.6	2465.4	2261.6	2078.9
25%	1894.7	3044.4	3011.8	2864.0	2657.3	2429.0	2229.2	2049.4
30%	1604.1	2531.8	2544.5	2427.2	2258.8	2057.3	1881.0	1720.9
40%	1228.4	1869.1	1877.0	1857.3	1721.0	1549.2	1399.8	1264.0
50%	1157.5	1744.0	1751.2	1750.2	1621.6	1455.6	1311.5	1180.5

Table G-15. Axial resistance in kN from proposed model with w/c: 0.50.

Rubber Content	w/c: 0.50							
Time	Cold	0	30	60	90	120	150	180
0%	2780.7	4607.0	4437.0	4183.9	3855.0	3546.0	3272.2	3031.9
5%	2993.3	4982.0	4782.7	4506.9	4166.9	3841.1	3553.0	3298.9
10%	2802.0	4644.5	4475.0	4222.7	3908.4	3599.3	3327.2	3086.8
15%	2483.0	4082.0	3957.1	3739.3	3445.1	3161.4	2911.4	2690.6
20%	2355.5	3857.0	3753.9	3553.1	3286.8	3015.4	2777.9	2566.8

<b>Rubber Content</b>	<b>w/c: 0.50</b>							
<b>Time</b>	<b>Cold</b>	<b>0</b>	<b>30</b>	<b>60</b>	<b>90</b>	<b>120</b>	<b>150</b>	<b>180</b>
25%	2242.1	3656.9	3569.9	3381.3	3123.1	2860.9	2631.3	2427.5
30%	1916.0	3081.8	3045.5	2894.8	2682.3	2451.1	2248.9	2067.4
40%	1575.7	2481.7	2494.1	2379.9	2198.9	1996.1	1819.0	1659.5
50%	1370.2	2119.1	2128.7	2071.4	1920.0	1736.3	1576.2	1430.9

*Table G-16. Axial resistance in kN from proposed model with w/c: 0.55.*

<b>Rubber Content</b>	<b>w/c: 0.55</b>							
<b>Time</b>	<b>Cold</b>	<b>0</b>	<b>30</b>	<b>60</b>	<b>90</b>	<b>120</b>	<b>150</b>	<b>180</b>
0%	3496.4	5869.5	5591.4	5253.3	4848.0	4477.3	4148.4	3863.6
5%	2965.0	4932.0	4734.7	4460.3	4113.7	3789.3	3501.4	3249.5
10%	2745.3	4544.5	4380.9	4133.0	3813.0	3507.5	3237.5	2999.3
15%	2575.2	4244.5	4104.7	3875.3	3565.9	3274.0	3015.7	2788.5
20%	2348.4	3844.5	3740.3	3538.6	3262.6	2990.7	2751.8	2540.5
25%	2100.3	3406.9	3339.1	3165.1	2912.6	2661.4	2441.1	2245.9
30%	1908.9	3069.3	3032.1	2880.7	2659.4	2426.1	2222.5	2040.7
40%	1639.6	2594.3	2596.7	2473.7	2277.1	2066.7	1883.1	1718.7
50%	1363.1	2106.6	2116.1	2059.6	1904.4	1720.5	1560.1	1415.0